AD NUMBER

AD839872

NEW LIMITATION CHANGE

TO

Approved for public release, distribution unlimited

FROM

Distribution authorized to U.S. Gov't. agencies and their contractors; Critical Technology; SEP 1968. Other requests shall be referred to Air Force Aero Propulsion Lab., Wright-Patterson AFB, OH 45433.

AUTHORITY

AFAPL ltr, 12 Apr 1972

AD839872

RESEARCH ON SLOT INJECTION INTO A SUPERSONIC AIR STREAM

JOSEPH A. SCHETZ

HAROLD E. GILREATH

PAUL J. WALTRUP

AND

DAVID P. LEWIS

DEPARTMENT OF AEROSPACE ENGINEERING

UNIVERSITY OF MARYLAND

SEPTEMBER 1968

Qualified requestors may obtain additional copies from the Defense Documentation Center.

CONDITIONS OF REPRODUCTION

AFAPL-TR-68-97

RESEARCH ON SLOT INJECTION INTO
A SUPERSONIC AIR STREAM

Joseph A. Schetz
Harold E. Gilreath
Paul J. Waltrup
David P. Lewis

Aerospace Engineering Department
University of Maryland

Technical Report AFAPL-TR-68-97

September 1968

FOREWORD

This work constitutes the final report on an investigation of slot injection into a supersonic stream. The work was performed under contract F33(615)-67-C-1805 by the Aerospace Engineering Department of the University of Maryland, College Park, Maryland, and was monitored by Mr. W. Lee Bain of the Ramjet Components B.anch (APRT) of the Aero Propulsion Laboratory. The time period covered was from June 1967 to August 1968.

The contribution of many people in addition to the authors is acknowledged. In particular, Mr. James Deveney performed valuable machine work, and Mrs. Edna Brothers typed the manuscript.

Publication of this report does not constitute Air Force approval of the report's findings or conclusions. It is published only for the exchange and stimulation of ideas.

W. Lee Bain

W. LEE BAIN
PROJECT ENGINEER
AF AERO PROPULSION LABORATORY

ii

ABSTRACT

The results of an experimental and analytical study
of tangential slot injection into a supersonic stream are
presented. The experiments were performed in an atmospheric
intake wind tunnel with freestream Mach numbers of 2.85 and
4.19. Injection of air, helium and carbon dioxide at various
subsonic Mach numbers and one supersonic condition was considered.
Experiments for the flow over of wedges with turning angles between
5° and 25° located on the wall downstream of the injection are also
reported.

The principal data are in the form of spark schlieren
photographs, interferograms and wall static pressure distributions.
Density profiles at several axial stations determined from inter-
ferograms are also presented. The transition to turbulence in
the shear layer and the character of the turbulence were observed
from the spark schlieren photographs. The presence of separation
zones was detected by small tufts or threads on the surface.

With subsonic injection, it is found that the initial
slot exit conditions are not arbitrary for a given injectant mass
flow but are determined by the downstream interaction between
the two streams. The flow field has many of the features of the
now well-known base-flow problem. A relatively simple analysis
is developed which predicts the initial jet exit conditions.
Very good agreement with the experimental observations is achieved.

TABLE OF CONTENTS

SYMBOLS

A	area/unit wi͏ ͏etween wall and dividing streamline
a	slot height
b	mixing zone width
h	A/A^*
k	mixing coefficient
K	constant in eddy viscosity model
M	Mach number
P	pressure
R	gas constant
S	test section span
T	temperature
u	x - component of velocity
x	streamwise coordinate
y	normal coordinate
z	spanwise coordinate
β	wedge angle
γ	ratio of specific heats
δ	boundary layer thickness
τ	shear stress
ρ	density

Subscripts

l	refers to conditions in undisturbed freestream
w	refers to conditions at the wall
j	refers to conditions in injectant at the point of injection
e	refers to conditions at edge of mixing zone
t	refers to stagnation conditions
d	refers to conditions along dividing streamline

Superscripts

*	refers to conditions at critical point
	ratio of injectant to freestream conditions
'	measured with critical point location as initial station

v

LIST OF FIGURES

1.0 INTRODUCTION

The tangential injection of a fluid into a moving stream by means of a wall slot is very often of interest in aerodynamic problems. Figure 1 presents a schematic representation of such a flow field corresponding to low-subsonic injection into a supersonic stream, and serves to introduce the general arrangement and some of the terminology used throughout the text. Examples of applications proposed for slot-injection devices can be drawn from a wide range of technological fields, but recent attention has focussed on those for which the external flow is supersonic or hypersonic. For instance, it is frequently necessary to provide protection for aerodynamic surfaces which would otherwise be exposed to high heat transfer rates. These problems become more severe in cases involving flow over flared junctions or deflected control surfaces. The purpose of injection under these circumstances is to supply a protective layer of fluid near the surface. Interest has also been expressed in combining these thermal protection advantages with a gaseous fuel injection system for supersonic combustion engines in which cooling problems are likely to be severe. Recently, there has been considerable interest in the possibility of re-energizing the innermost portion of a boundary layer that is near separation so that it might undergo a further pressure rise without separating.

Various aspects of the applications just cited have been studied experimentally. Within the past five years, the NASA Langley Research Center has conducted several investigations of slot injection as a drag reduction device (1,2,3,4), but these were strictly application-oriented and did not discuss the fundamental processes involved in the flow development. A number of experimental studies have been made in which both primary and secondary streams are subsonic (5,6,7,8) and several in which the primary flow alone is supersonic (9,10,11,12). All of these cases, however, involve turbulent mixing, and with the exception of Ref. 12, all of the supersonic experiments employed very thick splitter plates. No previous experimental results have been presented in which the mixing region is laminar, and studies of the important initial

1

adjustments between streams have been notably lacking.

The only results related to supersonic injection into a supersonic freestream appear to be those of Ref. 13 which was a limited study of the turbulent mixing region between uniform treams and not directly concerned with the tangential injection problem. In addition, aside from a brief discussion in Ref. 12, there have been no experiments relevant to the important question of transition from laminar to turbulent mixing. Considering the high altitude, high Mach number flight regimes currently receiving attention, an understanding of the conditions under which transition occurs becomes increasingly important since some laminar mixing is likely to be encountered.

The present work was undertaken to extend the experimental investigation of tangential injection into several new areas. First, due to the practical importance attributed to transition to turbulence in flows of this type, certain facets of the stability problem were studied. In particular, the relative change in transition location with a change in injection rate and the influence of foreign gas injection were considered. Second, an examination of the interactions in the vicinity of the point of injection for both subsonic and supersonic injection into a supersonic freestream was conducted. Third, the development of the flow field arising from injection over wedges located on the main surface was investigated. Last, the development of the flow field with an artificially generated "near separation" initial splitter plate boundary layer was considered.

In considering the possibility of a theoretical treatment of the flow field, one is tempted to formulate the problem in terms of an initial value problem in boundary layer theory in which initial velocity and enthalpy profiles are specified at the injection station together with a streamwise pressure distribution and the solution then "marched" downstream. Approximate techniques based upon a linearization of the boundary layer equations have been used in this manner (14,15,16) and results are available for constant pressure flow including the effects of compressibility, initial splitter plate boundary layers, and

2

combustion. However, except under very restrictive circumstances, such a formulation is inadequate in describing the basic structure and development of the flows under study here. As will become apparent later, in the case of subsonic injection this is due to the fact that the initial conditions are not arbitrary out are fixed by the interaction between streams. In the case of supersonic injection, significant wave patterns develop unless the injectant and freestream static pressures are closely matched. Therefore, the present analytical efforts were directed toward (1) accounting for the influence of the mixing, and pressure interaction between streams in determining the conditions at the point of injection for subsonic injection, and (2) assessing the utility of inviscid theory in analyzing the basic structure of supersonic injection flows.

The experimental portion of the work was conducted in the atmospheric intake wind tunnel at the University of Maryland at freestream Mach numbers of 2.85 and 4.19, and the principal results are presented in the form of 0.4 microsecond spark Schlieren photographs, wall pressure distributions, and the results of surface flow studies. In addition, density profiles obtained with a Mach-Zehnder interferometer are presented for several cases. Tests were run with air-to-air, He-to-air and CO_2-to-air injection with the total temperatures of the primary and secondary streams essentially equal.

3

2.0 APPARATUS AND TEST METHODS

2.1 Wind Tunnel Facilities

The experiments were conducted in the supersonic wind tunnel facility at the Gasdynamics Laboratory of the University of Maryland. The tunnel is an in-draft type and employs a regenerative silica-gel bed dryer to prevent condensation. For the present experiments, the test section was fitted with either of two nozzle blocks which permitted test Mach numbers of 2.85 and 4.19. A fixed-geometry diffuser was de- signed to allow operation at both Mach numbers without modification, and with a starting back pressure of roughly 1/2 psia this configuration produced a maximum run time of about 25 seconds at either Mach number.

At test Mach numbers of 2.85 and 4.19 the Reynold's numbers per foot were 2.5 and 1.3 million respectively.

2.2 Model

The basic injection model was adaptable to both subsonic and super- sonic injection experiments. The subsonic configuration is shown in Fig. 2a with the model side-plates removed in order to indicate the internal arrance- ment. The complete assembly forms the upper wall of the test section with the splitter plate lying along the plane of symmetry of the 2-dimensional super- sonic nozzle block attached at the opposite wall. Control of the freestream Mach number was obtained by installing the appropriate nozzle block while retaining the basic injection model structure.

The change-over from subsonic to supersonic injection consisted of replacing the surface block in the injection model (c.f., Fig. 2a). The upstream end of this block forms one wall of the injection channel, and in the case of supersonic injection was contoured to produce a converging- diverging section. This is illustrated in Fig. 2b. The injection slot measured 0.50 inches in height and 5.94 inches in span regardless of whether the model was configured for subsonic or supersonic experiments. The distance between the primary nozzle throat and the injection station was 5.5 inches, which placed the point of injection about 1 inch downstream of the beginning of the test section rhombus at Mach number 4.19 and 1/4 inch downstream at Mach number 2.85. The major portion of the model was fabricated

4

from laminated mahogany; however, dimensionally critical components as
well as parts serving as attachment points were constructed of metal.
In particular, the splitter plate was machined from brass with a great
deal of emphasis placed on maintaining a straight and sharp trailing
edge. After several attempts using both brass and stainless steel, it
was found that .005 inch was the smallest trailing edge thickness con-
sistent with a reasonable requirement for straightness. At this thickness,
the amount of spanwise bow at the trailing edge was held to a maximum of
about .010 inch.

For the air injection experiments the injectant was drawn from
the atmosphere through a regulating valve and a remotely actuated on-off
valve. For He or CO_2 injection, a manifold of commercial gas bottles,
followed by a pressure regulator, a surge tank and a metering valve pre-
ceded the on-off valve. The total temperatures of the injectant were $535^\circ R$
for air, $525^\circ R$ with Helium and $485^\circ R$ with CO_2. From this point, connection
was made to the model through a specially constructed fitting at the top of
the tunnel. Very careful attention to the manner in which the injectant entered
the model was required in order to achieve acceptably uniform injection. To
this end, a T-shaped header was employed to pre-distribute the flow in the
model plenum (cf. Fig. 2b). The flow entered the stem of the tee and ex-
hausted into the plenum through a number of spanwise ports arranged along
the head of the tee. Further smoothing of the flow prior to injection was
achieved by requiring it to pass through a straightening section composed of
eight layers of 14 mesh x .012 inch diameter wire screen. Spanwise static
pressure distributions measured just downstream of the injection station are
presented in Fig. 3 for several air injectant Mach numbers and a freestream
Mach number of 2.85. It is emphasized that these represent the least uniform
of the cases encountered in either the Mach 2.85 or 4.19 tests. The maximum
deviation from the average spanwise pressure is seen to be generally less
than about 1.5%. The distribution shown for an injectant Mach number of
2.0 was measured with the distributing header removed from the model plenum,
which was the arrangement used in most of the supersonic injection tests at
Mach 2.85. A survey with the header installed indicated a deviation of only

5

1.3%. Since, in addition, surface oil-flow studies revealed no appreciable spanwise component of flow, it is concluded that the level of non-uniformity experienced in the tests had only a minor effect on the overall results.

Pressure orifices were also located at eleven streamwise stations near the centerline within the first nine slot-heights in order to obtain the near-field pressure distribution along the wall. The injectant total pressure was measured by means of a static tap downstream of the straightening screens in the model plenum. Based upon area ratio considerations, at injection Mach numbers near unity the static pressure at this point was estimated to be within about one percent of the total pressure and virtually indistinguishable from it at low injection Mach numbers or when used in conjunction with the supersonic injection configuration.

The entire injection chamber was enclosed by .030 inch thick sideplates and sealed with "0"-rings. The sideplates were in turn sealed against the tunnel walls with 1/16 "0"-ring material. As evident from Fig. 2, similar sealing provisions were also made between the tunnel walls and the main components in the test section.

For experiments involving injection over wedge surfaces, the surface block was fitted with a slotted attachment plate which permitted positioning the various wedge models at any streamwise location between zero and about 10 slot-heights (cf. Fig. 2b). When the wedges were not in use a solid blank replaced the attachment plate. Typically, the wedge models were 1-inch thick with turning angles between 5 and 25 degrees in 5 degree increments. Again, the sides of the wedges were sealed against the tunnel walls with "0"-rings. In addition, the interface between the injection model surface and the wedge vertex was coated with a thin film of General Electric RTV-102 Silastic, since the development of the flow was known to be very sensitive to leakage in this area. This proved to be a most reliable and durable sealant and did not alter the geometry of the surface significantly.

In studies involving the limiting case of flow over a rear-facing step, the injection model was replaced with a solid, laminated-mahogany block with a step one slot-height deep located at the point corresponding to the injection station. It is of interest to note that the flow over a solid step is not equivalent to the situation of zero injection using the injection model. This is due to the fact that the restraining influence of the step face is lacking in the latter case, leading to a highly three-

6

dimensional separated region and a somewhat lower base pressure.

A few tests were conducted to investigate the development of the boundary layer over wedges with no injection, and in this case the injection model was replaced with a straight block to form essentially a half-nozzle test section. The wedge models and attachment plate described earlier were also utilized in these tests.

2.3 Test Methods

2.3.1 Optical tests. Schlieren and interferometric methods of flow visualization were used extensively throughout the experimental program. The Schlieren system employed either a continuous, high-intensity mercury vapor light source (PEK 110) or a short duration spark source of relatively low intensity (EG & G Type 2307). The latter was adjusted to produce .006 candlepower-seconds at 0.4 microseconds duration which is the maximum output available with this instrument. Most of the photographic data was obtained using the spark source with the test section image condensed to a magnification of 1/2. The wind tunnel windows used in these tests were of interferometric quality, i.e., about 0.1 fringe in flatness and 1 second in parallelism. The photographs were taken with a Model FP Speed Graphic camera with an open shutter using type 57 (ASA 3000) Polaroid film. The continuous source was used primarily to visually monitor the flow during testing. All tests were observed in this fashion in order to assess the steadiness of flow as well as to afford a quick interpretation of any variation in normal operating conditions.

In order to obtain detailed information concerning the streamwise development of the flow, a Mach-Zehnder interferometer was used to measure density profiles at various axial stations. The optics in this instrument are nine inches in diameter and are set at an incidence of 60 degrees. The continuous mercury-vapor source was used in conjection with a Baird-Atomic interference filter centered at $4376A^{\circ}$ to provide the necessary monochromatic beam. The interferograms were taken with the Speed Graphic camera using a focal plane shutter and type 57 Polaroid film at a shutter speed of 1 millisecond.

2.3.2 Pressure measurements. The vacuum-reference manometer shown in Fig. 4 was used in gathering most of the pressure data. The accuracy of the measurements was estimated to be $\pm$ 2%. In addition to the manometer measurements, spanwise pitot pressure surveys were made of the freestream flow in order to

7

determine the primary Mach number and to check the uniformity.

2.3.3 <u>Surface flow studies</u>. The surface flow studies were conducted in order to obtain confirmation of the occurence of flow separation independent of the measured pressure distribution. An oil-graphite mixture was used in the tests for which the freestream Mach number was 2.85, and a distribution of fine tufts for those at Mach 4.19.

3.0 TEST RESULTS FOR INJECTION ON A FLAT SURFACE

In this section specific test results are presented and discussed. First, the related problem of the flow over a rearward facing step is considered, which introduces several important concepts that carry over to injection flows. Next, the results for subsonic and supersonic injection are presented with particular emphasis on the nature of the initial adjustments between the injected and primary flows. In the sub-section dealing with supersonic injection, the experimental results are compared with an inviscid analysis in which the interface between the streams is a slip-line. Results relevant to transition from laminar to turbulent mixing are shown next, and finally, interferometric measurements of the development of density profiles are presented for several cases.

3.1 **Flow Over a Rearward-Facing Step**

Due to its close connection to the present work, it is appropriate to discuss briefly the limiting case in which there is no injection and the slot-opening is replaced by a solid step. If the base press.re is specified under these circumstances, an approach-ing inviscid supersonic stream will expand to this pressure at the point of sudden change in the surface and continue in a straight path toward the lower wall. At reattachment, the flow is suddenly turned parallel to the original flow direction through an oblique shock wave. It is obvious that this solution does not involve a unique determination of the base pressure, its specification being required a priori. However, when the effects of viscosity are added, it is found that the details of the mixing between the outer flow and the "dead air" in the base region fix the base pressure.

An important concept first introduced by Chapman (17) is the dividing streamline which separates the outer flow from that recirculated at the base. In the part of the mixing zone beneath this streamline, the flow is accelerated by shear forces, but this acceleration begins to be counterbalanced by the increasing pressure as the outer flow turns parallel to the lower wall. At reattachment, the flow above the dividing streamline continues downstream whereas the flow beneath is turned back, not having been able to negotiate the

9

pressure rise. Under steady-state conditions, the amount of accelerated
flow beneath the dividing streamline and the amount returned must be
equal since otherwise mass would be continually added or removed from
the base region. Therefore, it is a balance between the flow scavenged
in the mixing region and the flow turned back which uniquely determines
the required solution. In this connection, it is apparent that the base
pressure depends greatly on whether the mixing region is laminar, transitional,
or turbulent since this affects the mixing rate and the magnitude or the
pressure rise which can be withstood at reattachment, thereby shifting the
overall balance. Chapman, Kuehn and Larson (18) conducted an extensive
experimental program from which evolved most of the present understanding of
separated flows. One of the major findings was that the pressure field is
greatly affected by the location of transition relative to the point of re-
attachment. They classify three types of separated flows: pure laminar,
in which transition is downstream of reattachment; transitional, in which
transition is between separation and reattachment; and turbulent, in which
transition is upstream of separation. It will be seen in a later section
that similar classifications can be made in the case of subsonic tangential
injection flows. It is also convenient to carry over the concept of the
dividing streamline to such flows with a definition such that the amount of
flow between it and the wall is the same as originally issued from the slot.

The picture of the flow over a discontinuous surface just
presented remains over-simplified since in an actual flow situation a
boundary layer develops on the upper wall before reaching the step.
This introduces several complications which also carry over to tangential
injection flows. The first is that the flow begins adjusting to the
base pressure prior to separation. An order to magnitude analysis
indicates that transmission through the subsonic portion of the boundary
layer has an upstream extent of the order δM, and can therefore be
an important effect at high Mach numbers (c.f., Ref. 19). In addition,
the corner expansion must now pass through the non-uniform supersonic
portion of the boundary layer giving rise to a continuous distribution
of internal reflections. The effects of these reflections can also
be significant at high Mach numbers and are discussed in detail in

10

Ref. 20. Perhaps the most readily observable complication is the existence of a lip shock following the corner expansion. Recent experiments by Hama (21) indicate that this phenomena is primarily due to flow separation on the face of the step wherein the highly viscous subsonic portion of the boundary layer "creeps" around the edge of the step with the outer flow over-expanding to a pressure less than the base pressure. Therefore, the pressure distribution on the step face is one increasing from this lower pressure to the final base pressure. Since the boundary layer cannot negotiate this rise it separates with the required pressure adjustment being made by means of a separation shock.

The flow over a rearward-facing step under the present experimental conditions was studied by means of spark Schlieren photographs, examples of which are shown in Fig. 5. Primary interest was directed toward locating the point of transition; however, rough estimates of the base pressure were made by measurement of the turning angles ($\Delta v = 19^\circ$ at Mach 2.85 and 5.2° at Mach 4.19) neglecting the strength of the lip shock. From Fig. 5 it is apparent that at Mach 2.85 transition occurs just before reattachment while at Mach 4.19 transition appears to occur after reattachment. It is also notable that the lip shock is oriented toward the wall at Mach 2.85 and is nearly horizontal at Mach 4.19, and that the recompression zone extends over a considerable streamwise distance at both Mach numbers. These results serve as a basis of comparison for some elements of the subsonic injection experiments presented below.

3.2 Subsonic Injection

Schlieren photographs together with the corresponding wall pressure distributions are presented in Figs. 6,7, and 8 for a freestream Mach number of 2.85 and injectant Mach numbers between 0.15 and 1.0. At low injection rates. the flow field is seen to resemble the flow over a rearward facing step in a number of aspects. The large corner expansion with following lip shock, and the recompression zone are easily identified in the photographs.

Separation occurs along the lower wall if the total pressure of the injected flow is insufficient to negotiate the pressure rise attending the recompression. Oil-flow studies indicated that with

11

an injectant Mach number of 0.153 (Fig. 6a) full-span separation
occurred about 3-1/4 slot-heights downstream of the injection station
(indicated by the symbol "s" in the figure). However, with an injectant
Mach number of 0.255 similar testing revealed a localized region of
separation at about 5-1/2 slot-heights which extended only part-span,
with the unseparated surface flow being constricted into the remaining
span at this station. This appears to be indicated in the slight
drop in pressure recorded in Fig. 6b. As the rate of injection is
increased there is a reduction in the initial amount of expansion
with a correspondingly higher initial pressure and less severe
recompression, so that beyond an injectant Mach number of 0.255 no
further incidence of separation was observed along the lower wall.

The adjustment between the streams which determines the
initial injectant pressure depends primarily on the mixing rate.
Since the mass flow rate per unit area of the injected flow is less
than that of the freestream, any mixing will cause the dividing
streamline to deflect toward the lower wall. In this regard the
nature of the boundary layer is seen to be of paramount importance.

At Mach 2.85, a further increase in the injection rate ultimately
leads to a marked change in the pressure distribution. As shown in
Fig. 7, a considerable pressure decrease occurs before recompression
at injectant Mach numbers of 0.434 and 0.706. Since no appreciable
spanwise velocity components were detected in the oil-flow tests, this
is perhaps best explained by the increasing importance of wall shear
and the dimunition of the driving shear along the dividing streamline
as the Mach number is increased. Coupled with the decreasing total
streamtube area of the injected flow, this tends to depress the
pressure gradient.

For all of the cases considered thus far, the pressure and
Mach number at the point of injection (or equivalently the pressure
and mass flow rate) could not be chosen independently, there being a
unique Mach number corresponding to a given initial pressure determined
by the interaction with the external flow. However, if the injection
rate is raised sufficiently, the condition is eventually reached for
which the slot exit is choked. Beyond this point the exit Mach number

12

is fixed near unity and the pressure (or equivalently the mass flow rate) can be increased independently. An example of choked injection is shown in Fig. 8a. A careful examination of the photograph discloses the existence of weak compression waves in the injectant near the exit, accounting for the somewhat erratic pressure distribution. (The measured Mach number was actually 1.01). Increasing the total pressure of the injectant flow beyond this point results in under-expanded sonic injection (Fig. 8b) with the flow passing into the supersonic regime through an expansion centered at the trailing edge of the splitter plate. The adjustment between the streams takes the form of a shock wave in the primary flow with the lip shock now follow-ing the expansion in the injectant. The upper limit on the injection rate established whenever the freestream shock is of sufficient strength to separate the splitter plate boundary layer.

Up to a certain point the trends observed for subsonic injection at Mach 2.85 were also found at Mach 4.19. Figure 9 presents the Schlieren photographs and pressure distributions obtained in this case for injectant Mach numbers between .232 and .570. Due to the higher freestream Mach number and initially laminar mixing, the amount of deflection at the injection station was considerably less than that observed at Mach 2.85. Separation was indicated on the lower wall at a location of about 6-1/4 slot heights with an injectant Mach number of 0.232, but was not detected in any of the other cases. As the injectant Mach number approached approximately 0.5 a drastic change in the development of the flow occurred with an increase in injection rate. Visual observation of the flow field indicated that at times the mixing zone as a whole became unsteady at a mass flow ratio of about 0.065, with the adjustment in the freestream occuring as a shock wave (Fig. 9c). If the mixing zone is visualized as a slip-line extending downstream from edge of the splitter plate, this line appeared to remain straight but with one end pivoted at the splitter plate and the other end oscillating several degrees to either side of the equilibrium orientation. An oil-flow test of the splitter plate surface revealed that the boundary layer was

13

separated less than .020 inch upstream of the trailing edge, so that
presumably the unsteadiness was due to alternating separation and
reattachment. The flow behavior at this particular injection rate
was extremely erratic, since it was possible to achieve both completely
steady flow with an initial injectant pressure slightly lower than the
freestream value, and also unsteady flow with a shock wave adjustment
in the freestream at the same injection rate. This is evident in
Fig. 9c, the pressure distribution corresponding to the steady case
and the photograph to the unsteady case. With a slight increase in
injection rate beyond this point, the flow appeared to develop normally
when the flow was first initiated, but after a few seconds a sudden
separation of the splitter plate boundary layer occurred. The separation
in this case always appeared stable.

It is believed that the explanation of this behavior lies
in a detailed consideration of the initial mixing between the two
streams. It is possible that the dividing streamline actually deflects
upward at first even though the mass flow ratio is low since this
initial deflection strongly depends on the profile shapes. Due to
the fact that the deflections involved are small, it is likely that
there would be some measure of sensitivity in this regard. It is
interesting to note that a complex initial adjustment was also ob-
served in Ref. 10 as the injectant Mach number approached 0.5. The
freestream Mach number in that case was 3.95; however, the initial
boundary layer was turbulent.

3.3 Supersonic Injection

Whenever the condition of injection is supersonic, it is
possible to identify three basic types of flow: overexpanded, fully-
expanded and underexpanded, corresponding to situations in which the
static pressure at the slot exit is less, equal or greater than
the static pressure of the undisturbed freestream. Fig. 10 presents
Schlieren photographs and pressure distributions for two cases of
overexpanded injection at Mach number 2.00 into a Mach 2.85 primary
flow. It is observed that the initial adjustment between the streams
occurs as a shock wave in the injectant and an expansion in the

14

freestream (with a following lip shock). The reflection of the shock wave at the wall is followed by an intersection with the mixing layer through which, in general, part of the incident wave is transmitted and part reflected. In a general case, this process of multiple reflection between the two streams progresses downstream, the type and strength of each interaction determined by the requirement of continuity of pressure and flow direction through the mixing layer. If the mixing layer is conceptually replaced by a slip-line separating two uniform supersonic streams of different Mach numbers, a simple inviscid analysis is possible for determining the pattern of these interactions (cf. Ref. 22).

The analytical solution corresponding to an inviscid flow is shown as the dashed line in each of the cases in Fig. 10. Although such a solution cannot be used to predict the detailed wall pressure distribution, it does provide excellent results for the wave pattern and overall pressure rises. For example, corresponding to the conditions in Fig. 10a, inviscid theory predicts a weak compressive reflection into the injectant from the point of the first downstre n intersection with the dividing streamline involving a pressure rise slightly greater than 1%. Although this reflection is not discernable in the photograph, its presence is nonetheless apparent in the measured pressure distribution. It can be expected that inviscid theory will provide a good description of the major features of the flow development provided the shear layer thickness and Mach number variation are not too large (in which case internal reflections in the layer are likely to become important), or that separation does not occur.

In this regard it is noted that in Fig. 10b the adjustment shock in the injectant produces separation along the lower wall which is evident both in the photograph and in the measured pressure distribution. Disturbances arising from the free-interaction between the injected stream and wall boundary layer upstream of shock-incidence propagates into the main flow through the transmitted waves which are observed just downstream of the point of injection. Similar waves are observed in Fig. 10a even though the flow remains unseparated, implying a considerable thickening of the wall boundary layer. A

15

furtner decrease in the exit pressure below that existing in Fig. 10b, eventually leads to internal separation of the flow in the injection nozzle, establishing a definite lower limit for the injection rate. On the other hand, an increase in the exit pressure results in a weakening of the adjustment waves and at a certain point the condition is reached for which the exit pressure and undistrubed freestream pressure are equal. In the ideal inviscid case this would produce a completely wave-free flow, however in an actual flow situation the finite thickness of the boundary layers and splitter plate lip cause some weak disturbances to always be present.

When the injection rate is increased beyond that corresponding to matched static pressures, the initial adjustment takes the form of a shock wave in the freestream and an expansion in the injectant with the lip shock now trailing the latter. Two examples of under-expanded flow are given in Fig. 11 for injection at Mach 1.98 into a Mach 4.19 freestream. The results of inviscid theory are again shown in Fig. 11a as the dashed line and a comparison serves to illustrate the effect of the lip shock. It is seen that this shock recompresses the flow to the inviscid level following an expansion which is larger than required by inviscid theory. Still further increases in injection rate lead to a separation of the splitter plate boundary layer as shown in Fig. 11b. It is apparent from the photograph that as the lip shock propagates through the expansion fan its strength decreases, but an appreciable adverse pressure gradient is still produced at the wall.

3.4 Foreign Gas Injection

This phase of the investigation was formulated to study the effects of using two different foreign gases as injectants with air as the external stream. Helium and carbon dioxide were chosen not only because one is a monatomic gas and the other is a diatomic gas, but because of their relative positions on the molecular weight scale when compared with air. Also, it was felt that helium would be a good simulant for the flow characteristics of hydrogen, which is of interest for the fuel injection application. The experiments consisted

16

of subsonically injecting the above gases into a Mach 2.85 freestream.

First, some streamwise static pressure distributions and Schlieren pictures will be presented for both helium and carbon dioxide injection and then a comparison of the results between the two will be discussed and compared to a special case with air as the injectant. Typical results are given for helium injection in Figs. No. 12 and 13 and for CO_2 injection in Figs. No. 14, 15 and 16. The two cases exhibit quite different distributions. In order to clarify some of these differences, a special case was run using air as the injectant at a Mach number of 0.290. Then the helium and carbon dioxide were run at the same Mach number and again at the same mass flow rate per unit area. The results are shown in Fig. 17 and 18.

Note that at the same Mach number, carbon dioxide and air exhibit almost identical pressure distributions whereas the helium is at a somewhat higher pressure and exhibits no recompression region as do the carbon dioxide and air. This may well be attributed to the fact that even though the mass flow rate of the helium is less than that of the carbon dioxide, as shown in Fig. 16, the higher static pressure of the helium at the slot exit is more than sufficient to over-come this deficit. This is also the case when the mass flow rates are matched, although the pressure distributions of the air and carbon dioxide are not then exactly the same.

An immediate consequence of this would be in the field of thermal protection and/or skin friction reduction where, for a fixed slot size and prescribed injectant Mach number or mass flow rate, one is interested in using the least amount of injectant to protect as much surface area as possible. In this case, as shown in Figs. 17 and 18, the lower molecular weight injectant; i.e., helium, would be the best choice because its protective influence is felt substantially further downstream than that of the carbon dioxide.

3.5 Interferometric Results

Examples of interferograms taken under various conditions with air injection are presented in Figs. 19 and 20. Those representing tests with a freestream Mach number of 4.19 demonstrate the restrictiveness of the small total fringe shift under low density conditions. Density profiles measured at several axial stations are given in Fig. 21 for sonic and supersonic injection into a Mach 2.85 freestream. The first profile in each case was taken near the beginning of fully turbulent mixing.

4.0 STABILITY OF THE SHEAR LAYER

Aside from purely scientific interest, the question of transition from laminar to turbulent mixing between coflowing streams is basic to applications in technological fields. Although the actual flow field under study herein is an extremely complex one, there has been a considerable amount of analytical work in the area of linear stability theory directed toward simpler but related flow problems. Specifically, these studies have been concerned with, (1) the stability with respect to infinitesimal disturbances of a plane vortex sheet between parallel streams and (2) the corresponding case of a continuous mixing layer between parallel streams.

It is well known that a vortex sheet in an inviscid incompressible fluid is unstable in an absolute sense in that any small disturbance is amplified exponentially with time (23). When the effects of viscosity are added the discontinuity is eliminated and a mixing layer is produced between the streams. The important destabilizing mechanisms, however, are still entirely inviscid ones with the viscous effects providing purely damping influences in contradistinction to problems involving flow along a wall. The theoretical results of Lessen (24) and Tatsumi-Kakutani (25) point to the exceedingly unstable nature of flows of this type, with critical Reynold's numbers based on mixing layer thickness of the order of 5.

The compressible counterparts of the cases just described are more complicated. For example, in considering incompressible flows, it is possible to deal only with two-dimensional disturbances insofar as stability boundaries are concerned since by Squire's Theorem every three-dimensional disturbance is equivalent to a two-dimensional one at a lower Reynold's number. Such a simplification is not possible in compressible flows where three-dimensional disturbances play an important role in the stability problem. In addition, one must now consider the possibility of both subsonic and supersonic disturbances, corresponding to circumstances for which phase velocity of the disturbance is less or greater than the local speed of sound.

The stability of a plane vortex sheet with respect to two-dimensional subsonic disturbances was examined by Lin (26) who found that the flow was stable if:

$$|u_1 - u_2| > a_1 + a_2 . \qquad (1)$$

19

However, if supersonic disturbances are admitted, Miles (27) showed that a more restrictive condition applied:

$$|u_1 - u_2| > (a_1^{2/3} + a_2^{2/3})^{3/2}. \tag{2}$$

This was later extended by Fejer and Miles (28) to include three-dimensional disturbances:

$$|(u_1 - u_2) \cos \emptyset| > (a_1^{2/3} + a_2^{2/3})^{3/2} \tag{3}$$

where $\emptyset$ is the angle of propagation of the disturbance with respect to the streamwise coordinate. This relation demonstrates that disturbances traveling at sufficiently obliques angles are unstable.

Similar results are found for the case of a mixing layer between uniform streams. The most recent results in this area are those of Lessen, Fox and Zien (29, 30) who found that the flow is generally unstable with respect to supersonic disturbances although the rate of amplification is less than in the subsonic category, and with three-dimensional disturbances, instability associated with the presence of subsonic disturbances exists even at very high Mach numbers.

In all of the preceding investigations, it was found that the flow became less unstable if the Mach number were increased; however, one is forced to conclude that the mixing layer between two uniform streams is generally unstable under any conditions. This discussion is quite aside from stability with respect to finite disturbances, which can lead to increased amplifications even for flows which are otherwise stable with respect to infinitesimal disturbances (31).

Now turning to an examination of the experimental results, the relative stability of tangential injection flows was studies by means of the spark Schlieren photographs already presented. In addition, the limiting case of the supersonic wall jet (quiescent "freestream") was examined in the same manner, and examples of the results are shown in Fig. 22 for various ratios of jet pressure to back pressure, P_j/P_b.

The onset of transition was gauged by the appearance of the first clearly defined disturbance in the mixing layer, and in applicable cases, the end of transition was identified by the complete dissolution of the "white line" into eddies (e.g., Figs. 6-8). It should also be noted that a considerable number of photographs were taken for each case and no large differences

20

were discerned in either location. The results of the photographic measurements for air injection are given in Fig. 22. The solid and open symbols refer to the beginning and end of transition, respectively. There are two main points of observation. First transition occurred in all cases, with those at the higher freestream Mach number appearing to have a later initiation to turbulent mixing. Second, there is seen to be a definite destabilizing trend as the injection rate is increased except in the case of the wall jet. Both of these results would certainly appear to be explicable in terms of an increase in Mach number alone, since for the injection flows the amount of initial expansion increases as the injection rate is lowered. A similar statement applies to an increase in injection rate in the case of the wall jet.

Since almost no control could be exercised over the Reynold's number of the primary flow in the present work, it is not possible to generalize about the location of transition. However, the results indicate that transition is to be expected even at Mach numbers in the high supersonic range, and that its occurrence is delayed by a Mach number increase.

The effects of foreign gas injection on the stability of the mixing layer can be seen in Figs. No. 24 and 25. The most striking effect is the greatly increased eddy size in the mixing layer for Helium injection when compared with either CO_2 or air injection. Secondly, with foreign gas injection, transition occurs at different axial locations on the top and bottom of the shear layer. Lastly, transition occurs closest to the injection station with CO_2 injection.

A point which it is appropriate to include in this section concerns the generation of "noise" in the freestream by the turbulent mixing zone. This can be observed in the spark Schlieren photographs as turbulent eddies in the freestream (e.g., Figs. 6-8). In order to assure that these disturbances were not confined to the side wall boundary layers alone, air was injected through one of the streamwise pressure taps situated near the centerline of the model. The disturbances arising from this injection were considerably distorted in passing through the free-stream turbulence. This "radiation" of turbulent energy from shear layers has also been observed in high speed wakes (32).

21

5.0 ONE-DIMENSIONAL ANALYSIS FOR SUBSONIC INJECTION

5.1 General Development

As pointed out several times previously, the initial injectant pressure and the mass flow ratio are not independent when the injected flow is subsonic. Therefore, the principal goal of this section is to analyze this dependence in as simple a manner as possible for prescribed freestream conditions and types of mixing (i.e., laminar o. turbulent).

This particular flow belongs to a general class of viscous-inviscid interaction problems which involve the coupled effects of mixing and pressure-interaction with an external stream. A pioneering study of flows in this category was published in 1952 by Crocco and Lees (33). In their formulation the flow was divided into two regions: an inner dissipative region adjacent to an inviscid external stream. The governing equations were derived in terms of suitably defined average variables in the inner portion of the flow and included a relation connecting the pressure interaction and the rate of entrainment of fluid into the dissipative layer. In order to complete the mathematical description, it was necessary to introduce several semi-empirical correlation functions, one of which related the entrainment rate to the other dependent variables. For the special case in which this relation was expressed in terms of a constant mixing coefficient, the equations of motion reduced to a single non-linear, ordinary differential equation. The most interesting feature of this equation was the existence of a critical point which fixed the initial conditions if the solution were required to pass continuously downstream through this point. The interest in flows with critical points aroused by the Crocco-Lees theory led to later refinements as embodied in Refs. 34 and 35, and recently a comprehensive discussion of the occurrence of these singularities in viscous-inviscid flows was given by Weinbaum (36).

The one-dimensional treatment of tangential injection presented in this section is closely related to the Crocco-Lees theory. The essential differences are in the choice of a control volume and in the method of handling the effects of non-uniform profiles. The control volume used in the present work consists of the region between the dividing streamline and the wall, and is shown schematically in Fig. 26. It is important to note that the shear along the dividing streamline is included in the analytical model, and

22

in effect, the flow is "viscous-driven." In the initial development of
the equations appropriate to this region, the general method used in
Ref. 37 is followed, and it will be found that again a critical point
appears.

In generating a one-dimensional system of equations it is conven-
ient to introduce the following notion of an average quantity:

$$\bar{q}(x) = \frac{1}{A(x)} \int_0^{A(x)} q(x,y)\,dy \tag{1}$$

where q is any of the dependent variables and $A(x)$ is the cross-sectional
area of the control volume per unit width. It is noted that in forming
products the average of the product of two quantities is not in general
equal to the product of the averages, the difference being known as the
covariance:

$$\overline{q_1 q_2} - \bar{q}_1\,\bar{q}_2 = \text{cov}(q_1,q_2). \tag{2}$$

The covariance is generally a function of x and clearly depends upon pro-
file shapes. In particular, it is seen that if either of the quantities
q_1, q_2 is constant the covariance is zero.

Since the boundaries of the present control volume are streamlines,
continuity requires:

$$\int_0^{A(x)} \rho u\, dy = \text{constant} \tag{3}$$

which upon averaging according to Eq. (1) becomes:

$$\frac{d}{dx}\,(A\,\overline{\rho u}) = 0. \tag{4}$$

Expanding and using the definition of the covariance this can be written
as:

$$\frac{1}{\bar\rho}\frac{\overline{d\rho}}{dx} + \frac{1}{\bar u}\frac{\overline{du}}{dx} + \frac{1}{A}\frac{dA}{dx}\left(1 + \frac{k_1}{\bar\rho\,\bar u}\right) + \frac{1}{\bar\rho\,\bar u}\frac{dk_1}{dx} = 0 \tag{5}$$

where

$$k_1 = \text{cov}\,(\rho,u).$$

23

The averaging process is applied to the equation of state in the same manner, so that:

$$\overline{T} = \frac{1}{R} \left[\frac{\overline{p}}{\overline{\rho}} + \text{cov} \left(p, \frac{1}{\rho} \right) \right]. \tag{6}$$

However, if we restrict consideration to "boundary layer-type" flows the pressure profile is uniform and the covariance term vanishes, i.e.,

$$p = \overline{\rho} \, R\overline{T}. \tag{7}$$

Returning to Fig. 26, it can be seen that the x-momentum equation can be written in the form:

$$\frac{d}{dx} \left(A \, \overline{\rho u^2} \right) = -A \frac{dp}{dx} + \tau_d - \tau_w \tag{8}$$

where the small difference between the direction of the dividing stream-line and the x-axis is ignored in accordance with the boundary layer approximations. These approximations also preclude consideration of the y-momentum equation. Upon averaging, Eq. (8) becomes:

$$\gamma \frac{\overline{dM^2}}{dx} = \frac{-\overline{(1+\gamma M^2)}}{p} \frac{dp}{dx} - \frac{\overline{\gamma M^2}}{A} \frac{dA}{dx} + \frac{\tau_d - \tau_w}{pA}. \tag{9}$$

In deriving the energy equation, it is presumed that the wall is adiabatic and that the initial total temperature profile across both streams is uniform. It is not necessary to invoke these conditions in general, but they comply closely to the present experimental situation. If in addition it is asserted that the appropriate Prandtl number (i.e., laminar or turbulent) is unity throughout then under these circumstances the profile remains uniform. From the standpoint of the control volume under consideration here, this implies that the shear work generated along the dividing streamline is exactly counterbalanced by the outward heat transfer. Therefore at any point in the flow the following relation holds:

$$T\left(1+\frac{\gamma-1}{2} M^2\right) = T_t = \text{constant}. \tag{10}$$

Averaging in the usual manner gives:

$$T_t = \overline{T}\left(k_0 + \frac{\gamma-1}{2} \overline{M^2}\right) \tag{11}$$

24

where

$$k_2 = 1 - \frac{\gamma-1}{2} \frac{cov(\rho,u^2)}{\gamma p} .$$

In order to relate the average Mach number, velocity, and temperature the following equation arising from the definition of Mach number is used:

$$\frac{1}{\overline{M^2} - k_3} \cdot \frac{d}{dx}(\overline{M^2} - k_3) = \frac{2}{\overline{u}} \frac{d\overline{u}}{dx} - \frac{1}{\overline{T}} \frac{d\overline{T}}{dx} \tag{12}$$

where

$$k_3 = \frac{1}{\gamma p}\left[cov(\rho,u^2) + \overline{\rho}\, cov(u,u)\right].$$

Combining Eqs. (5), (7), (9), (11) and (12) yields:

$$\frac{d\overline{M^2}}{dx} = \frac{-(1+\gamma\overline{M^2})}{\gamma}\left\{ -\frac{1}{2}\left[\frac{1}{(\overline{M^2}-k_3)}\frac{d}{dx}(\overline{M^2}-k_3) + \frac{1}{(k_2 + \frac{\gamma-1}{2}\overline{M^2})}\frac{d}{dx}(k_2 + \frac{\gamma-1}{2}\overline{M^2})\right] \right.$$

$$\left. + \frac{1}{A}(1 + \frac{k_3}{\overline{\rho}\,\overline{u}})\frac{dA}{dx} + \frac{1}{\overline{\rho}\,\overline{u}}\frac{dk_3}{dx}\right\} - \frac{\overline{M^2}}{A}\frac{dA}{dx} + \frac{\tau_d - \tau_w}{\gamma p A} . \tag{13}$$

The covariance terms have been carried to this point in the derivation in order to demonstrate from a one-dimensional perspective the influence of profile shape. However, these terms cannot be evaluated beforehand, and to proceed further would require the assumption of a family of profiles or some other approximate means for specification of the covariance. However, it is reasonable to expect that actual profiles which are not severely distorted would lead to relatively small covariance terms, and therefore a substantial simplification in the analysis could be effected by setting them equal to zero. When this is done, Eq. (13) becomes:

$$\frac{dM^2}{dx} = \frac{-2M^2 (1+\frac{\gamma-1}{2}M^2)}{1 - M^2}\left[\frac{1}{A}\frac{dA}{dx} + \frac{\tau_d - \tau_w}{Ap}\right] \tag{14}$$

where the bar has been dropped and average quantities are understood. It is seen that similar to the case of Crocco-Lees, Eq. (14) has a singularity at M=1, and the nature of this point will be discussed in detail later

25

in this section. It is also noted that in neglecting shape effects,
the governing equations reduce to the familiar ones for strictly one-
dimensional flow which are thoroughly treated in Ref. 38. For completeness
these are given below in integrated form with respect to conditions at the
critical point ($M = 1$):

$$\frac{p^*}{p} = \frac{A}{A^*} M \left[\frac{2}{\gamma+1} \left(1 + \frac{\gamma-1}{2} M^2 \right) \right]^{1/2}$$

$$\frac{u}{u^*} = M \left(\frac{T}{T^*} \right)^{1/2}$$

$$\frac{\rho^*}{\rho} = \frac{p^*}{p} \frac{T}{T^*} \tag{15}$$

$$\frac{T^*}{T} = \frac{2}{\gamma+1} \left(1 + \frac{\gamma-1}{2} M^2 \right)$$

$$\frac{P_t}{P_t^*} = \frac{p}{p^*} \left[\frac{2}{\gamma+1} \left(1 + \frac{\gamma-1}{2} M^2 \right) \right]^{\frac{\gamma}{\gamma-1}} .$$

5.2 Interaction With the Outer Flow

One of the important characteristics of this flow, and one which
must be accounted for in a physically reasonable analysis, is the pressure-
interaction between the primary and injected streams. This arises from
the fact that area changes occurring in the inner flow produce corres-
ponding changes in direction in the external supersonic flow, resulting
in significant pressure variations. For situations in which the stream-
line curvature is not extreme, this pressure change is at the same time
impressed on the inner region.

In the present case, the following approximate relation is asserted
between the change of flow direction for the inviscid streamline at the
outer edge of the mixing layer and the curvature of the dividing stream
line:

$$\frac{d\theta_e}{dx} \doteq \frac{d^2 A}{dx^2} \tag{16}$$

This is reasonable for small turning angles and thin mixing layers, and

26

in any case reflects the desired connection between inner and outer flows.

A pressure-area relation can now be obtained by the use of the Prandtl-Meyer simple-wave equation:

$$\frac{1}{p}\frac{dp}{dx} \doteq \frac{\gamma M_e^2}{\sqrt{M_e^2 - 1}} \frac{d^2 A}{dx^2} \ . \tag{17}$$

The edge Mach number, M_e, is in general a function of the streamwise coordinate, but in order to preserve the simplicity of the analysis Eq. (17) is linearized by replacing M_e with the undisturbed freestream Mach number, M_1.

A second pressure-area relation for the inner flow is obtained by combining the one-dimensional continuity and energy equations and the equation of state. The results are:

$$\frac{1}{p}\frac{dp}{dx} = -\frac{1}{2}\frac{1}{M^2}\frac{dM^2}{dx}\left[\frac{1+(\gamma-1)M^2}{1+\frac{\gamma-1}{2}M^2}\right] - \frac{1}{A}\frac{dA}{dx} \ . \tag{18}$$

Equating Eqs. (17) and (18) and integrating between the critical point and an arbitrary streamwise station leads to:

$$\frac{dA}{dx} = \left(\frac{dA}{dx}\right)^* \frac{\sqrt{M_1^2-1}}{\gamma M_1^2}\ \ln\frac{A}{A^*}\ M\left[\frac{2(1+\frac{\gamma-1}{2}M^2)}{\gamma+1}\right]^{1/2} \ . \tag{19}$$

This equation expresses the functional connection between area and Mach number necessary to assure matching pressure along the dividing stream-line for the assumed interaction relation (Eq. (17)), and is to be used in conjunction with Eq. (14). Specification of the shear term in Eq. (14) closes the system mathematically with two equations relating two unknowns, area and Mach number.

5.3 Evaluation of the Shear Term

An entirely satisfactory specification of the shear term in Eq. (14) would again require a detailed study of the development of velocity and temperature profiles. Of course, if this were to be done there would be little point in adopting the present one-dimensional approach. Accordingly, a simple specification of the shear is made by means of the relation

$$\tau_d = k(u_e - u(x)) \tag{20}$$

where u_e is the edge velocity (assumed constant in the present analysis)

27

and $u(x)$ is the average velocity of the inner flow. In this form, k has the units of viscosity/length, and obtaining an approximation of its value for laminar and turbulent mixing is considered below. As an additional simplification, the wall shear is neglected in comparison with the shear along the dividing streamline, so that $\tau \equiv \tau_d - \tau_w \doteq \tau_d$.

For laminar mixing k has been approximated by $\bar{\mu}/\delta_0$, where $\bar{\mu}$ is the average viscosity across the layer and δ_0 is the initial splitter plate boundary layer thickness. Additionally, in view of the fact that deflections of the dividing streamline are typically small in laminar flow, the ratio τ/p was taken as nearly equal to τ/p_1. In this case, the shear term in Eq. (14) becomes:

$$\frac{\tau}{p} \doteq \frac{\gamma R T_t}{P_{te}} \left(1 + \frac{\gamma-1}{2} M_e^2\right)^{\frac{\gamma}{\gamma-1}} \frac{\bar{\mu}}{\delta_0} \left[\left(\frac{M_e^2}{1 + \frac{\gamma-1}{2} M_e^2}\right)^{1/2} - \left(\frac{M^2}{1 + \frac{\gamma-1}{2} M^2}\right)^{1/2} \right]. \quad (21)$$

Such a straightforward approximating procedure is not possible in situations involving turbulent mixing since the apparent, or eddy, viscosity coefficient depends on the variables of the mean flow. In order to develop a simple expression for the eddy viscosity, use was made of a model adopted in Ref. 39 wherein the low-speed form for wakes and jets proposed by Prandtl was extended to include compressible flows. Specifically, the low-speed form

$$\epsilon = Kb(u_{max} - u_{min}) \quad (22)$$

was generalized to

$$\rho\epsilon = kb(\rho_e u_e - \rho_j u_j) \quad (23)$$

as originally proposed by Ferri (40), where b is the mixing width.

Equation (23) is appropriate for the free-mixing region between streams of constant velocities u_e and u_j and therefore cannot be justifiably extended into the recompression region in which the mixing layer begins to approach the lower wall. Therefore, in the present work Eq. (22) was further modified to

$$\rho\epsilon = Kb(\rho_e u_e - \rho u) \quad (24)$$

where ρ and u refer to average values of the inner flow. In the free-mixing region ρu does not differ greatly from $\rho_j u_j$, and in the recompression zone Eq. (24) can be somewhat justified in that it involves the average of local conditions. In any case, the formulation is consistent with the level of approximation in the analysis.

28

In free-mixing flows, the mixing width b is proportional to x, i.e., $b = mx$, where for low-speed coflowing streams

$$m = c\lambda. \tag{25}$$

c is an empirical constant in the range 0.2 to 0.3 (cf. Ref. 41) and

$$\lambda = \frac{u_{max} - u_{min}}{u_{max} + u_{min}}. \tag{26}$$

In the classical treatment m, K and λ are combined into a spread parameter defined by

$$\sigma^2 = \frac{1}{4Km\lambda} = \frac{1}{4Kc\lambda^2}. \tag{27}$$

According to Sabin (42)

$$\sigma = 13.5/\lambda. \tag{28}$$

Taking $c = 0.25$ and solving for K between Eqs. (25), (27) and (28) leads to a value of 0.0055. This result is based on low-speed free-mixing arguments but is carried over to the present case in the spirit of Eqs. (23) and (24). However, K must in general be considered a purely empirical quantity to be adjusted to provide the best correspondence with the experiments. However, as will be seen later, the low-speed value yielded good agreement with the experiments without adjustment in the present work.

Returning to the central problem of approximating the shear term for turbulent mixing, this term can now be written as

$$\frac{\tau}{\rho} = \frac{\rho\epsilon}{\rho}\left(\frac{u_e - u}{b}\right) = \frac{K}{RT}\left(u_e\frac{T}{T_e} - u\right)(u_e - u) \tag{29}$$

where again b is the mixing width. Further rearranging leads to

$$\frac{\tau}{\rho} = K\gamma\left[M_e\left(1 + \frac{\gamma-1}{2}M_e^2\right)^{1/2} - M\left(1 + \frac{\gamma-1}{2}M^2\right)^{1/2}\right]\left[\left(\frac{M_e^2}{1 + \frac{\gamma-1}{2}M_e^2}\right)^{1/2} - \left(\frac{M^2}{1 + \frac{\gamma-1}{2}M^2}\right)^{1/2}\right] \tag{30}$$

with K taken equal to 0.0055.

The only variable appearing in Eqs. (21) and (30) is the Mach number of the inner flow since in the present treatment M_e is approximated by M_i; therefor, when non-dimensionalized in terms of conditions at the critical point, Eqs. (14) and (19) constitute a system of two non-linear ordinary differential equations for the Mach number and area ratio. However, due to the existence

29

of the singular point in Eq. (14) these equations are not easily integrated from given initial conditions.

This is discussed in the following section.

5.4 Nature of the Critical Point

Before proceeding, it is helpful to briefly re-examine the problem at hand. Figure 27 illustrates the approximations made in the development of the analytical model to this point. The important features found in the actual flow, that is, the mixing and pressure-interaction between streams, have been retained but with liberal simplifications which permit the flow beneath the dividing streamline to be described in terms of ordinary differential equations. However, the experimental results also indicate that arbitrary initial conditions are not possible, and therefore a physically realistic analytical model must reflect this behavior. This is, in fact, found within the present formulation, the initial conditions being fixed by the necessity of satisfying certain conditions at the critical point.

As in cases of one-dimensional isentropic channel flow, Fanno flow, etc., it is convenient to non-dimensionalize the variables with respect to conditions at the critical point. If we take

$$h = A/A^*$$
$$x \rightarrow x/A^*$$

then Eqs. (14) and (19) become

$$\frac{dM^2}{dx} = \frac{2M^2 \left(1 + \frac{\gamma-1}{2} M^2\right)}{h(1-M^2)} \left[\frac{dh}{dx} + \frac{\tau}{p}\right] \tag{31}$$

$$\frac{dh}{dx} = \left(\frac{dh}{dx}\right)^* - \frac{\sqrt{M_1^2 - 1}}{\gamma M_1^2} \ln \left[hM \frac{2\left(1 + \frac{\gamma-1}{2} M^2\right)}{\gamma+1}\right]. \tag{32}$$

It is clear from a consideration of Eq. (31) that unless the condition $M=1$ and the vanishing of the bracketed factor occur simultaneously, the flow cannot pass continuously through the critical point and the Mach number gradient becomes infinite. Thus, for a physically possible flow it is necessary that

$$\left(\frac{dh}{dx}\right)^* = -\left(\frac{\tau}{p}\right)^*. \tag{33}$$

30

One can imagine a procedure of specifying trial initial values for Eqs.
(31) and (32) and repeatedly integrating the system until a set is found
for which Eq. (33) is satisfied. However, it is preferable to begin the
integration at the critical point where the starting values are h = M = 1
and carry the solution both upstream and downstream from there. Since Eq.
(31) is indeterminate at this point it must be evaluated by means of l'Hospital's
rule. The value for $(dM^2/dx)^*$ thus obtained together with $(dh/dx)^*$ from Eq. (33)
permits a first integration step to be taken, and thereafter Eqs. (31) and (32)
can be used directly.

For laminar mixing the derivatives at the critical point are given
by:

$$\left(\frac{dh}{dx}\right)^* = c_\ell \left[\left(\frac{M_e^2}{1+\frac{\gamma-1}{2}M_e^2}\right)^{1/2} - \left(\frac{2}{\gamma+1}\right)^{1/2} \right] \tag{34}$$

$$\left(\frac{dM^2}{dx}\right)^* = \frac{1}{2}\left\{ -\left[\frac{\sqrt{M_e^2-1}}{M_e^2} + \frac{2}{\gamma+1}c_\ell\right] \right.$$

$$\left. + \left[\left(\frac{\sqrt{M_e^2-1}}{M_e^2} + \sqrt{\frac{2}{\gamma+1}}c_\ell\right)^2 - 4\left(\frac{\gamma+1}{\gamma}\right)\frac{\sqrt{M_e^2-1}}{M_e^2}\left(\frac{dh}{dx}\right)^*\right]^{1/2} \right\} \tag{35}$$

where

$$c_\ell = \frac{\sqrt{\gamma R T_t}}{P_{te}}\left(1+\frac{\gamma-1}{2}M_e^2\right)^{\frac{\gamma}{\gamma-1}}\frac{\bar{\mu}}{\delta_o}$$

and for turbulent mixing by

$$\left(\frac{dh}{dx}\right)^* = -\gamma K\left[M_e\left(1+\frac{\gamma-1}{2}M_e^2\right)^{1/2} - \left(\frac{\gamma+1}{2}\right)^{1/2}\right]\left[\left(\frac{M_e^2}{1+\frac{\gamma-1}{2}M_e^2}\right)^{1/2} - \left(\frac{2}{\gamma+1}\right)^{1/2}\right] \tag{36}$$

$$\left(\frac{dM^2}{dx}\right)^* = \frac{1}{2}\left\{-\left[\frac{\sqrt{M_e^2-1}}{M_e^2} - \bar{\gamma}+1)c_t\left(\frac{dh}{dx}\right)^*\right]\right.$$

$$\left. + \left[\left(\frac{M_e^2-1}{M_e^2} - (\gamma+1)c_t\left(\frac{dh}{dx}\right)^*\right)^2 - 4\left(\frac{\gamma-1}{\gamma}\right)\frac{\sqrt{M_e^2-1}}{M_e^2}\left(\frac{dh}{dx}\right)^*\right]^{1/2}\right\} \tag{37}$$

where

$$c_t = \frac{\frac{\gamma}{2}\left(\frac{2}{\gamma+1}\right)^{1/2}}{M_e\left(1+\frac{\gamma-1}{2}M_e^2\right)^{1/2} - \left(\frac{\gamma+1}{2}\right)^{1/2}} + \frac{\left(\frac{2}{\gamma+1}\right)^{1/2}\left(\frac{1}{\gamma+1}\right)}{\left(\frac{M_e^2}{1+\frac{\gamma-1}{2}M_e^2}\right)^{1/2} - \left(\frac{2}{\gamma+1}\right)^{1/2}} .$$

31

It is seen that $\left(\dfrac{dM^2}{dx}\right)^*$ is double-valued, and the proper branch in the present situation requires the choice of the positive square root in Eqs. (35) and (37).

Equations (33) and (34)-(37) indicate that conditions at the critical point depend directly on the value of the shear term. This suggests that subsonic tangential injection flows can be classified into laminar, transitional and turbulent categories analogous to the classifications mentioned in Section II-A for separated flows. The points of separation and reattachment in the latter case then have their analogs in the point of injection and the critical point. It should also be mentioned that a comparison of Eqs. (31) and (13) indicates that critical point conditions are likely to be significantly different for flows in which the covariance terms are important.

5.5 Comparison with Experiments

Equations (31) and (32) were integrated numerically using a standard computer program for systems of ordinary differential equations developed in Ref. 43. The other flow variables were computed using Eqs. (15).

Typical results for turbulent mixing and a freestream Mach number of 2.85 are shown in Figs. 28 and 29. Due to the manner in which the equations were posed, these curves represent the solution for all possible cases of subsonic injection for the given external Mach number. As in other one-dimensional flows involving singularities, the physical dimensions are scaled in terms of the area at the critical point. Of course, in a particular problem the actual magnitude of this area depends upon the slot height and the initial Mach number (or equivalently, mass f'w rate).

The information of central interest is the dependence of the initial injectant pressure on either the mass flow ratio or the initial injectant Mach number. The analytical results are compared with those from the experiments in Figs. 30 and 31. The laminar shear term was used in the calculations for the Mach 4.19 cases, and the turbulent term for those at Mach 2.85. It is noted that the results agree well with the experimental data.

The fact that the laminar results show poorer agreement at low injection rates can very likely be attributed to the limitations of the experimental measurements in this regime. For instance, the difference between the injectant total and static pressures was of the order of 0.1 mm. in this range, which is near the accuracy limit of the manometer system. This, coupled with the problems associated with the asymptotic approach of the

32

measurements to the true pressure probably resulted in recording a higher Mach number than was actually the case.

Although in order to better show the trend of the experiments plotted points are presented for flow without injection, the analysis is not valid in this limit. In addition, it is emphasized that it was not necessary to adjust the empirical constants in the analysis to achieve the indicated correspondence with the experimental data.

The effect of neglecting profile shapes in the analysis is demonstrated in Figs. 32 and 33. The first presents comparisons with experimental results for the streamwise pressure distributions, and the second, the corresponding dividing streamline trajectories. For the Mach 2.85 test, it is seen that the analysis predicts a continuously increasing pressure in contrast to the sharp rise actually found. This is evident also in the concave-outward shape of the dividing streamline (Fig. 33), and both results can be primarily attributed to the fact that $\overline{\rho u}$ is not equal to $\overline{\rho}\,\overline{u}$. In the test at Mach 4.19, with less rapid mixing, the effects are less pronounced.

An attempt was made to effect a comparison of the one-dimensional analysis to the experimental results of Refs. 9, 10 and 11 which involved very thick splitter plates. The agreement in these cases was not entirely satisfactory. For example, the experiments in Ref. 9 covered a range of about 0.12 to 0.54 in injectant Mach number and were performed with a freestream Mach number of 3.01 and a ratio of splitter plate thickness to slot height of about 0.3. At the higher injection rate the initial injectant pressure differed from that obtained with the one-dimensional analysis by only about 1%; however, there was a steady worsening of the correspondence as the injection rate was lowered, so that at the lowest rate the predicted pressure was nearly 40% too low. This indicates the important influence of the splitter plate thickness in controlling the initial adjustment between streams.

33

6.0 FLOWS WITH SURFACE TURNING

6.1 Flow over Wedges without Injection

In order to better adjudge the effect of injection in flows involving a wall turn, it is helpful to consider the more familiar situation without injection. The flow of a Mach 2.85 freestream over wedges with turning angles between 0 and 25 degrees was studied by means of spark Schlieren photographs, shown in Fig. 34. The wedges were situated at the same streamwise location used in most of the injection studies (i.e., about 9 slot-heights downstream of injection), and the arrow in the uppermost photograph indicates the position corresponding to the injection station. The Reynolds number based on freestream conditions and the distance from the primary nozzle throat to the wedge location was 2.15 × 10^6 for these tests.

Transition is noted at a streamwise location near the injection station and the boundary layer becomes fully turbulent before reaching the wedge position. A slight "bridging" separation first occurs at a turning angle of 20 degrees, the pressure ratio across the shock wave being about 3.78. The pressure ratio at 15 degrees, for which separation does not occur, is about 2.71. Since an interpolation of data from Ref. 18 for the pressure ratio at turbulent separation for flat plate-mounted models gives a value of 2.07 (i.e., about a 10^0 turning angle) it is seen that the pressure rise which can be negotiated with the present experimental arrangement is higher than on a conventional flat plate apparatus. In the latter case, the history of the boundary layer development is significantly different than in the present work. At a turning angle of 25 degrees a full separation in front of the wedge occurs, followed by an intermittent reattachment.

At this point it is helpful to review briefly some aspects of the pressure distributions representative of laminar, transitional and turbulent separation in front of wedges. A more complete description can be found in Ref. 18. In the case of pure-laminar flows, an initial pressure rise leading to separation is followed by a plateau of nearly constant pressure, indicative of the "dead air" in the separated region. Reattachment on the wedge surface is generally accompanied by an abrupt pressure rise. The pressure distribution is only mildly influenced by a variation in Reynold's

number provided completely laminar flow remains between separation and reattachment. A variation in Mach number produces a qualitatively similar distribution with the principal changes exhibited in the overall pressure levels and a slight influence on the streamwise extent of separation.

The pressure rise to separation is about the same for transitional separations as for those in the laminar regime. However, the most distinctive feature found in these flows is the correlation between the location of transition and a sharp rise in the pressure distribution before reattachment. Transitional flows are markedly affected by changes in Reynold's number when transition is relatively near reattachment. In addition, the effect of increasing the Mach number is to move the location of transition closer to reattachment, possibly resulting in a large variation in the pressure distribution.

In the case of turbulent flows, the pressure rise to separation is much higher and the streamwise extent of separated flow much smaller than in the other cases. The pressure distribution begins to level off after separation, but because of the substantial velocities in the separated region, a plateau is not generally observed. Again, at reattachment there is an abrupt pressure rise. Turbulent separations are affected only to a small extent by variations in Reynold's number, but the peak pressure levels are greatly influenced by variations in Mach number.

6.2 Flow over Wedges with Injection

Turning consideration now to flows with injection, it was observed that the nature of the wall pressure distribution could be classified in much the same manner as those without injection with regard to whether the separation of the injectant boundary layer in front of the wedge was laminar, transitional or turbulent. In fact, the class of separation on the lower wall was found to be of major significance in determining the overall structure of the flow field. Spark Schlieren photographs and pressure distributions are shown in Fig. 35 for flows with turning angles of 10 and 15 degrees. The freestream Mach number in these cases was 2.85 and the mass flow ratio was about equal to 0.22, which in the absence of the wedges produced choked flow at the slot exit. It is apparent that transition in the separated injectant boundary layer (identified by the diffusion of the white line adjacent to the surface and denoted in the figure by the symbol "t") is closely correlated with a sharp increase in pressure. The figure also reveals

35

the importance of the interaction between the streams in these cases, with the turning of the main flow beginning just downstream of the separation point. Oil-flow studies indicated that in Fig. 35a re-attachment may have occurred in front of the wedge since a second oil accumulation was observed at a location about 6-1/2 slot-heights from the injection station. Reattachment followed by another separation has been observed in the transitional regime for the case of forward-facing steps in subsonic flows (cf. Ref. 18).

A somewhat different situation was found with subsonic injection into a freestream at Mach 4.19. Several results of these tests are given in Fig. 36 for flow over 5 and 10 degree wedges at a mass flow ratio of 0.04, and over a 5 degree wedge with a mass flow ratio of 0.06. Surface flow studies failed to give indication of separation in any of these cases, but the pressure distributions tend to show that separation did occur in those represented by Figs. 36b and 36c. The interesting feature of the results is the lack of any appreciable interaction between the streams in the region in front of the wedge. However, the presence of the wedge produced a significant change in the initial adjustment between the streams. Figure 37 serves to show that at a fixed injection rate, an in-crease in the turning angle raised the pressure at the injection station, eventually leading to a separation of the splitter plate boundary layer for the tests at Mach 4.19.

Perhaps the most evincive evidence supporting the importance of the class of lower-wall separation in injection-wedge flows was found in the supersonic injection experiments. Figures 38, 39 and 40 a and b present results for injection at Mach 2.00 into a freestream at Mach 2.85. This series of tests covered a range of 5 to 25 degrees in turning angle with the wedges mounted either 4-3/4 or 9 slot-heights from the point of injection. The separations are observed to fall into the transitional catagory in all cases, exhibiting the characteristic increase in the pressure distribution. At a turning angle of 25 degrees separation occurred internally in the injection nozzle. It can be seen in the photographs that considerable interaction between the streams occurs after separation, particularly at the higher wedge angles. This is also indicated by the fact that the pressure level just in front of the wedge is higher than would be anticipated for transitional separation in a Mach 2.00 stream.

A very different flow situation is seen in Figs. 40c,d, 41 and 42 for

36

injection at Mach 1.98 into a Mach 4.19 freestream over about the same range of turning angle. The lower-wall separation is pure-laminar with the plateau pressure typical of this category apparent in the measured distribution. It is also clear that the streamwise extent of separation is much greater in these cases. In this connection it is noted that in Fig. 41b and c an increase of about 50% in injection rate produces only a very slight change in the location of separation.

Viewing the results as a whole, the following picture can be inferred for injection over wedges in supersonic flow: the separation characteristics and wall pressure distribution are determined by the nature of the wall boundary layer, and can be grouped into laminar, transitional, and turbulent categories. Beyond separation, the interaction between streams wherein the inner flow begins to turn the outer flow determines the magnitude of the overall pressure rise. This view of the flow field has some significance in regard to applications in practical devices. For example, one of the limitations met in considering the use of slot injection to prevent or reduce separation is the apparent need to inject at a higher kinetic energy than that of the freestream. At high flight Mach numbers this quickly becomes impractical. The present results lead to speculation that under certain circumstances this limitation is not as great as previously thought if the character of the injectant boundary layer is controlled. Thus, under flight conditions that would produce a laminar separation in the freestream, it is likely that the extent of separation could be altered by injecting at a substantially lower Mach number if the injectant boundary layer were made turbulent. Under these conditions, the value of the injectant Mach number would be determined primarily by the need of the turbulent boundary layer to negotiate the expected overall pressure rise generated in the freestream. That this is a significant reduction in injection requirements can be shown by a rough estimate of the effect on a laminar separation caused by a 5 degree turn in a Mach 10 freestream. Under these conditions injection at a Mach number of somewhat less than 3 would be necessary if the injectant boundary layer were tripped, implying a total pressure ratio, P_{t_j}/P_{t_1}, of only 0.00036 for fully-expanded injection. It should be noted, however, that as the injectant Mach number is increased it becomes more difficult to induce a turbulent boundary layer, particularly at the low Reynold's numbers anticipated.

37

in addition, supersonic injection flows leading to a laminar separation in front of wedges are considered to offer some benefits in the area of thermal protection. These separations are observed to be stable and the present results seem to indicate that they are effective in turning the outer flow efficiently. This leads to a gradual deceieration of the main flow along a fluid interface rather than along the surface.

6.3 Analysis

In this section, we treat the extension of the analysis e :loped in Sect. 5 to cases with surface turning of the lower wall. The work remains, of course, limited to those situations where separation does not occur. There are two basic cases which are differentiated by whether the surface turning begins before or after the critical point. If the turning only begins after the critical point, it is in an all-supersonic region and does not effect the initiai injectant conditions. On the other hand, surface turning before the criticai point can have a profound effect upon the initial conditions and this is the case of interest here.

The inclusion of lower wall turning in the analysis is straight forward and can be easily described by referring to the development and equations for the simpler case in Sect. 5.0. Equ. (i4) remains unchanged since the flow is one-dimensional. The important contribution of surface turning is as an additive term in the expression for the change in flow direction of the inviscid streamline at the edge of the mixing layer. Thus, Equ. (16) is replaced by:

$$\frac{d\theta_e}{dx} = \frac{d^2A}{dx^2} + \frac{d\theta_w}{dx} \qquad (16a)$$

where θ_w is the local angle that the lower wall makes with the initial flow direction. Accordingly, Equ. (17) is replaced by:

$$\frac{1}{p}\frac{d\rho}{dx} = \frac{\gamma M_e^2}{\sqrt{M_e^2-1}}\left[\frac{d^2A}{dx^2} + \frac{d\theta_w}{dx}\right] \qquad (17a)$$

Combining this with Equ. (18) in the same way as before, a new version of Equ. (19) emerges

$$\frac{dA}{dx} = \frac{dA^*}{dx} - \frac{\sqrt{M^2-1}}{\gamma M^2}\ln\left\{\frac{A}{A^*}M\left[\frac{2(1+\frac{\gamma-1}{2}M^2)}{\gamma+1}\right]^{1/2}\right\} - \frac{dy_w}{dx} + (\frac{dy_w}{dx})^* \qquad (19a)$$

38

In the special case of a simple wedge surface turn (dy_w/dx) is a constant so that Equ. (19a) reduces to the same form as Equ. (19). The pressure at the critical point will, however, differ from that without turning by an amount proportional to (dy_w/dx) as can be seen from Equ. 17a).

A calculation for a particular case with a wedge turn is given in Fig. No. 43 in terms of the wall static pressure distribution. The injected flow is sonic but becomes subsonic immediately downstream due to the wedge. The average Mach number becomes sonic about 5 1/2 slot heights downstream. The pressure distribution for the same case without the wedge is also shown. One can see that the wedge induces a severe adverse pressure gradient in spite of the fact that the injectant flow is not supersonic and the stream tube area is locally decreasing.

6.4 Initial Boundary Layer Profile Effects

To this point, all the experimental results have been for cases where the initial boundary layer on the outside of the splitter plate was that which developed naturally by travelling along the upper tunnel (see Fig. 2a). This layer was laminar but approaching transition. The boundary layer profile obtained by interferometric measurement is shown in Fig. 44. As mentioned under the discussion of the flow past surface wedges without injection, this layer had traversed a strong favorable pressure gradient as the main supersonic flow developed along the nozzle and hence it was able to withstand a greater pressure rise to separation than that for a constant pressure case.

The utility of slot injection in energizing the wall region of a "near separation" profile in order to enable it to sustain a further pressure rise without separation cannot be tested with an initial boundary layer of the type described above. Efforts were, therefore, made to artificially generate a near separation profile at the injection station.

The first attempt involved the placement of a drag strut in the initial boundary layer upstream of the injection station as shown in Fig. 45a. The purpose of this strut is to remove momentum from the wall region of the natural profile. The effect produced on the flow over a solid rearward facing step at Mach 2.85 is shown in Fig. 45 b,c. This is to be compared with Fig. 5a for the case with the natural initial boundary layer. Experiments were then performed with surface wedges downstream without slot injection. Results for a 20° wedge located 1" and 2" downstream of the injection station

39

are shown in Fig. 46 a,b. These are to be compared with the picture in Fig. 34 for the 20° wedge. The clear result is that the placement of a relatively large drag body in the initial boundary layer with the complicated flow interaction around it had no net effect on the pressure rise capability of the boundary layer! One can note that the size and appearance of the boundary layer at the injection station with or without the upstream strut are indistinguishable. It is felt that the result is similar to that observed on inlets with boundary layer "bridging." In that case, a boundary layer is observed to separate after negotiating some distance of adverse pressure gradient; it then reattaches to the surface and is able to negotiate a further pressure gradient without separation.

On the basis of these results, an alternative arrangement was conceived and constructed. This configuration is shown in Fig. 47. The injection slot is divided into two passages with the dividing surface contoured to provide different Mach numbers in each passage at the exit. The smaller passage nearest the free stream is constructed to provide a low subsonic Mach number. The flow of the free stream boundary layer and that issuing from the smaller slot are viewed together as the initial "outer" boundary layer profile for the inner channel injection which is at Mach 2.0. Preliminary results at Mach 2.85 are shown in Fig. 48 with extensive throttling in the subsonic passage.

7.0 CONCLUSIONS

An evaluation of the results presented in the previous
sections leads to the following principal conclusions, considered
valid in cases for which the splitter plate boundary layer and
lip thicknesses are small compared to the overall slot height.

(1) For subsonic injection flows, the Mach number and
pressure for a given area and mass flow rate are fixed by the
interaction due to the mixing between streams. A simple one-
dimensional description of this flow field exhibits a critical point
which serves to determine conditions at the injection station,
and leads to a good qualitative and quantitative agreement with
experimental results.

(2) Supersonic injection flows are classifiable into
overexpanded, fully-expanded and underexpanded categories, and
inviscid theory provides a satisfactory means of determining the
wave patterns and overall pressure rises. Underexpanded flows show a
distinctive overexpansion with the recompression through a lip
shock producing a significant adverse pressure gradient along
the lower wall.

(3) In the case of injection over wedge surfaces,
the separation characteristics and wall pressure distributions are
determined by the nature of the injectant boundary layer and can be
grouped into the familiar laminar, transitional and turbulent categories.
Beyond separation, the interaction between streams resulting in a
turning of the outer flow determines the magnitude of the overall
pressure rise.

(4) The profile shape of the boundary layer on the free stream
side of the splitter plate has a strong influence on the development
of the flow field.

41

(5) With regard to the transition from laminar to turbulent mixing increasing the injection rate is destabilizing, but this is probably due to a decrease in the initial amount of expansion in the outer flow. Transition is considered likely to occur even at high supersonic Mach numbers, but a Mach number increase delays its appearance.

(6) Two distinct initial shear flows with different transition points are present when an unlike gas is used as the injectant.

(7) The scale of the turbulence in the mixing region is increased for a low molecular weight injectant.

(8) For a given injectant Mach number or mass flow rate, the lower molecular weight injectant, i.e. helium, provides substantially more protection of the wall region than does carbon dioxide.
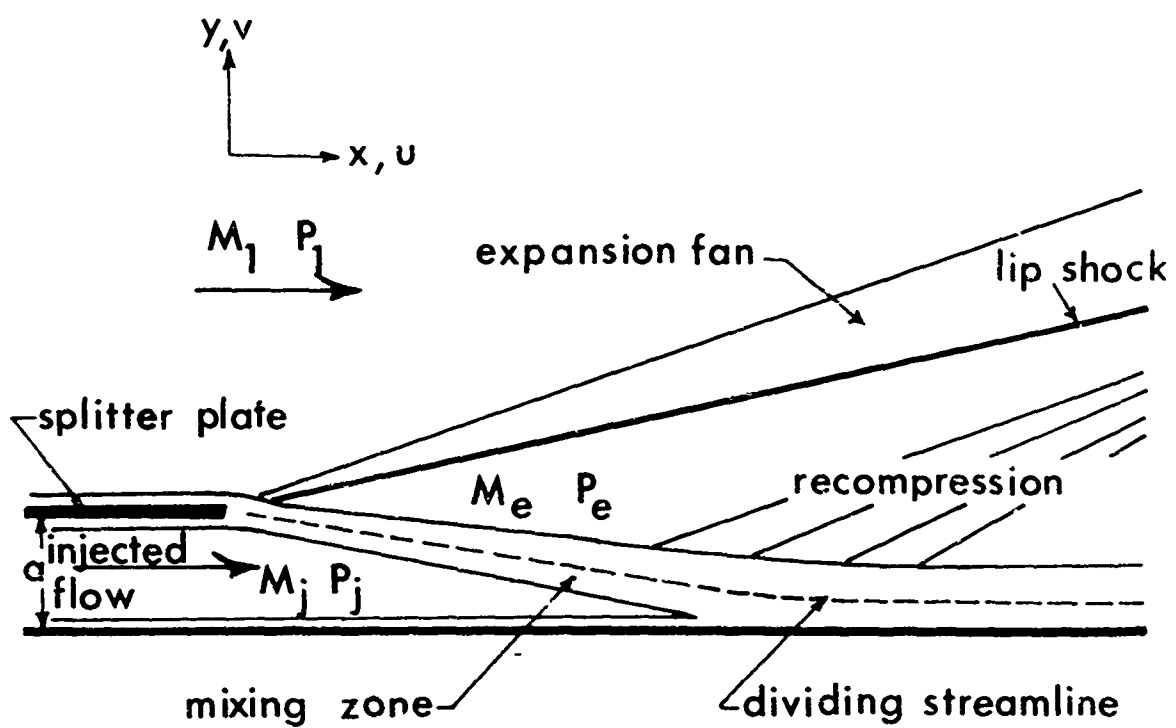
Fig. 1   Schematic Representation of Flow Field for
Low-Subsonic Injection into a Supersonic
Freestream

surface
block

nozzle
block

(a) Subsonic configuration

straightening
screens

header

attachment
plate

wedge
model
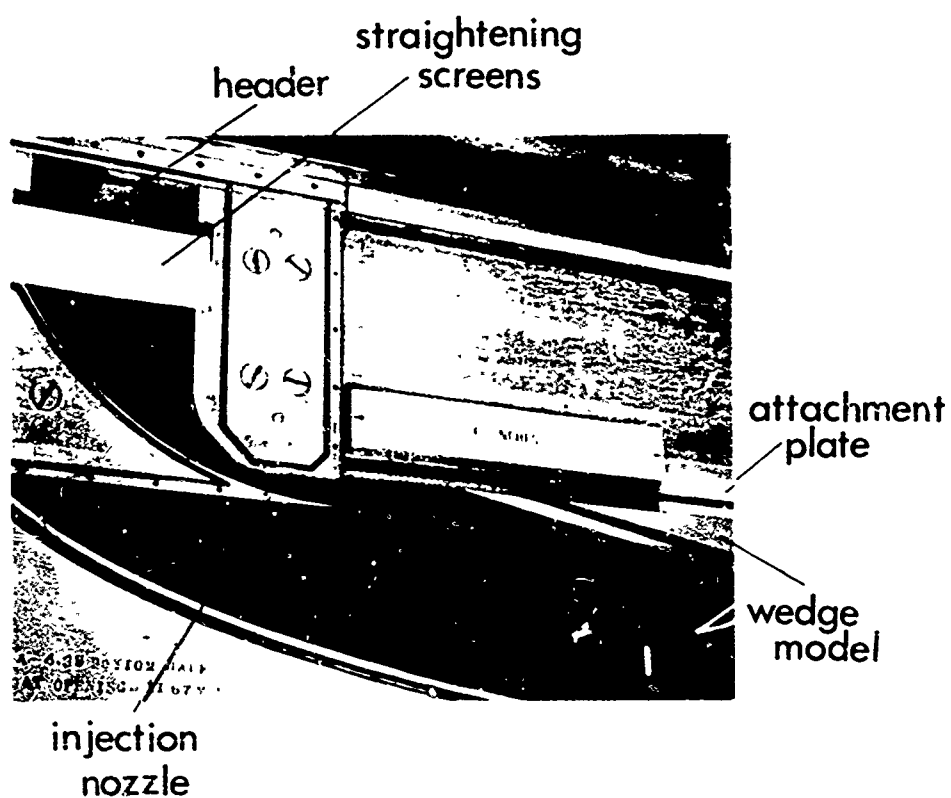
injection
nozzle

(b) Supersonic configuration with wedge model installed

Fig. 2   Injection Model

44
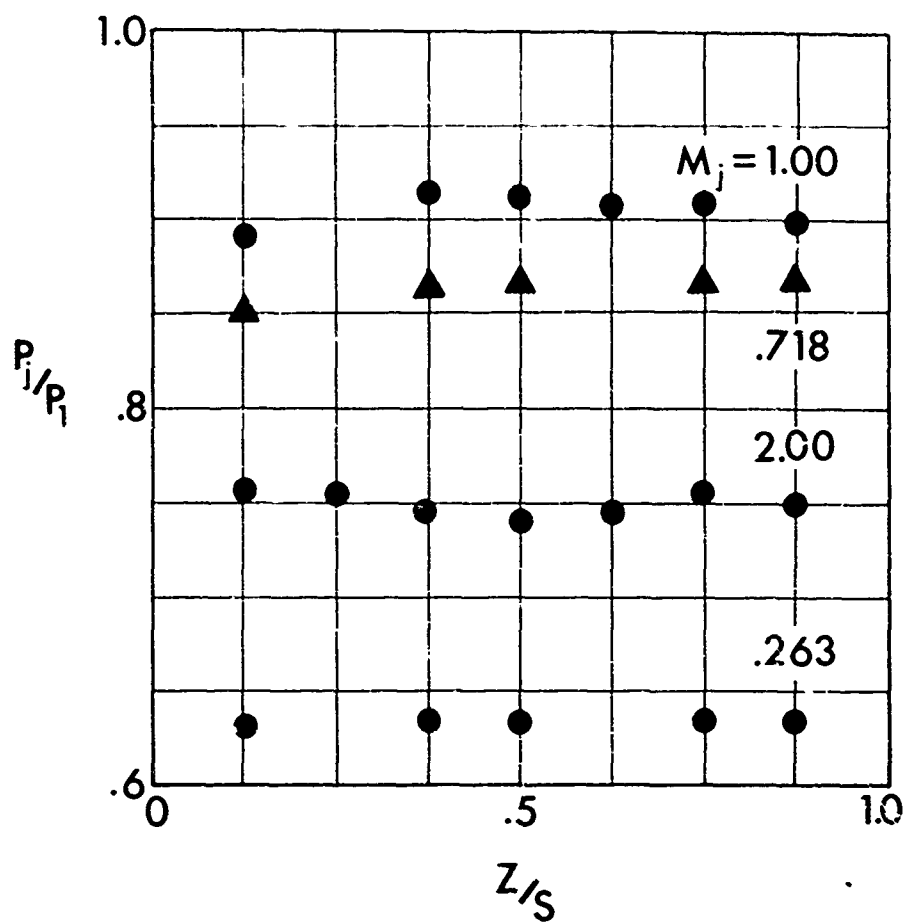
Fig. 3 Spanwise Pressure Distributions Measured at Injection Station, $M_1 = 2.85$

45
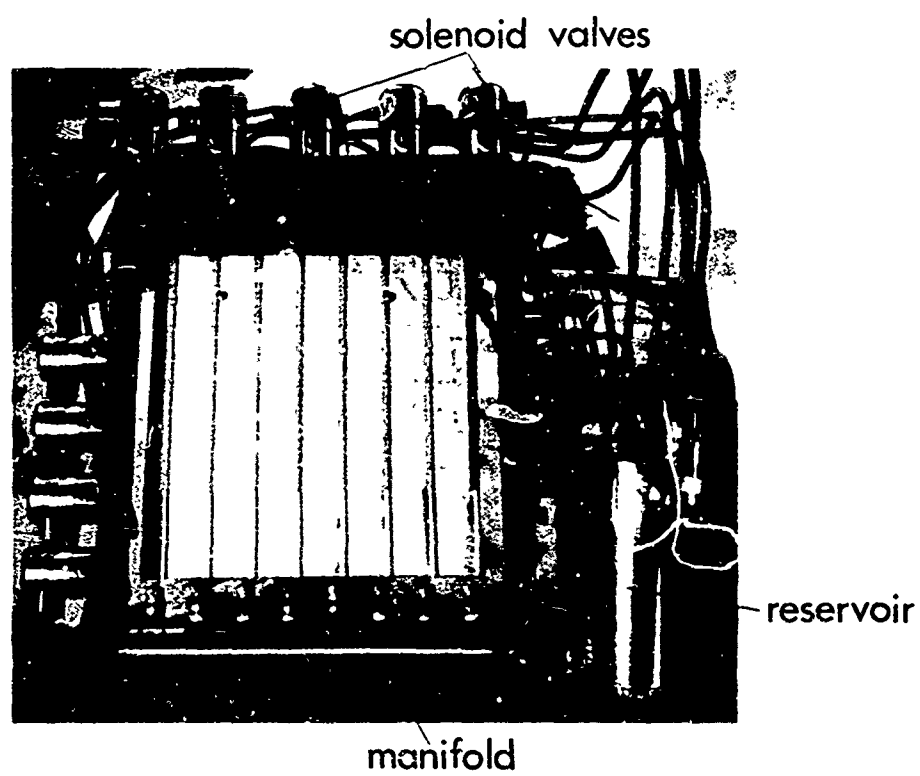
Fig. 4   Vacuum - Reference Manometer

(a) $M_1 = 2.85$

(b) $M_1 = 4.19$

Fig. 5   Flow Over a Rearward-Facing Step

47

(a)
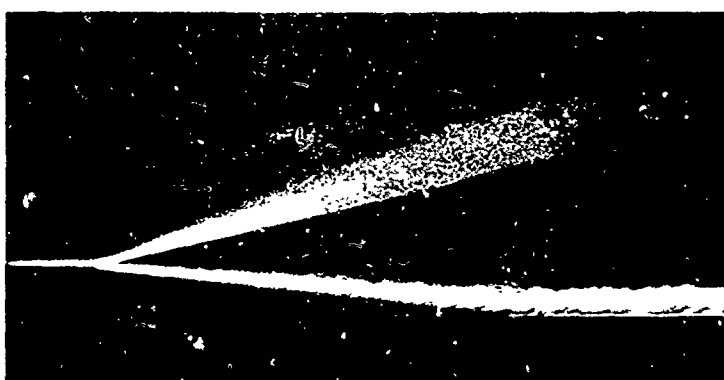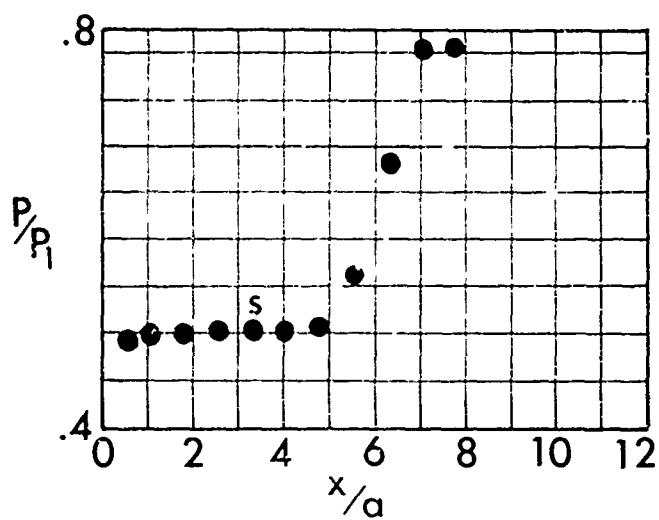
(b)
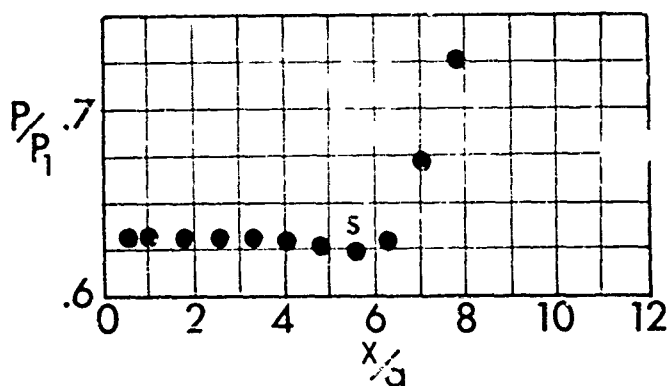
Fig. 6   Subsonic Injection, $M_1 = 2.85$

(a) $M_j = 0.153$ (b) $M_j = 0.255$

(a)
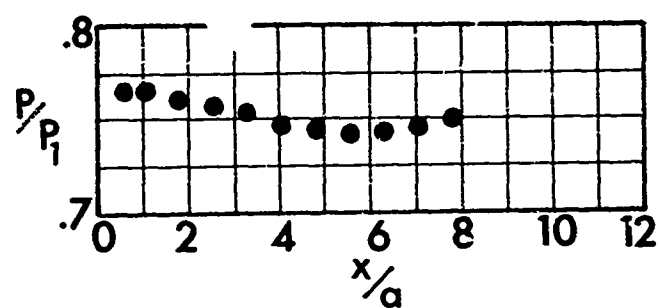
(b)
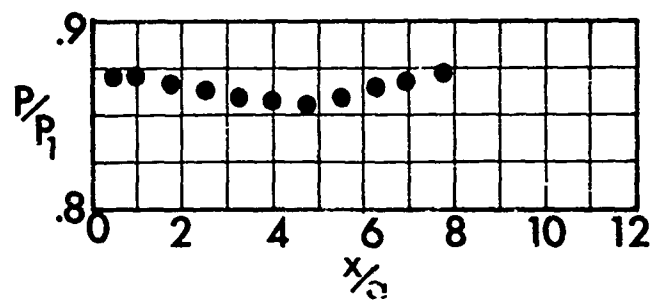
Fig. 7   Subsonic Injection, M_1 = 2.85

(a) M_j = 0.434   (b) M_j = 0.706
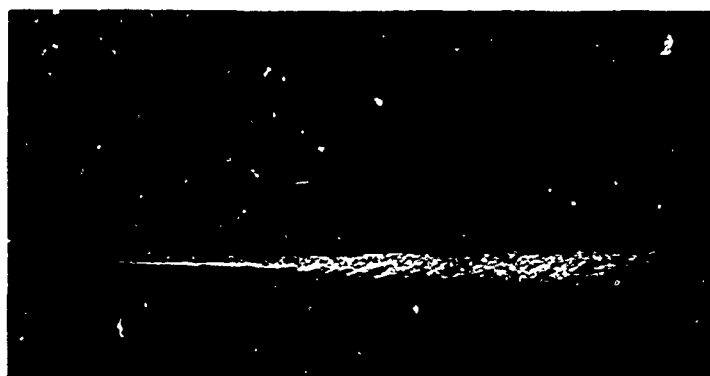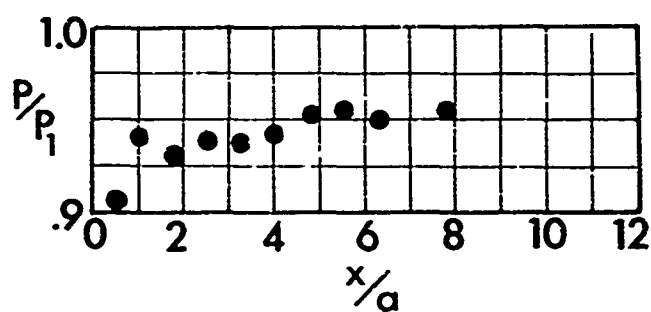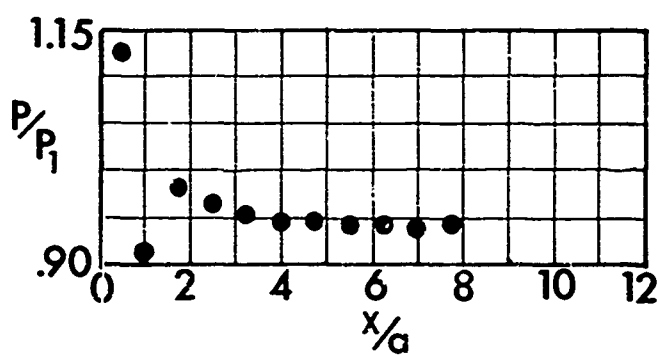
Fig. 8   Sonic Injection. M_1 = 2.85

(a) M_j = 1.00   (b) underexpanded sonic
injection
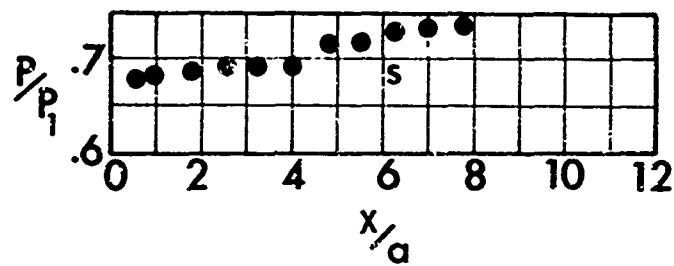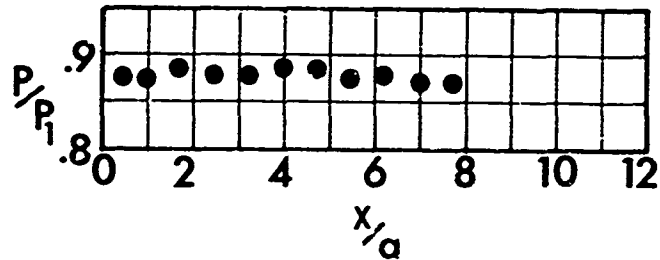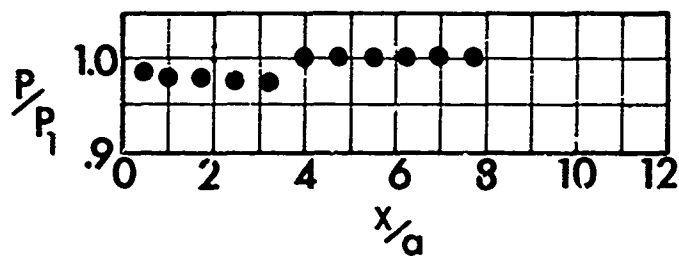
Fig. 9   Subsonic Injection, $M_1 = 4.19$
(a) $M_j = 0.232$ (b) $M_j = 0.403$ (c) $K_j = 0.570$
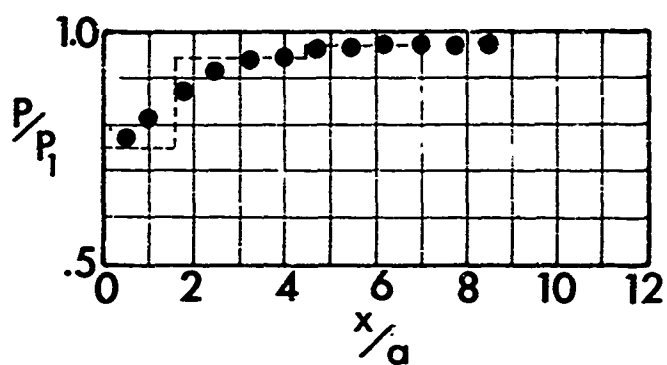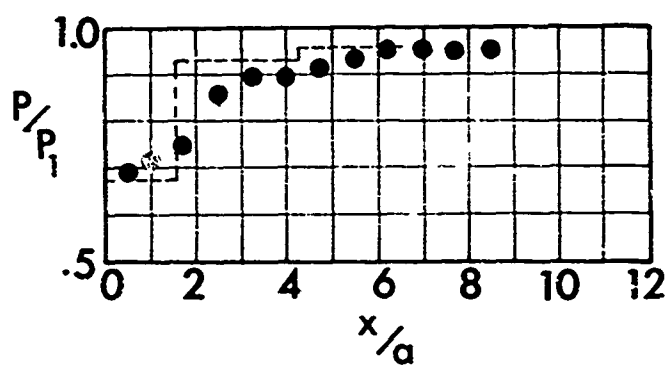
Fig. 10   Supersonic Injection, $M_1 = 2.85$, $M_j = 2.00$
(a) $\widetilde{\rho u} = 0.444$ (b) $\widetilde{\rho u} = 0.401$
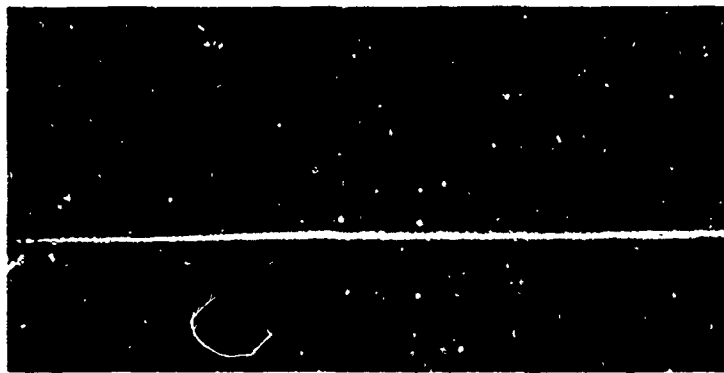
(a)
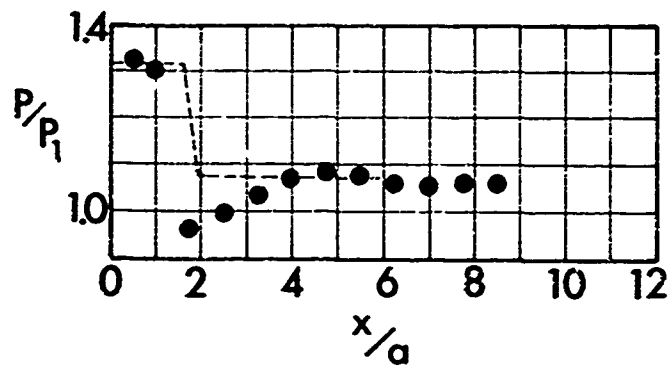
(b)
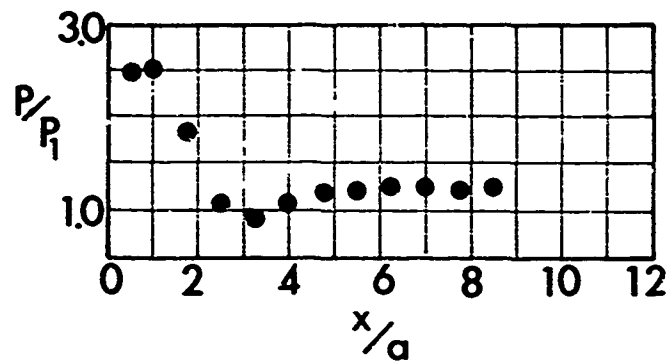
Fig. 11   Supersonic Injection, $M_1 = 4.19$, $M_j = 1.98$
(a) $\tilde{\rho u} = 0.384$ (b) $\tilde{\rho u} = 0.739$

53

(a)
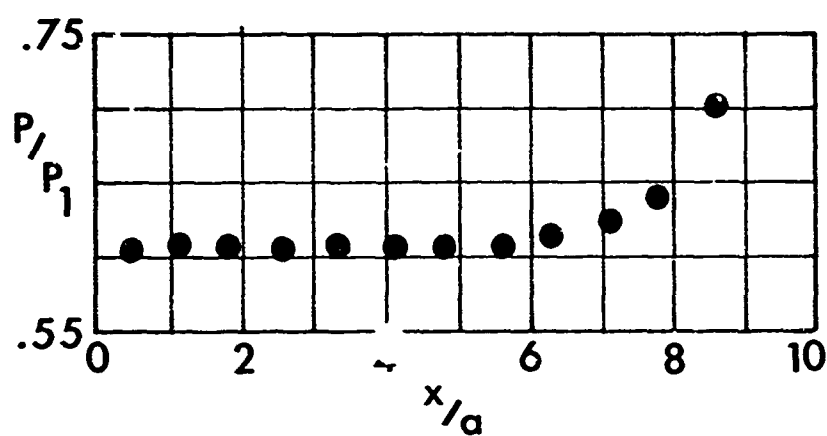
(b)
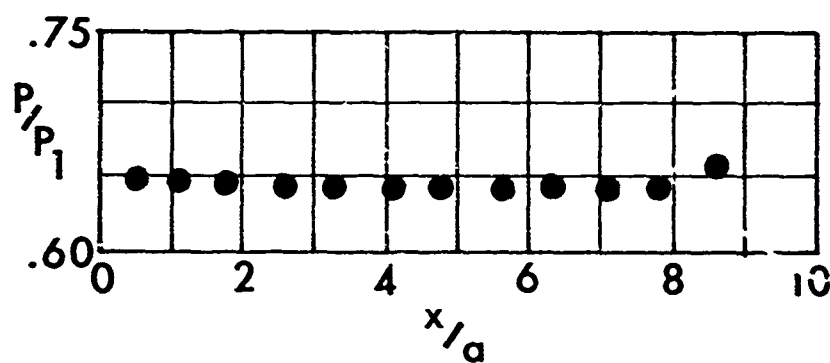
Figure 12a

HELIUM INJECTION; (a) M_j=.181, (b) M_j=.202

(a)
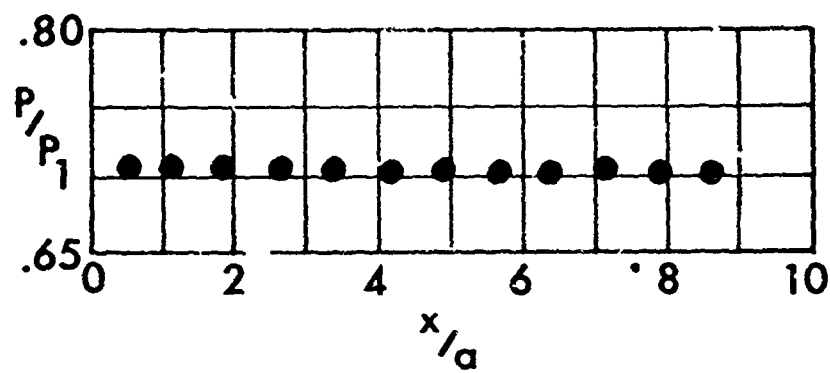
(b)
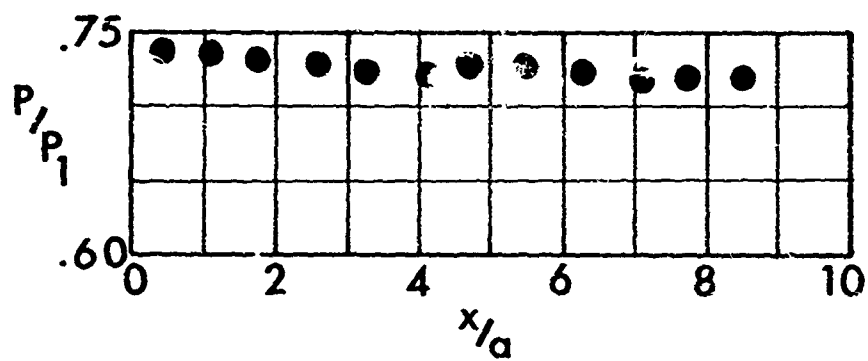
Figure 12b

HELIUM INJECTION; (a) M_j=.254, (b) M_j=.292

(a)
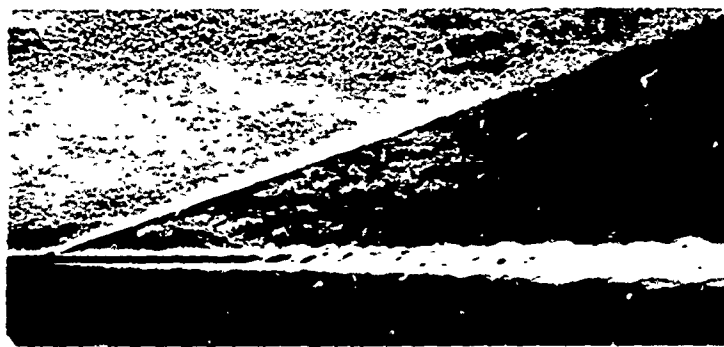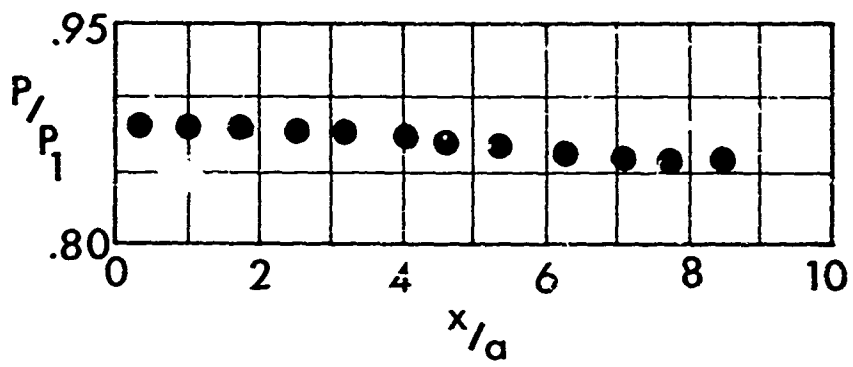
(b)
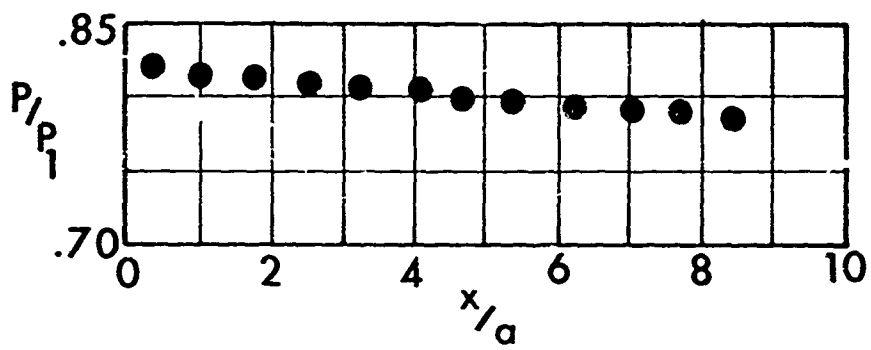
Figure 12c

HELIUM INJECTION; (a) $M_j = .448$, (b) $M_j = .511$

56

(a)

(b)
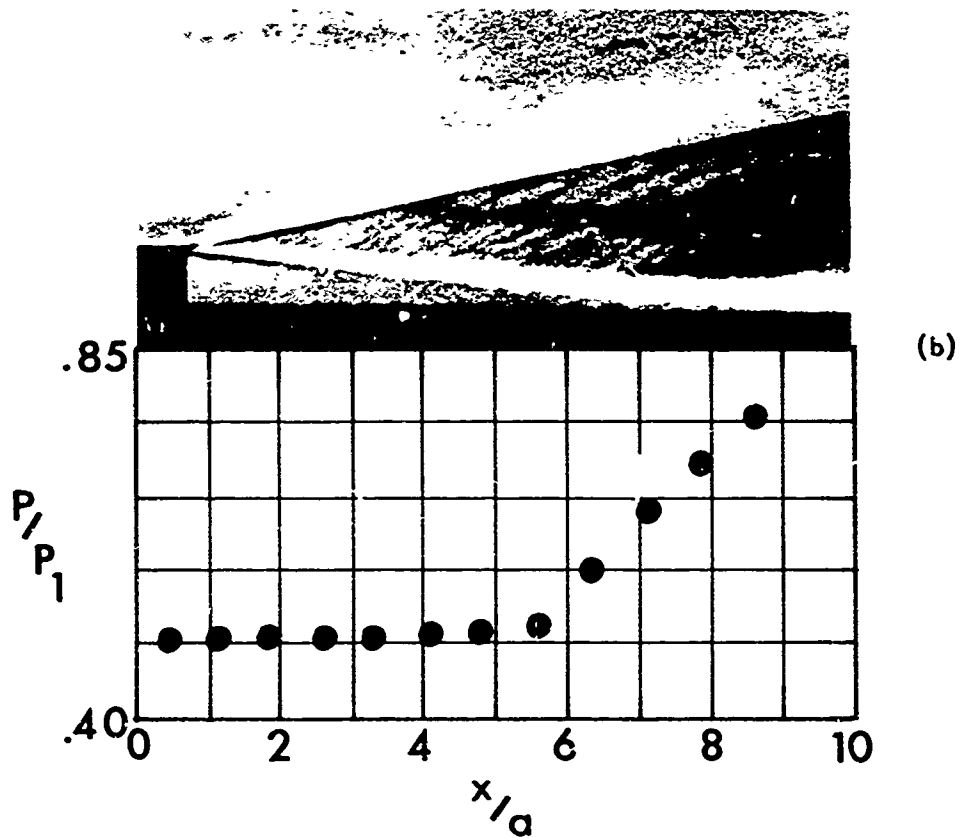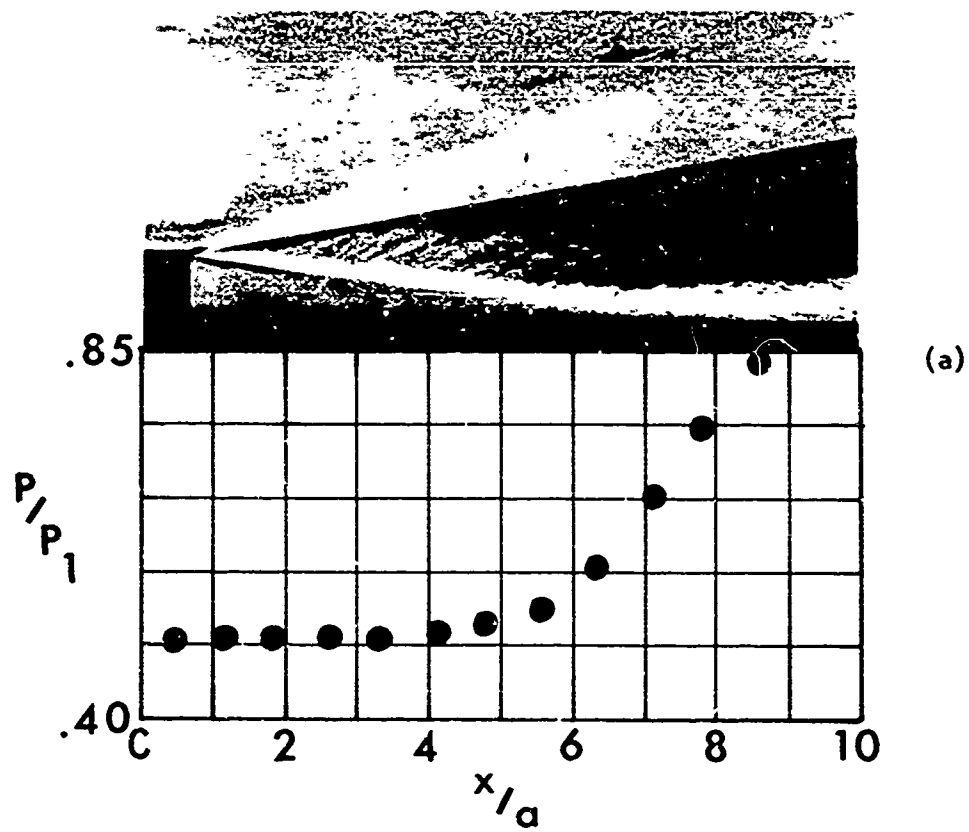
Figure 13a

CARBON DIOXIDE INJECTION; (a) $M_j=.212$, (b) $M_j=.276$
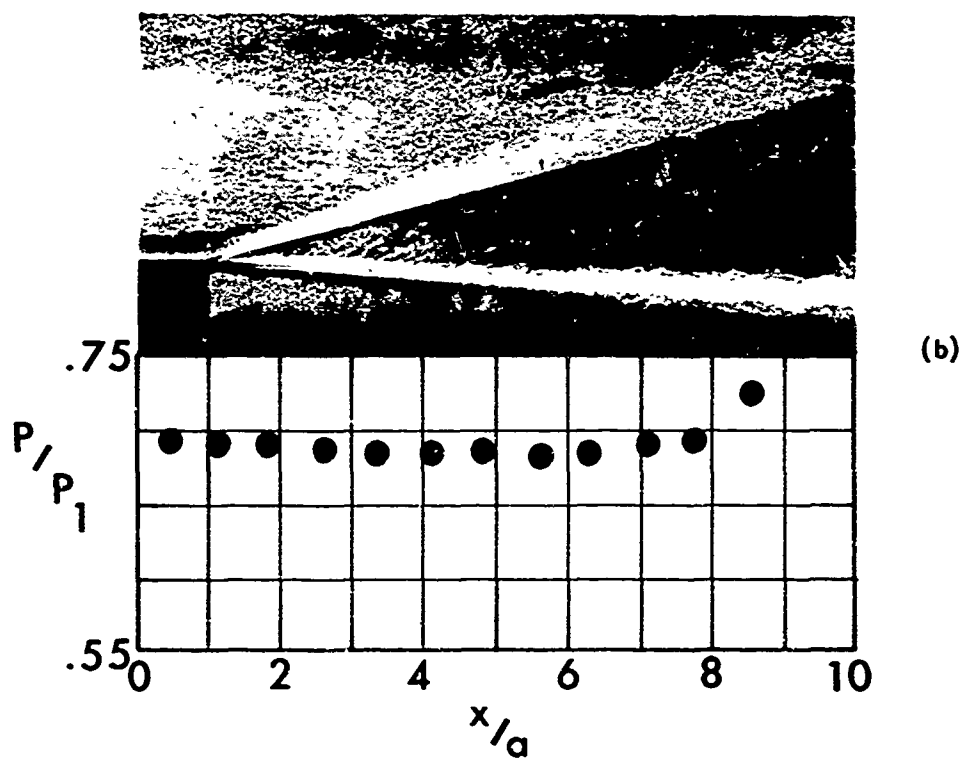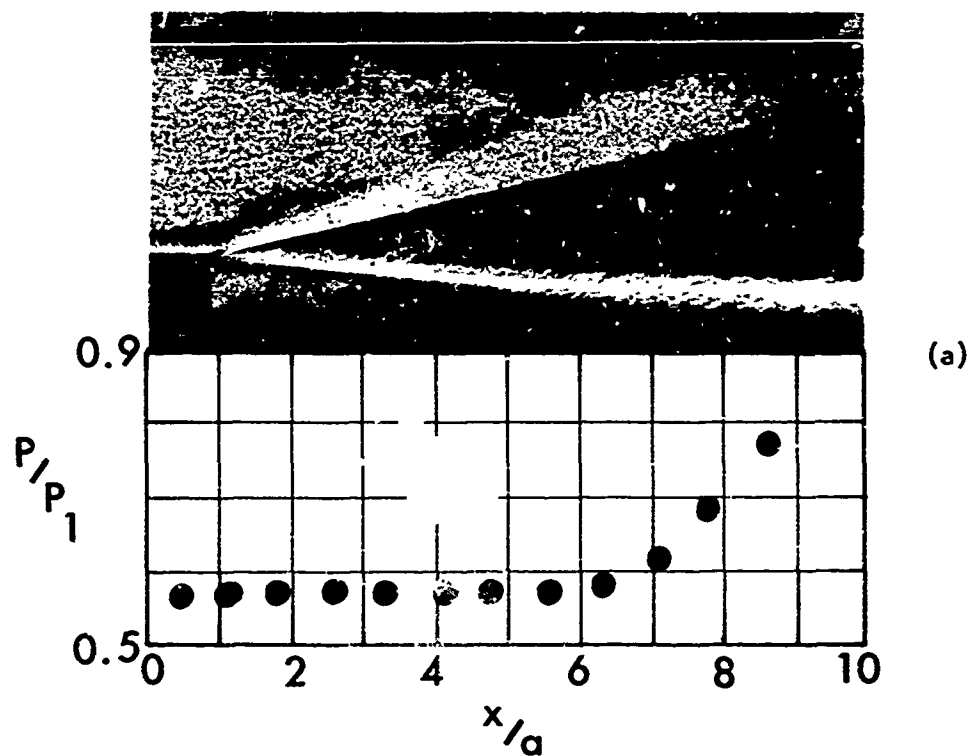
Figure 13b

CARBON DIOXIDE INJECTION; (a) $M_j = .293$, (b) $M_j = .378$

(a)
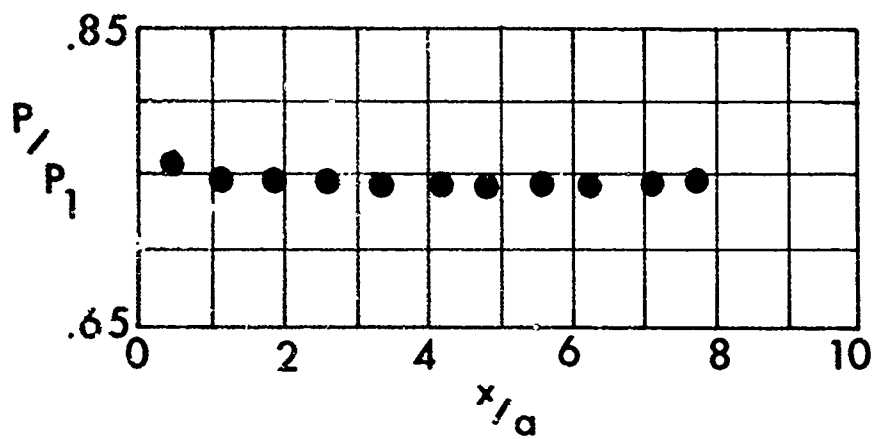
(b)
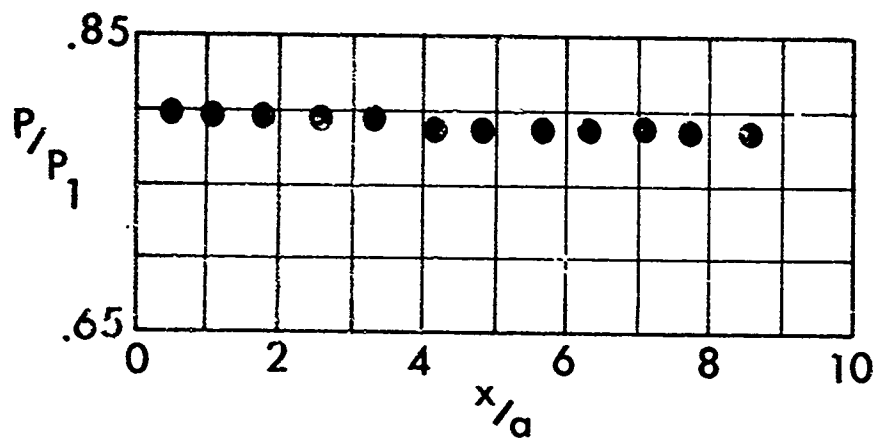
Figure 13c

CARBON DIOXIDE INJECTION; (a) $M_j = .543$, (b) $M_j = .663$

59

(a)

(b)
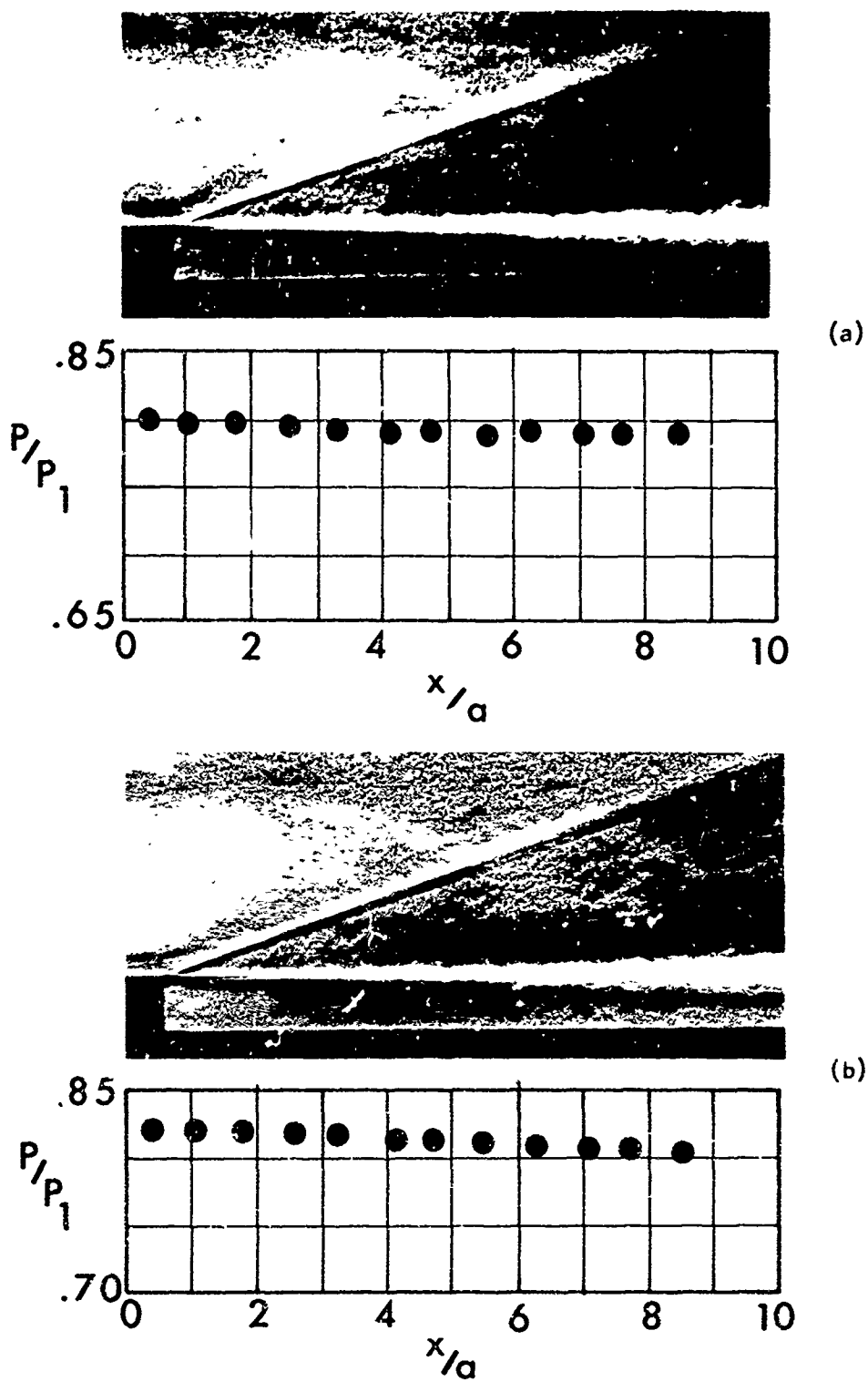
Figure 13d

CARBON DIOXIDE INJECTION; (a) $M_j = .743$, (b) $M_j = .954$

60
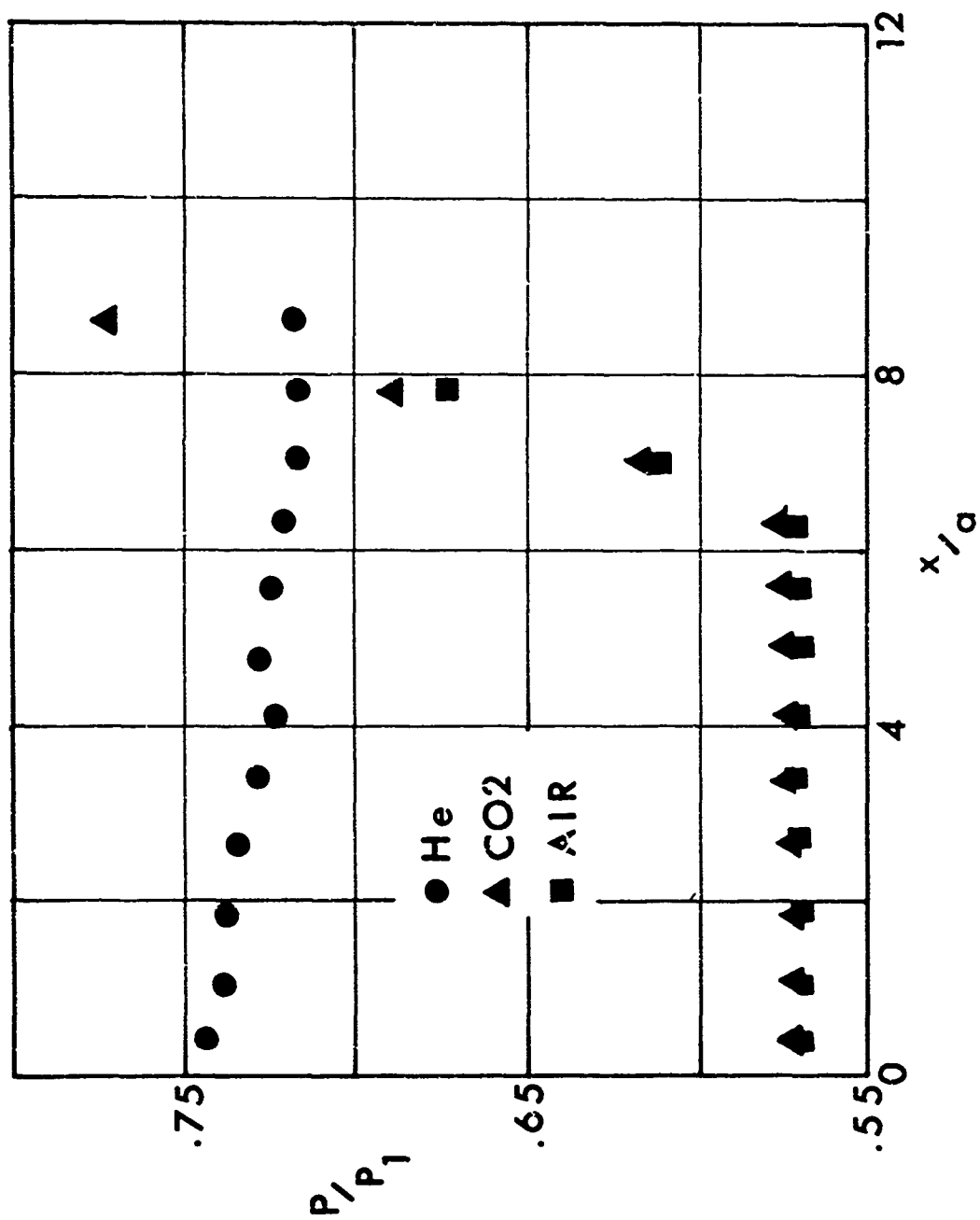
Fig. 14 WALL PRESSURE DISTRIBUTIONS FOR HELIUM, CARBON DIOXIDE,
AND AIR AT THE SAME MACH NUMBER ($M_j = .290$)

61
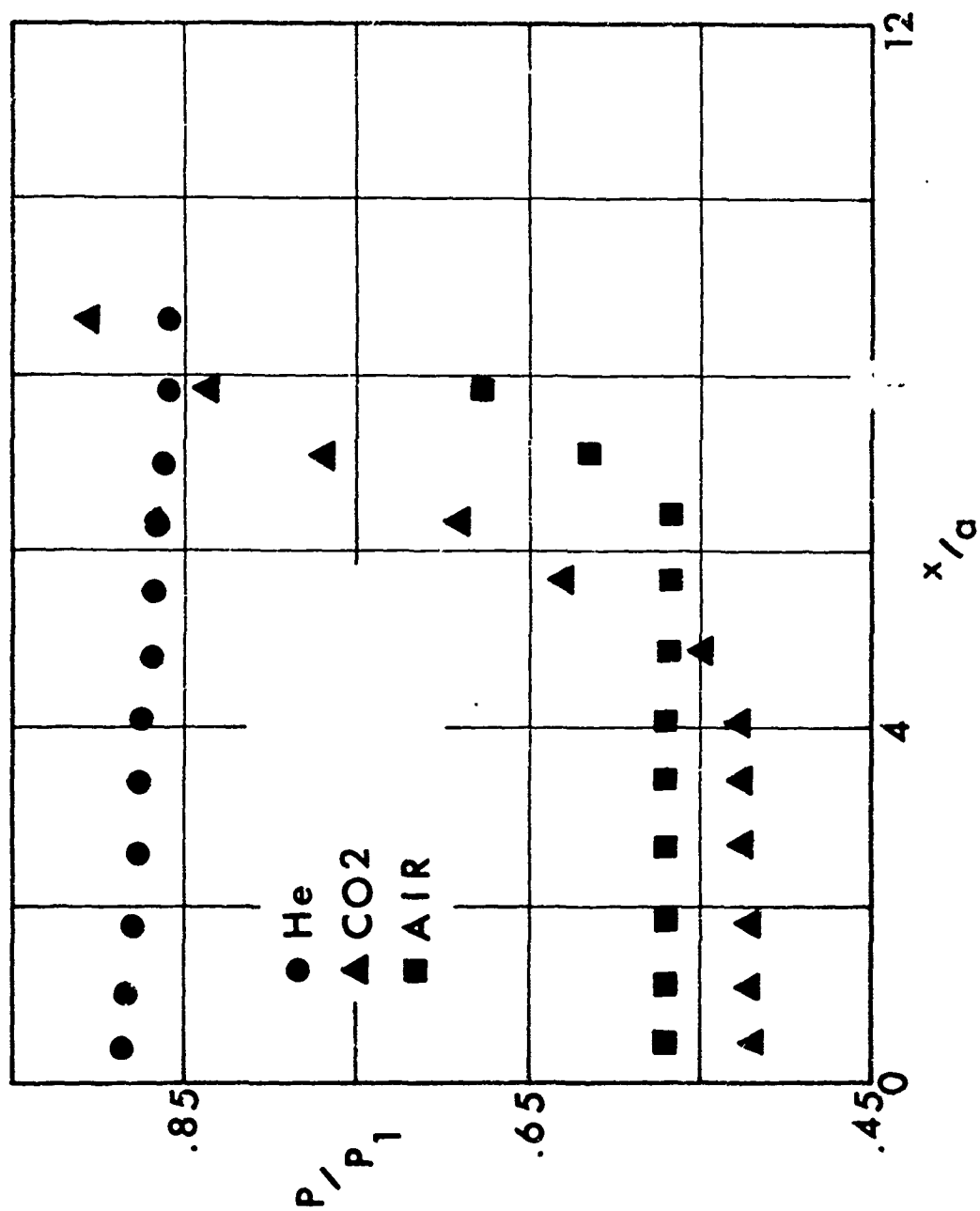
Fig. 15   WALL PRESSURE DISTRIBUTIONS FOR HELIUM, CARBON DIOXIDE, AND AIR AT THE SAME MASS FLOW RATE/UNIT AREA ($\rho u = 1.741 \times 10^{-2}$ slugs/sec.-ft.^{2})

62
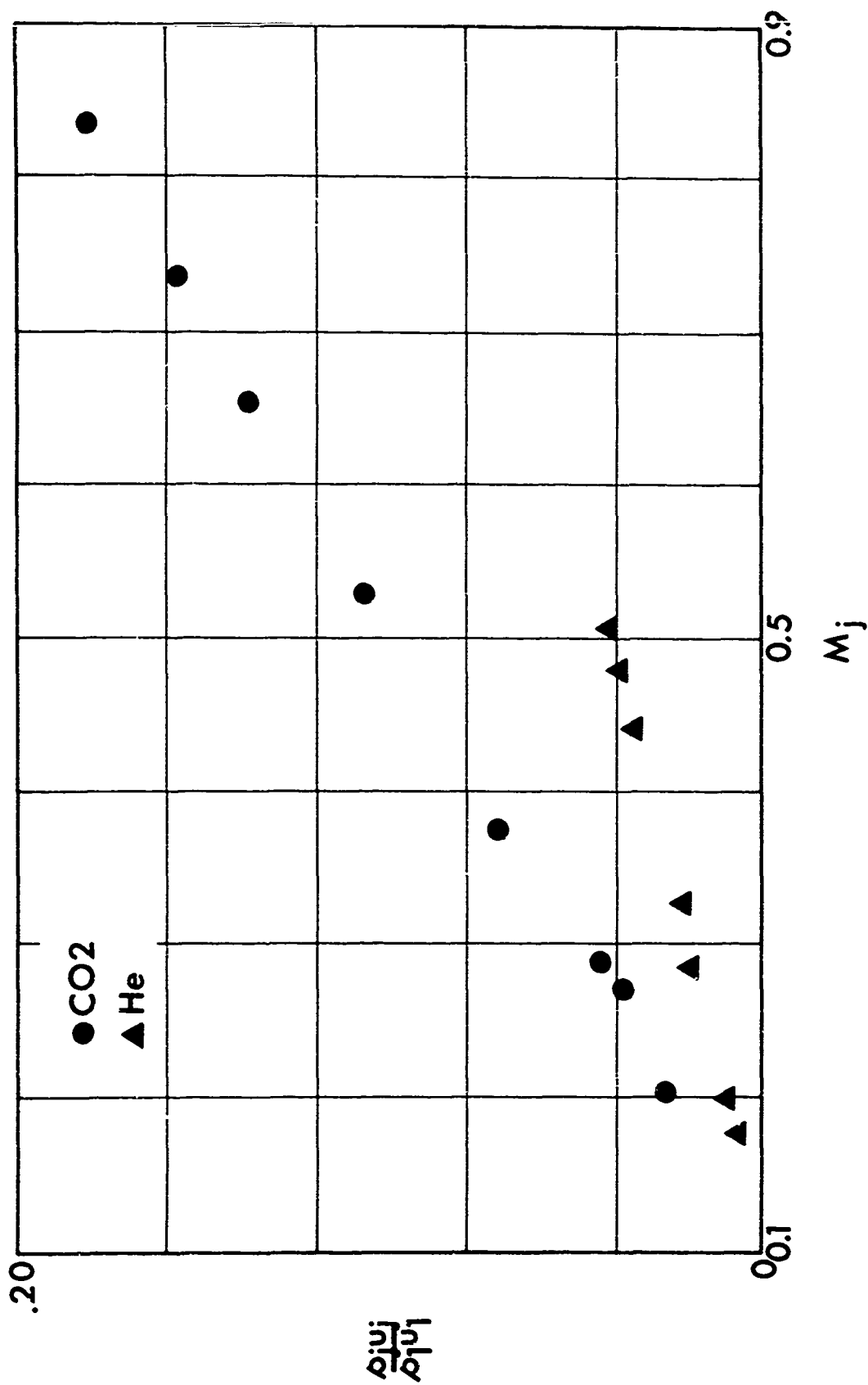
Fig. 16 MASS FLOW RATE/UNIT AREA vs MACH NUMBER FOR HELIUM AND CARBON DIOXIDE
INJECTION

63
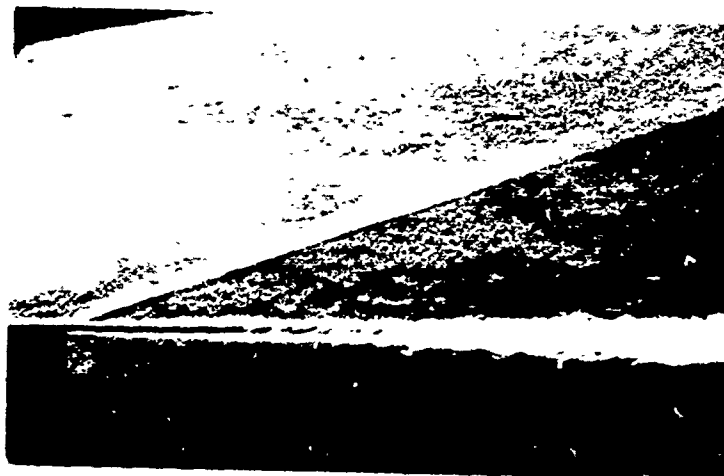
(a)

(b)

Figure 17

EXTENT OF WALL PROTECTION AT THE SAME MASS FLOW RATE/
UNIT AREA ($\rho u = 1.741 \times 10^{-2}$ slugs/sec.-ft.^{2}); (a) He-M_j=
.448, (b) CO_2-M_j=.276
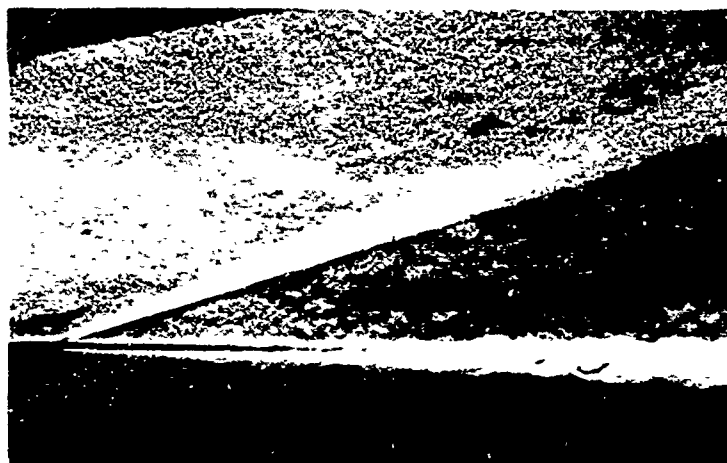
(a)
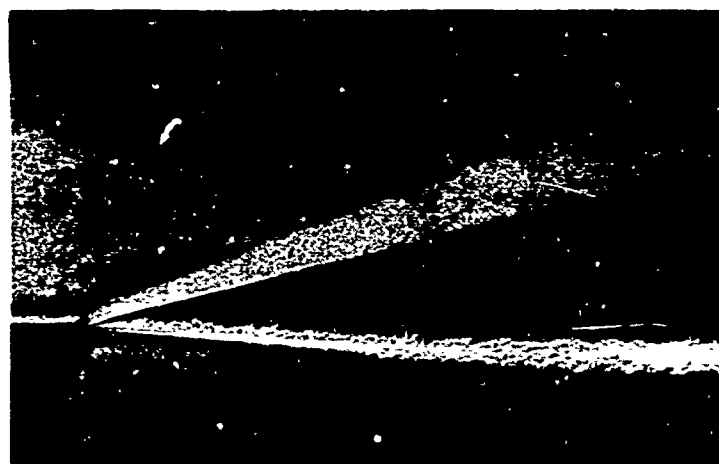
(b)

Figure 18

EXTENT OF WALL PROTECTION AT THE SAME MACH NUMBER
$(M_j = .290)$; (a) He, (b) CO_2
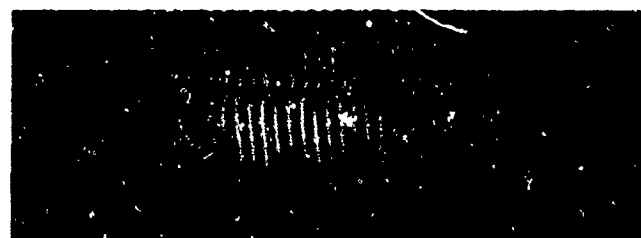
(a) $M_1 = 4.19$, $M_j = 0.403$

(b) $M_1 = 4.19$, $M_j = 0.570$
(Infinite Fringe)

(c) $M_1 = 2.85$, $M_j = 1.00$

Fig. 19. Interferograms - Subsonic Injection

66

(a) Infinite Fringe, $p_j/p_b \doteq 1.40$

(b) Infinite Fringe, $p_j/p_b \doteq 1.09$
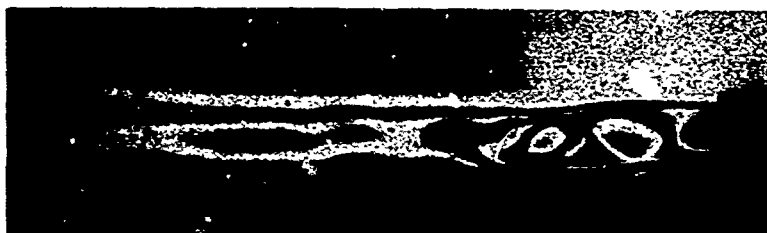
(c) Infinite Fringe, $p_j/p_b \doteq 0.80$
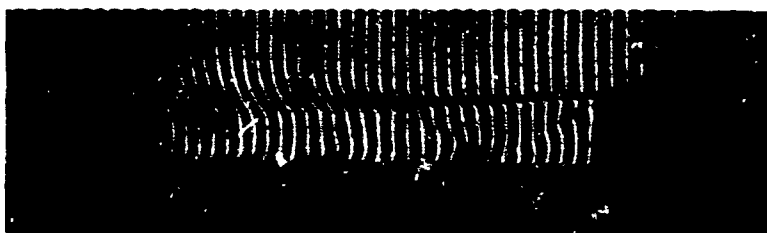
(d) $p_j/p_b \doteq 1.00$

Fig. 20. Interferograms - Supersonic Wall Jet

67
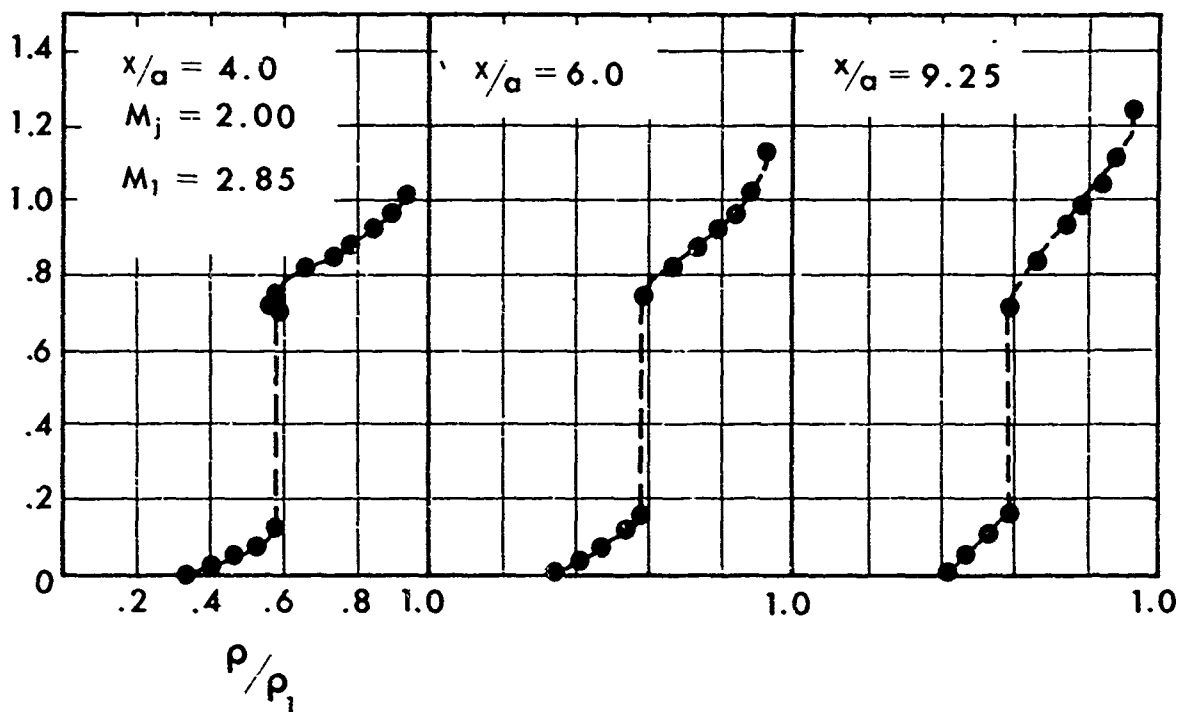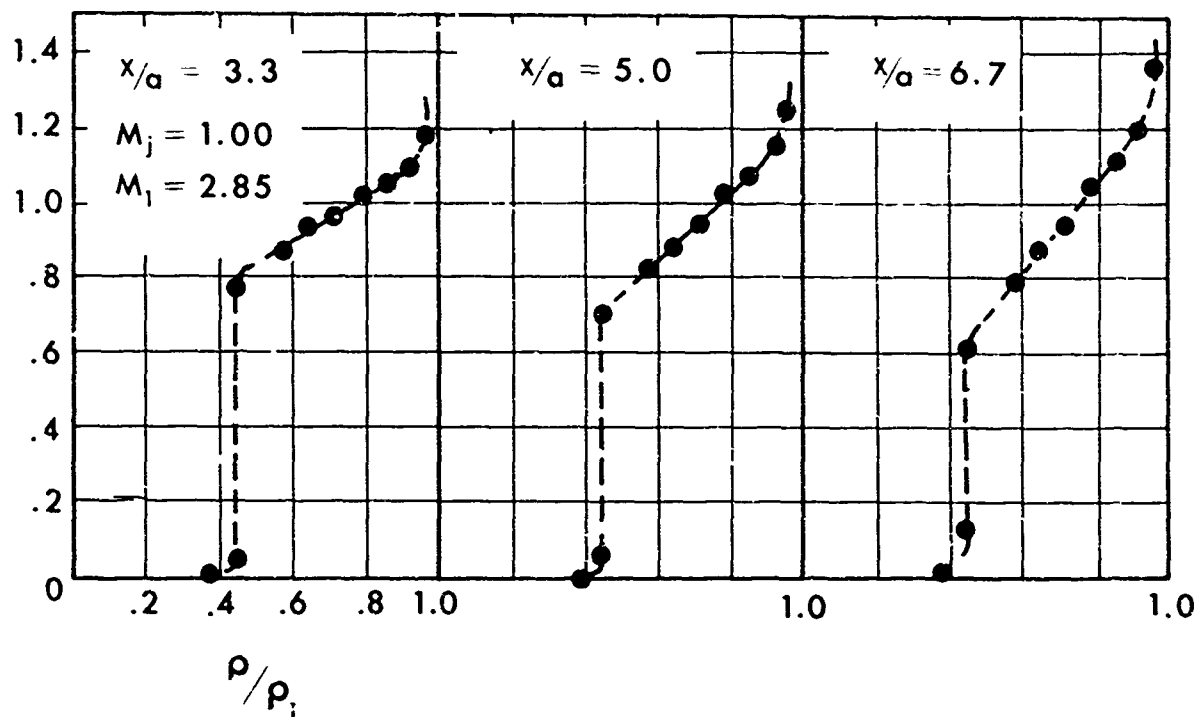
Fig 21 Density Profiles for Sonic and
Supersonic Injection, $M_1 = 2.85$

(a) $p_j/p_b \doteq 1.50$
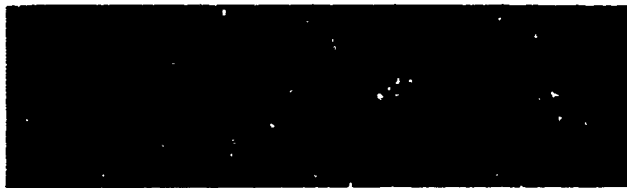
(b) $p_j/p_b \doteq 1.01$

(c) $p_j/p_b \doteq 0.81$

Fig. 22.   Supersonic Wall Jet, $M_j = 2.00$

69
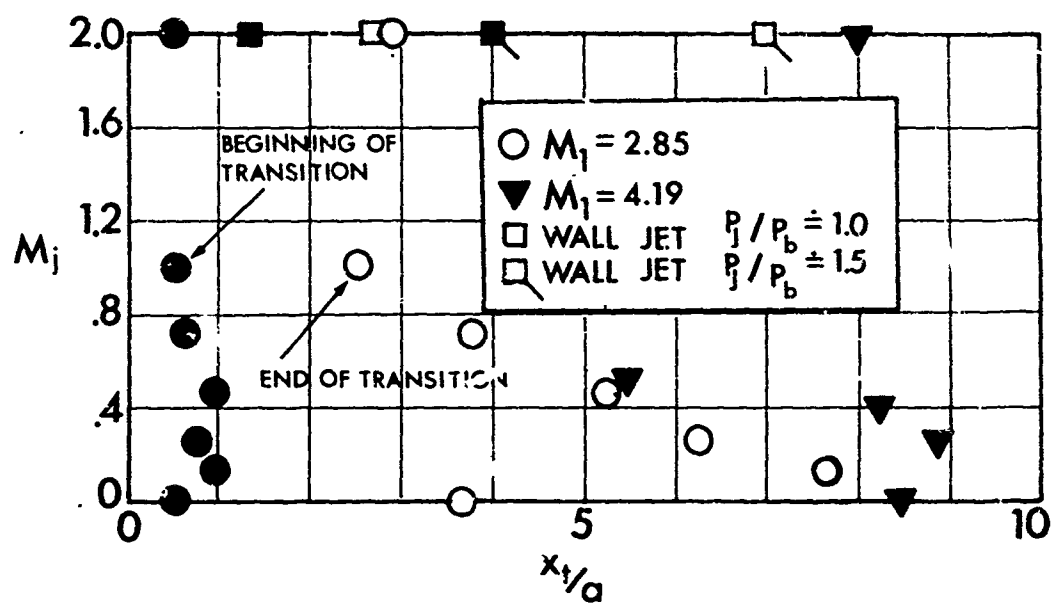
Fig. 23 Effect of Injection on Location of Transition
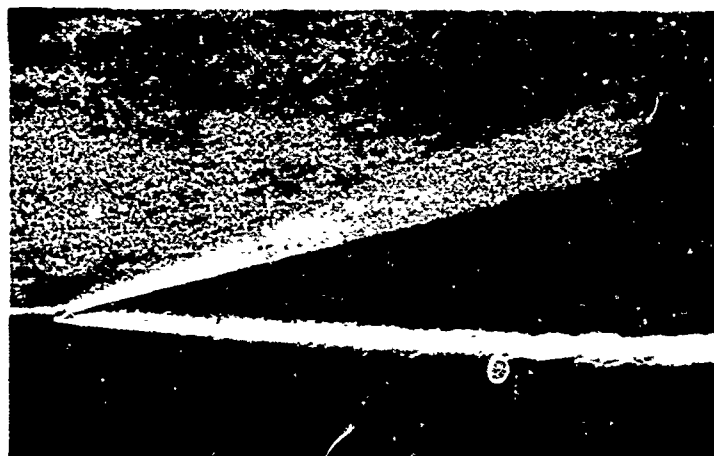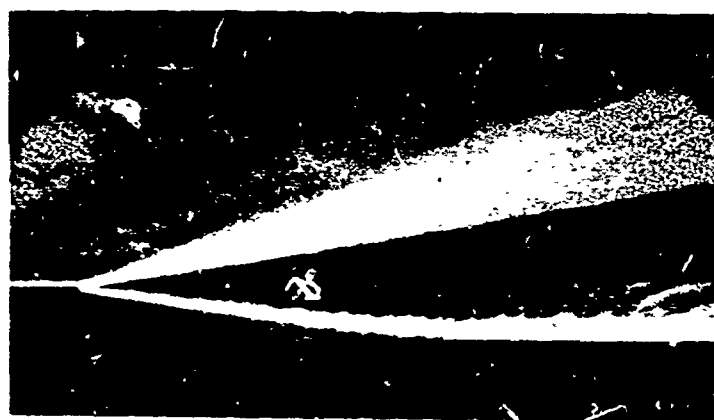
Figure 24

INFLUENCE OF INJECTANT ON THE SHEAR LAYER; (a) He-M_j=.181, (b) CO_2-M_j=.212, (c) Air-M_j=.290

(a)
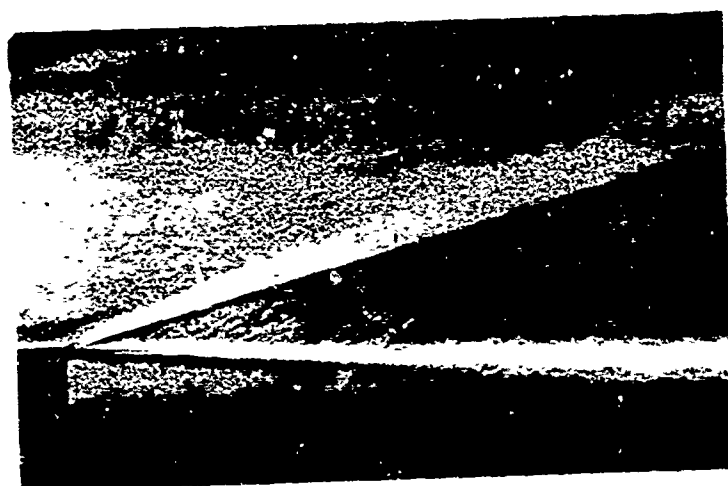
(b)

Figure 25

COMPARISON OF THE SCALE OF TURBULENCE: (a) $He-M_j=.254$, (b) $CO_2-M_j=.378$
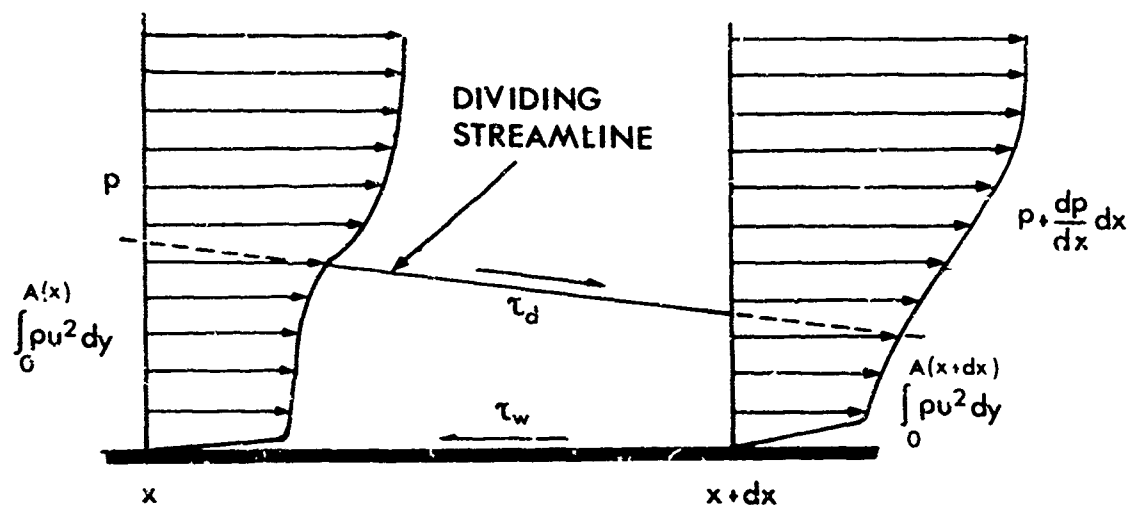
Fig. 26 Control Volume for One-Dimensional Analysis
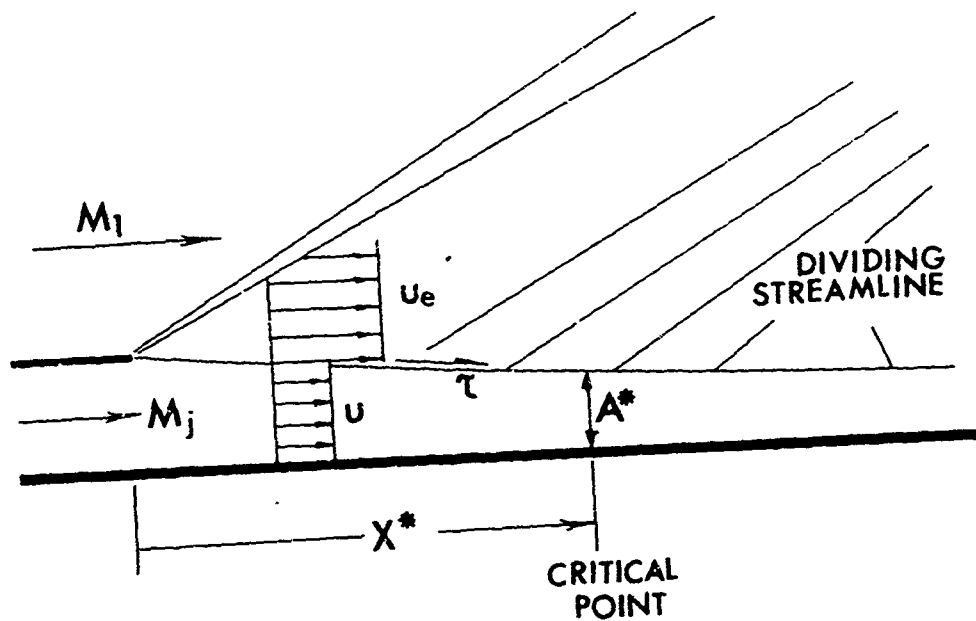
Fig. 27 Schematic of One-Dimensional Analytical Model
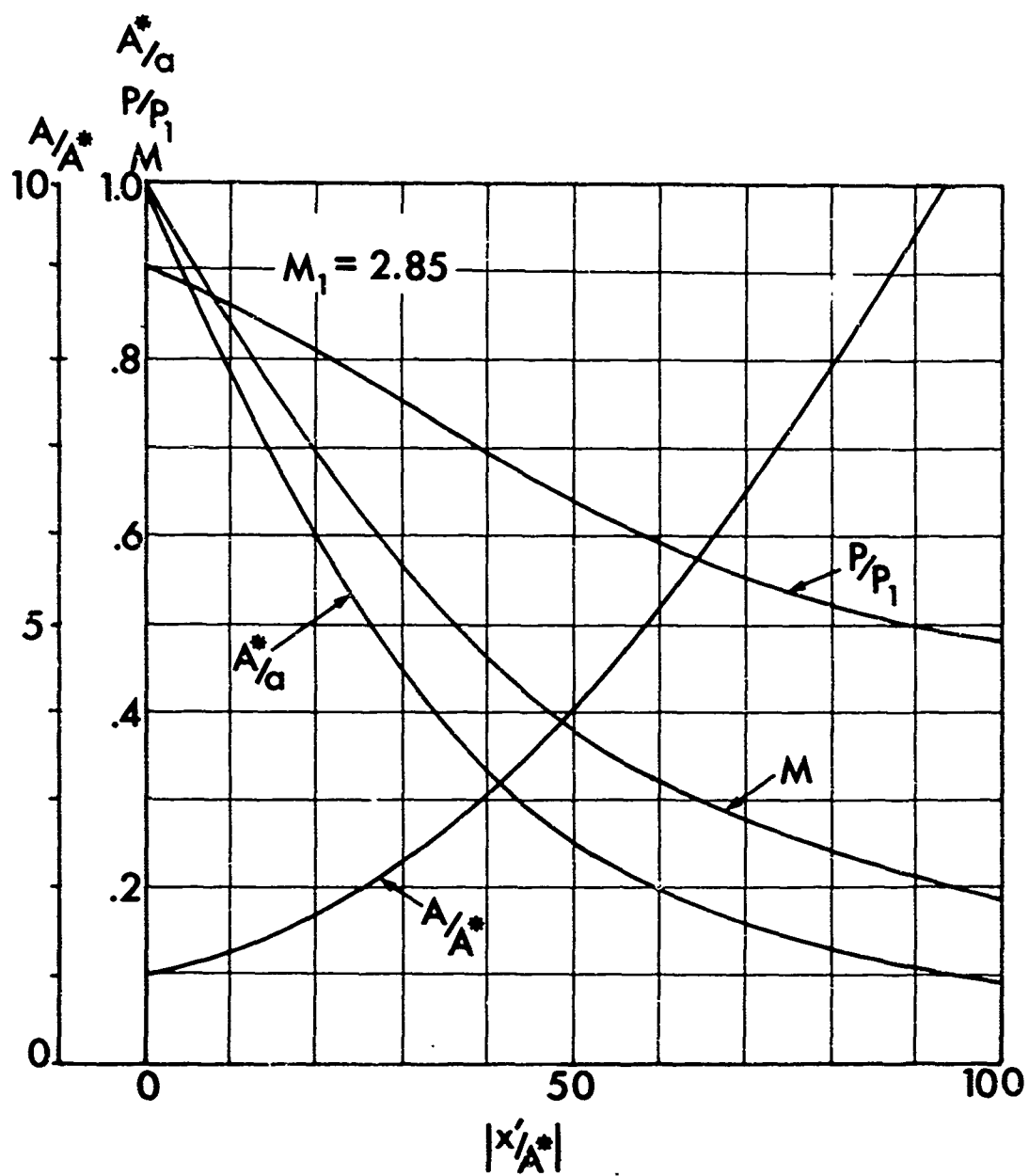
Fig. 28 **Solution Curves for Turbulent Mixing, M_1 = 2.85**
(Note: x'=0 corresponds to critical point location
Curves shown are for upstream values only.)

75
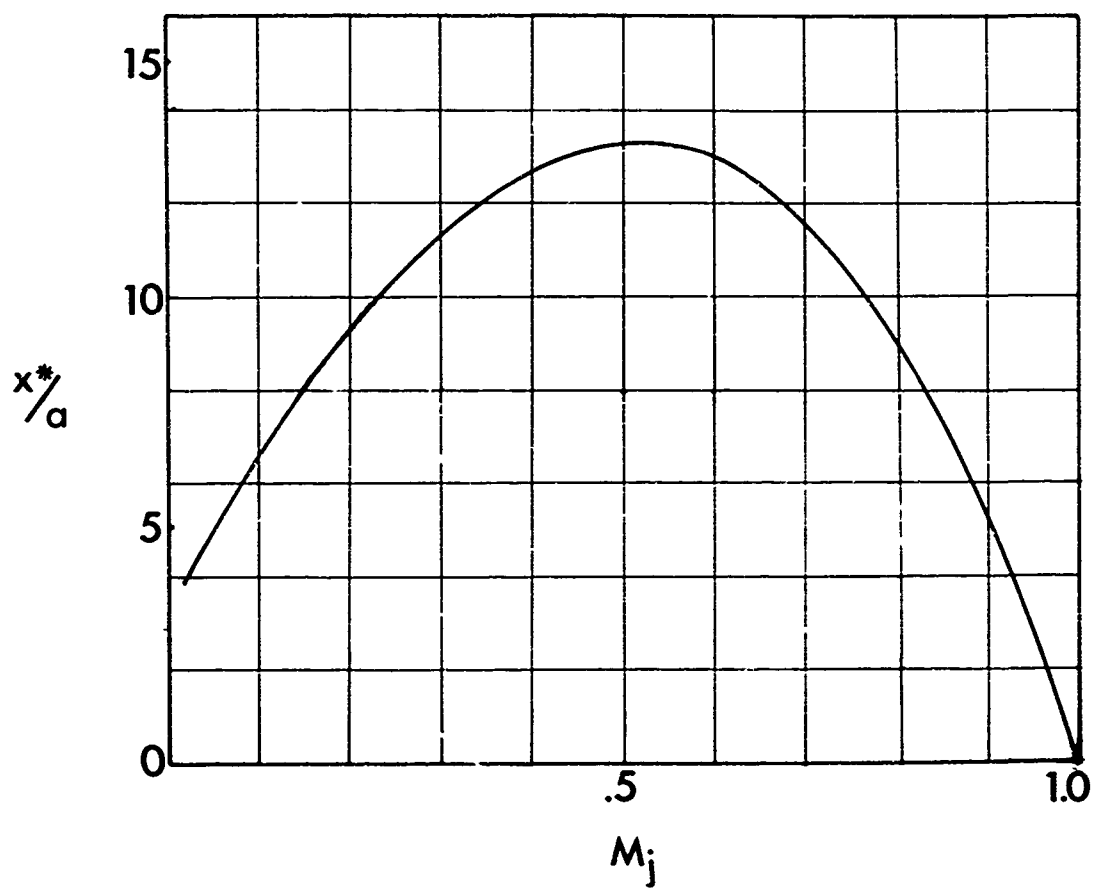
Fig. 29 Solution Curves for Turbulent Mixing, $M_1 = 2.85$
(concluded)
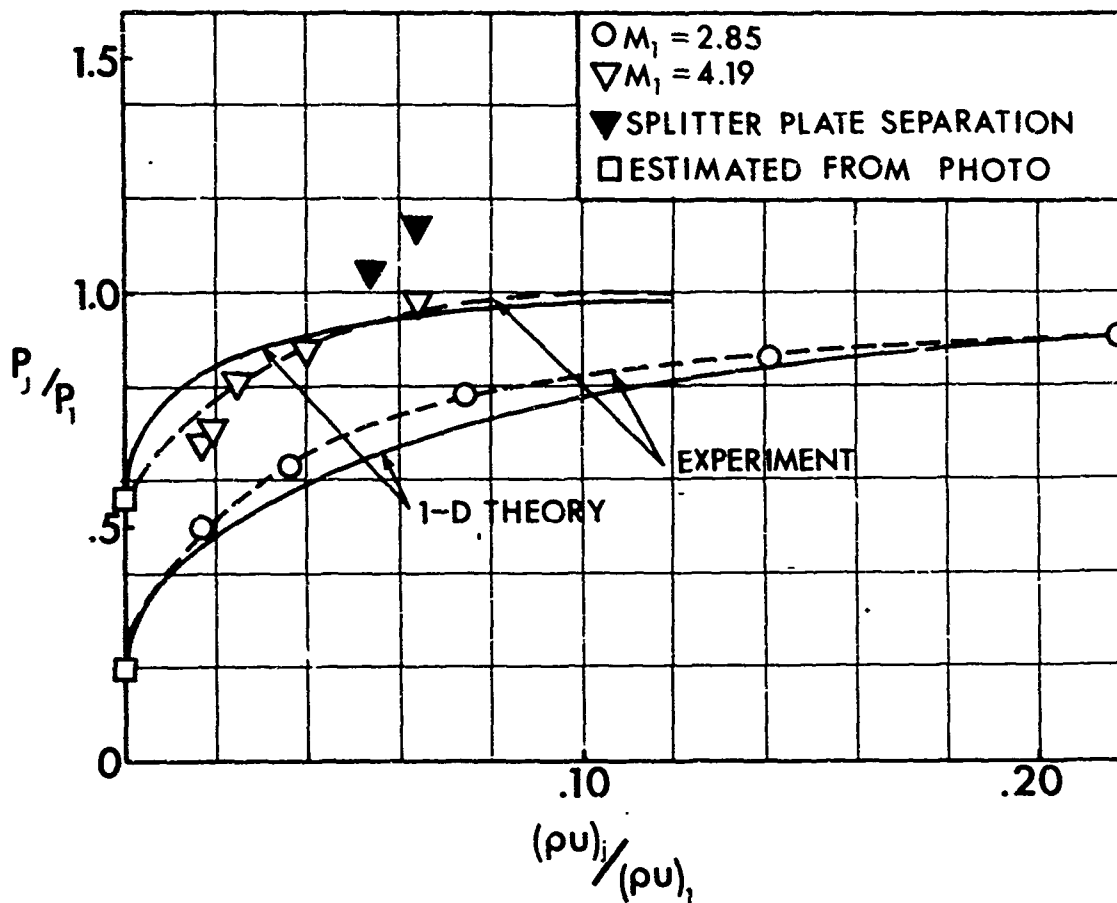
Fig. 30 Comparison of Theory and Experiment, Mass Flow
Ratio vs. Initial Injectant Pressure Ratio
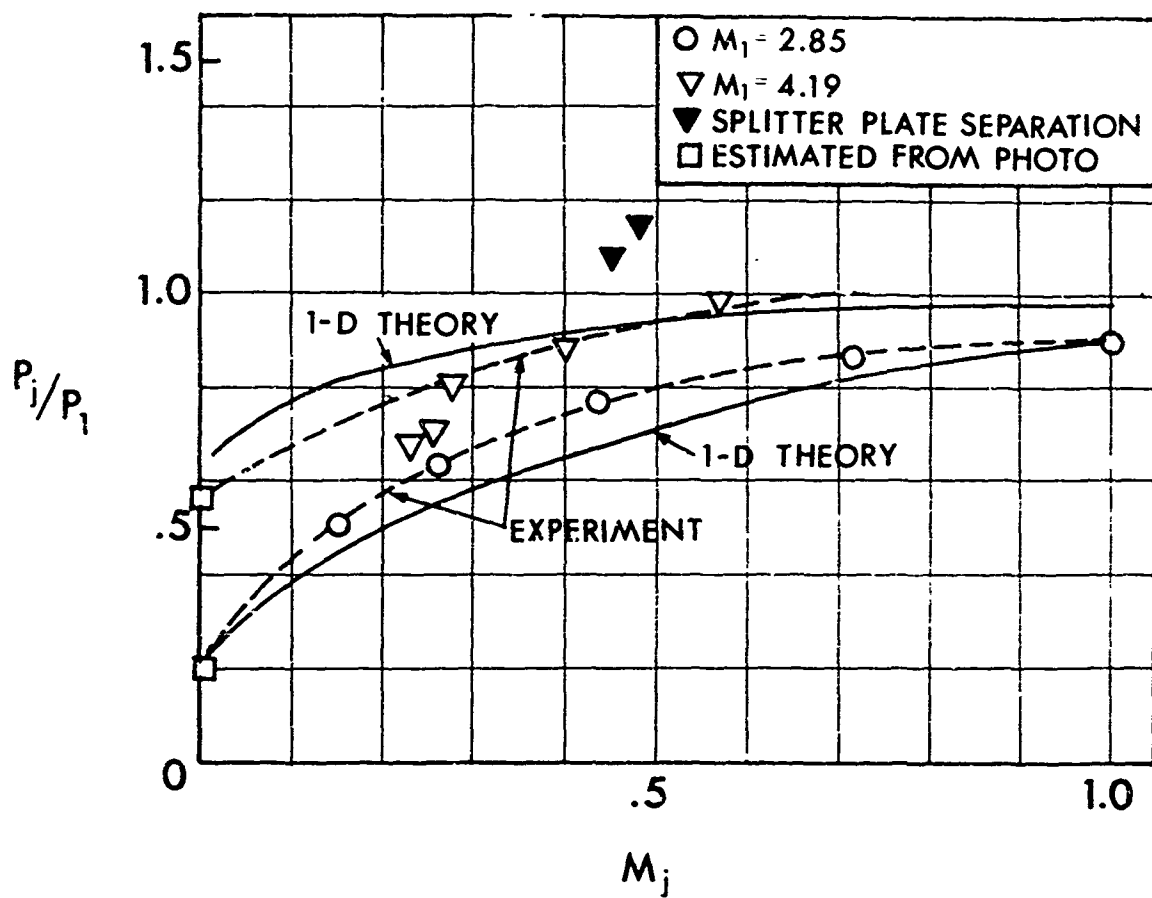
Fig. 31 Comparison of Theory and Experiment, Initial
Injectant Mach No. vs. Initial Injectant Pressure Ratio
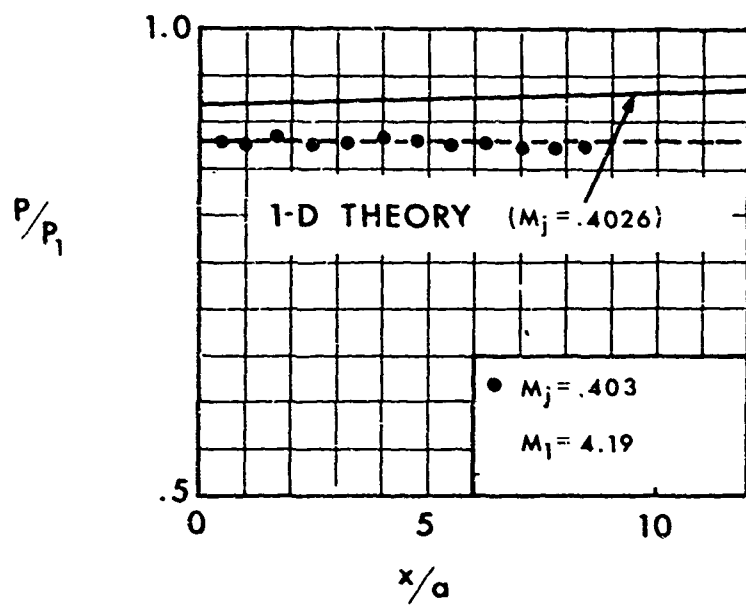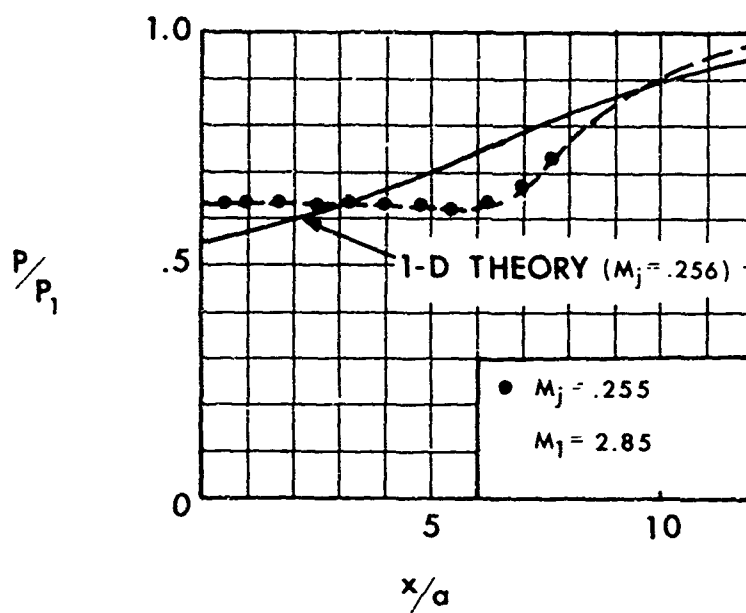
Fig. 32 Comparison of Theory and Experiment, Wall Pressure Distribution

79

$M_j = .255$, $M_1 = 2.85$
1-D THEORY, $M_j = .256$
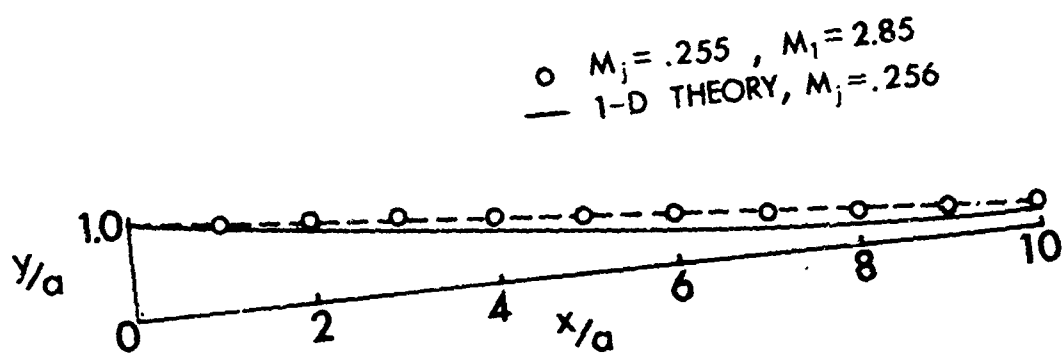
(Note: Experimental points estimated from photographic measurements.)

$M_j = .403$, $M_1 = 4.19$
1-D THEORY, $M_j = .4026$
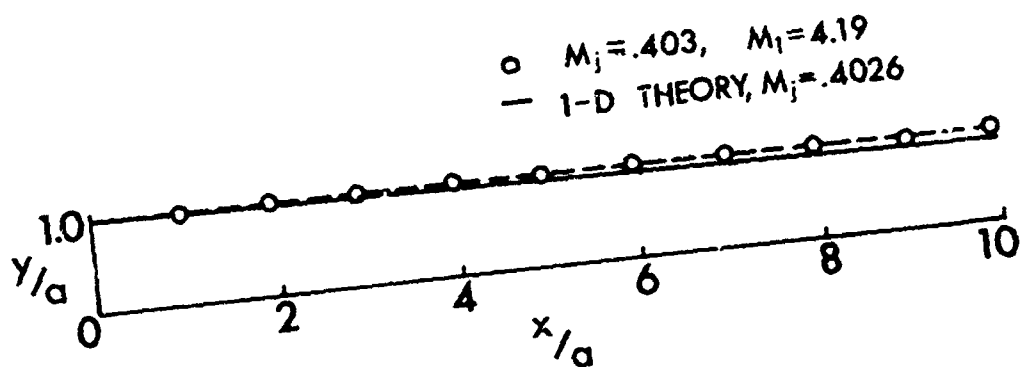
Fig. 33 Comparison of Theory and Experiment, Dividing Streamline Trajectories

0°

10°

15°

20°

25°
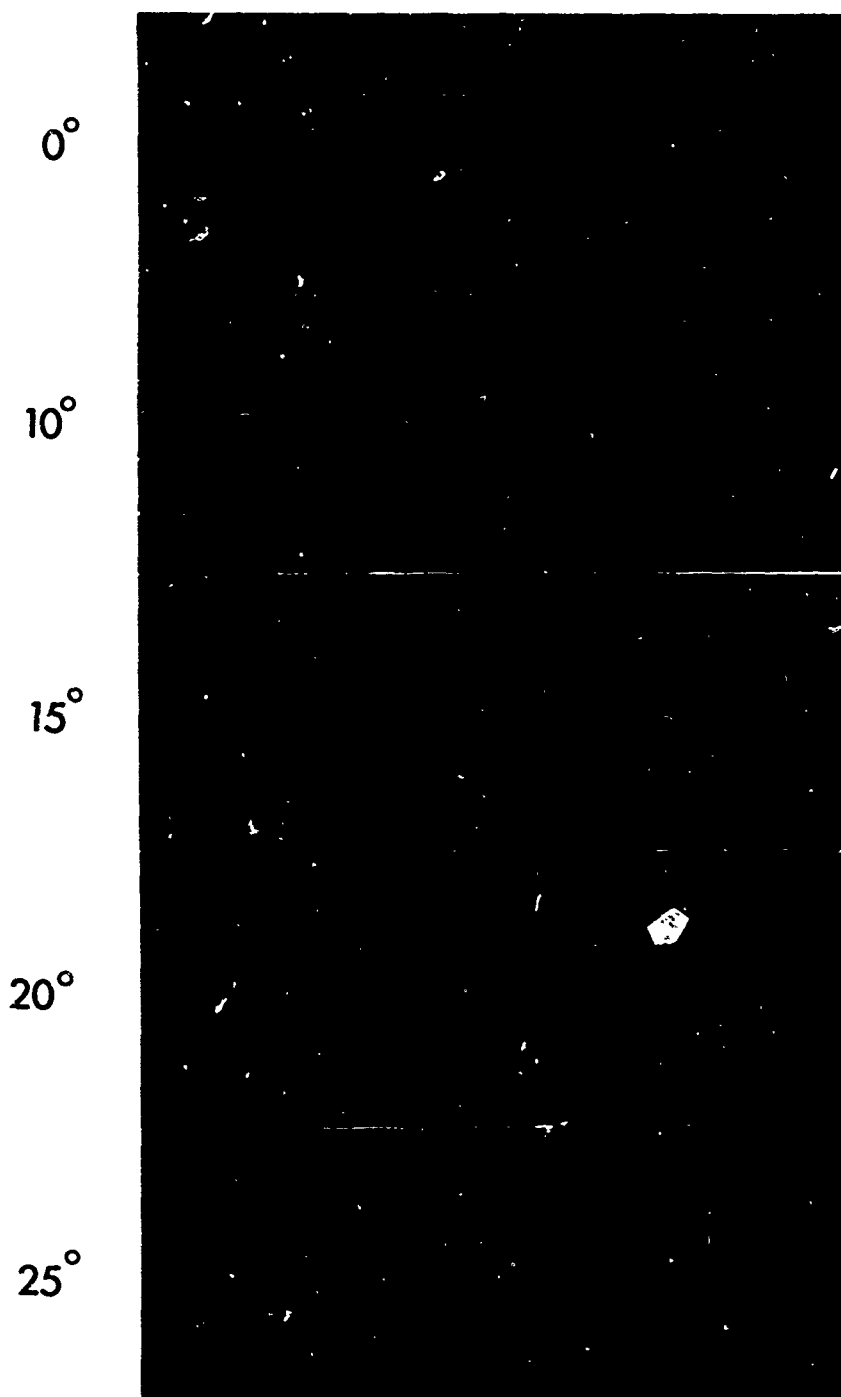
Fig. 3⁻. Supersonic Flow Over Wedges without Injection
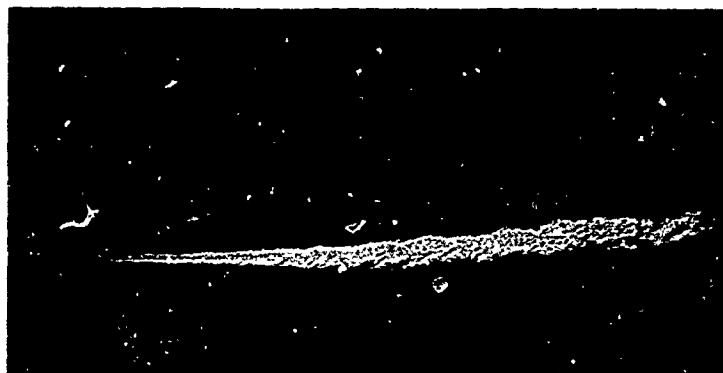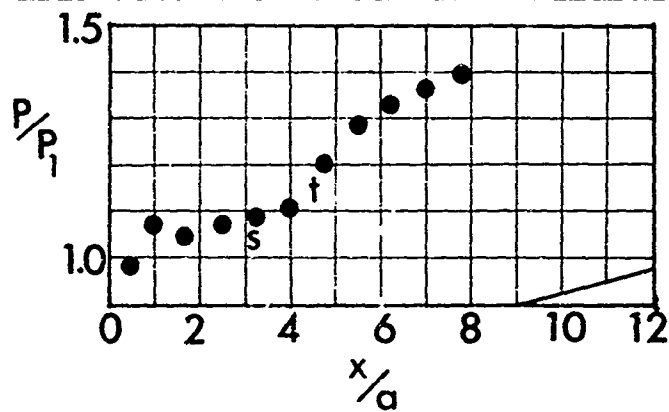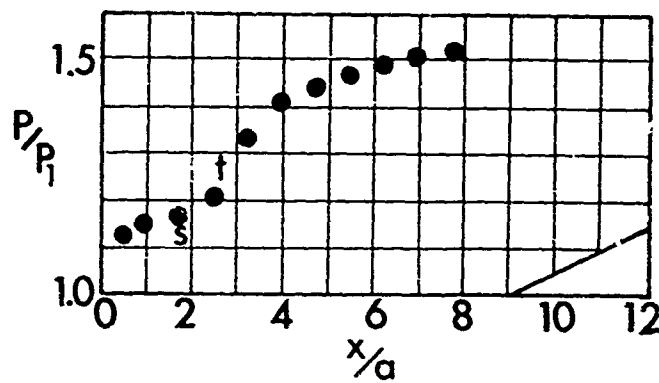
Fig. 35. Injection Over Wedge Surfaces, $M_1 = 2.85$, $\widetilde{\rho u} = 0.22$
(a) $\beta = 10°$ (b) $\beta = 15°$

82
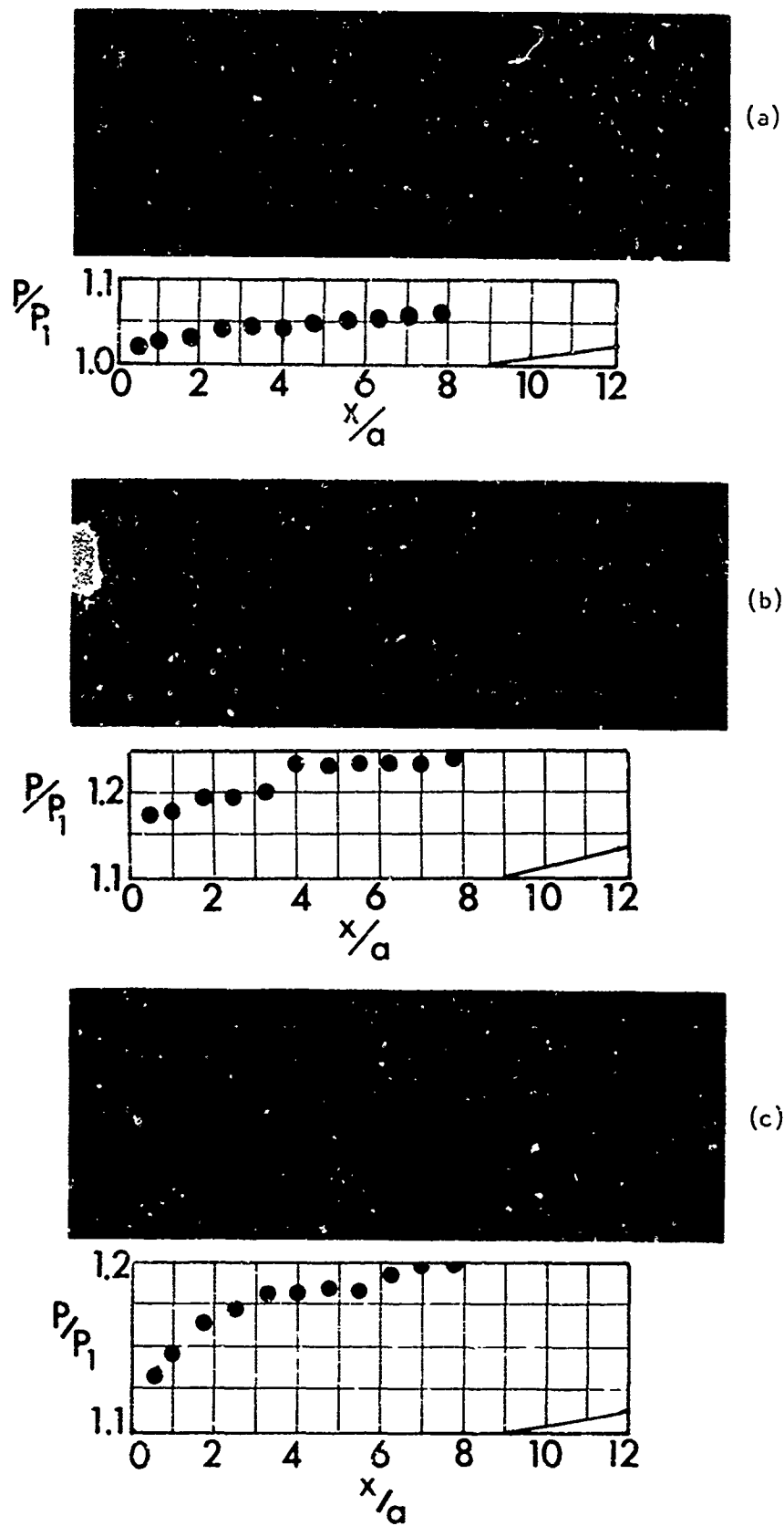
Fig. 36. Injection Over Wedge Surfaces, $M_1 = 4.19$
(a) $\widetilde{\rho u} = 0.04$, $\beta = 5°$ (b) $\widetilde{\rho u} = 0.04$, $\beta = 10°$ (c) $\widetilde{\rho u} = 0.06$, $\beta = 5°$

83
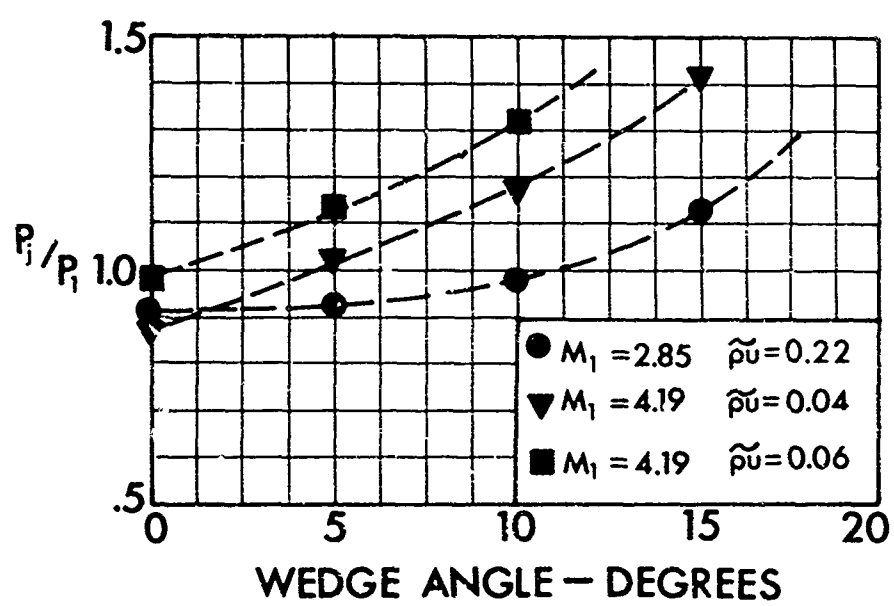
Fig. 37 Effect of Wedges on Initial Injectant Pressure
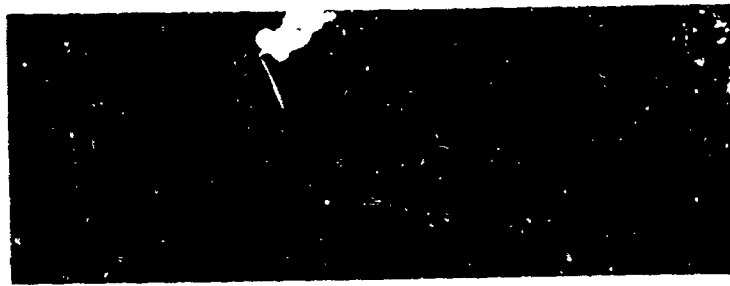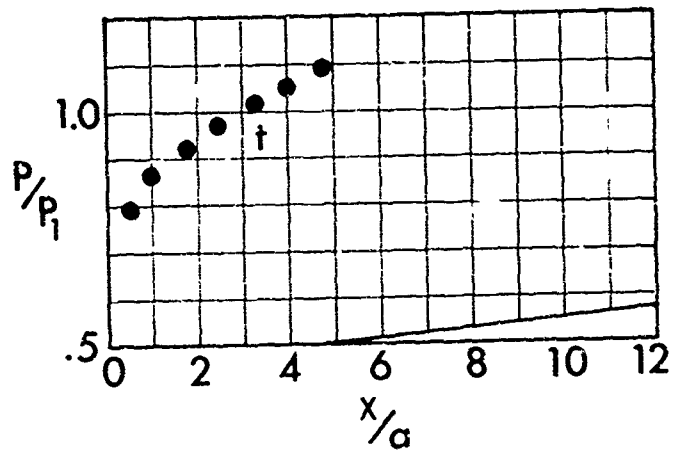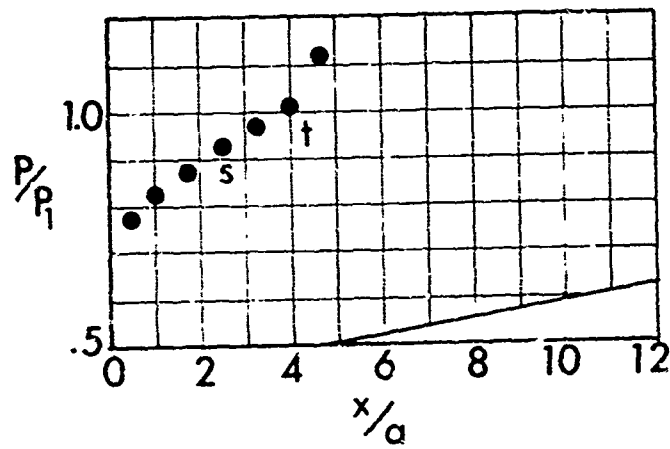
Fig. 38.   Supersonic Injection Over Wedge Surfaces
$M_1 = 2.85$, $\tilde{\rho u} = 0.44$ (a) $\beta = 5°$ (b) $\beta = 10°$

85
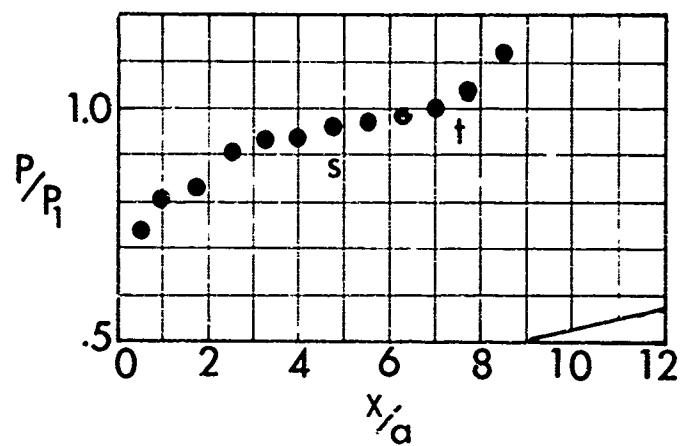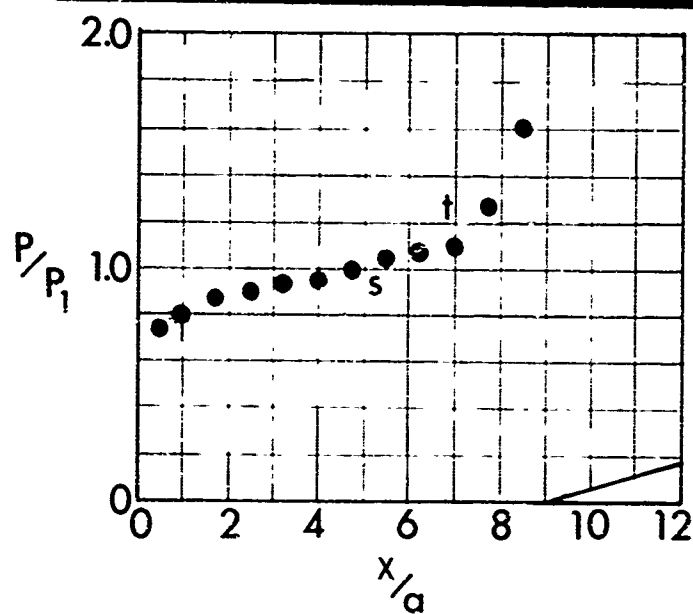
Fig. 39. Supersonic Injection Over Wedge Surfaces
$M_1 = 2.85$, $\widetilde{\rho u} = 0.44$ (a) $\beta = 10°$ (b) $\beta = 15°$

86
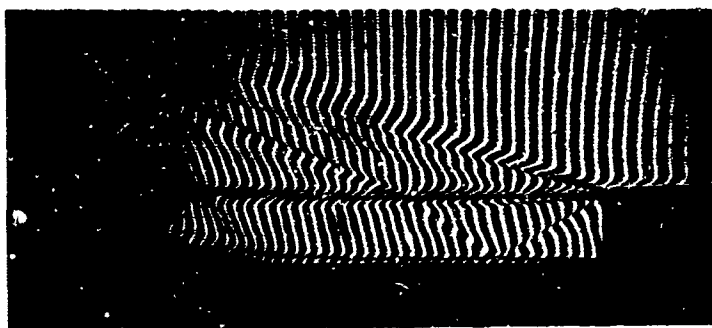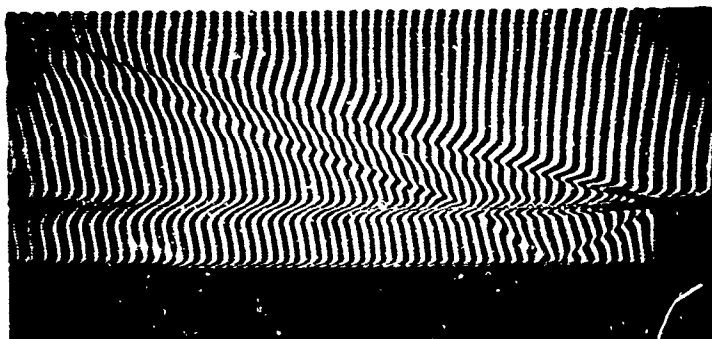
(a) $M_1 = 2.85$, $\widetilde{\rho u} = 0.44$

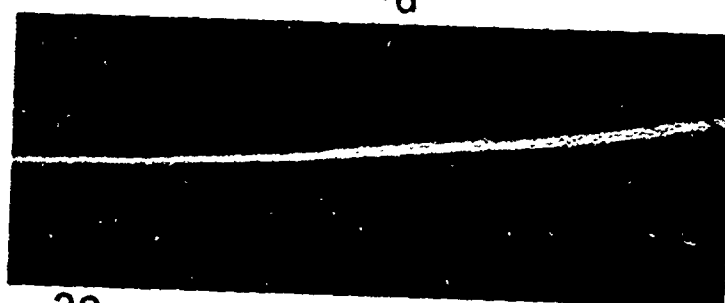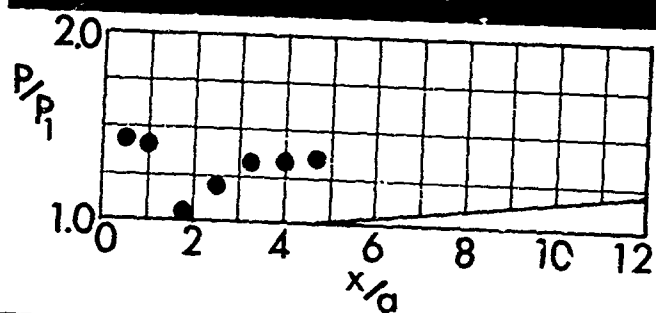(b) $M_1 = 2.85$, $\widetilde{\rho u} = 0.44$, $\beta = 10°$
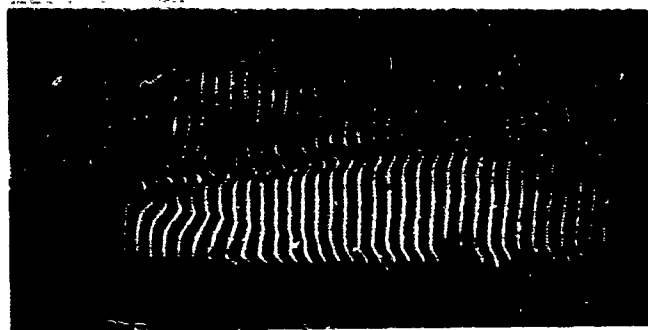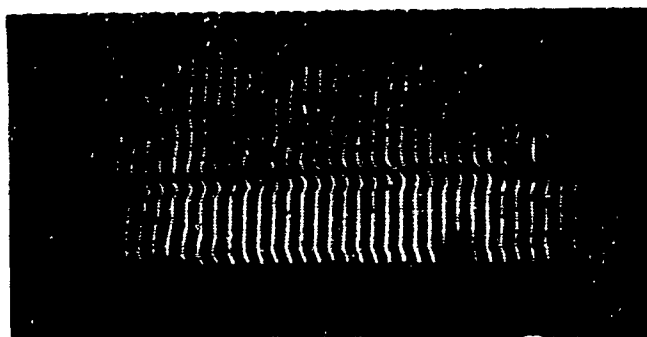
(c) $M_1 = 4.19$, $\widetilde{\rho u} = 0.38$
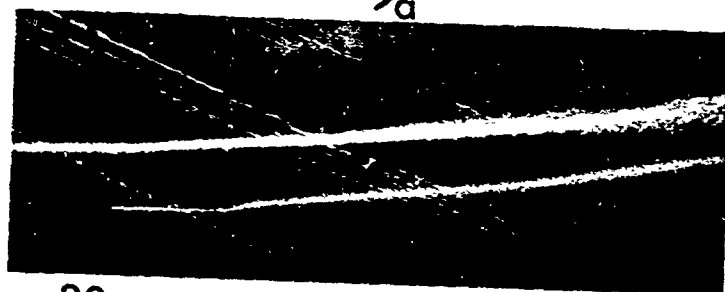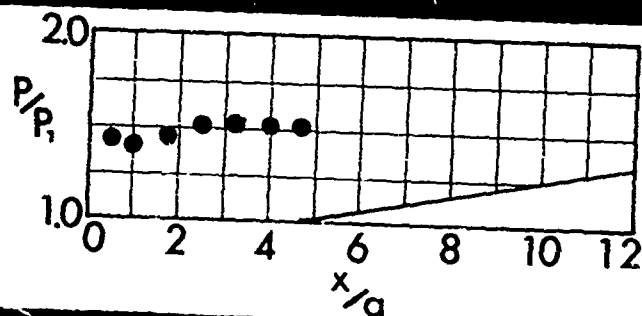
(d) $M_1 = 4.19$, $\widetilde{\rho u} = 0.74$
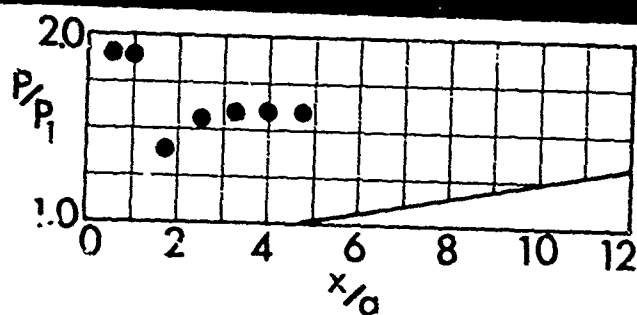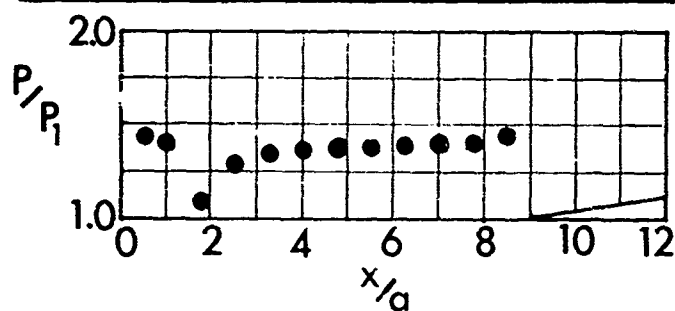
Fig. 40. Interferograms - Supersonic Injection

87
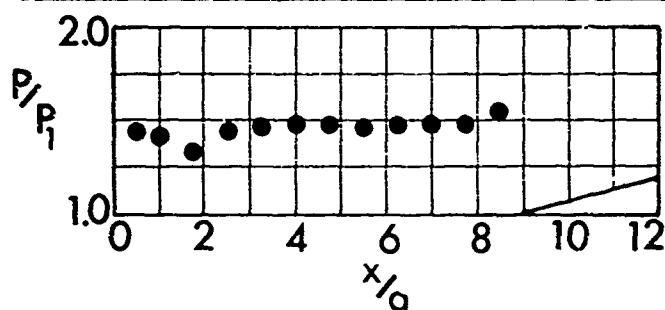
Fig. 41. Supersonic Injection Over Wedge Surfaces, $M_1 = 4.19$
(a) $\tilde{\rho u} = 0.43$, $\beta = 5°$ (b) $\tilde{\rho u} = 0.43$, $\beta = 10°$ (c) $\tilde{\rho u} = 0.56$, $\beta = 10°$
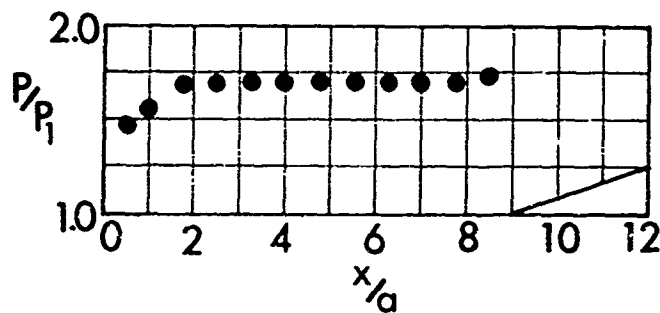
Fig. 42. Supersonic Injection Over Wedge Surfaces, $M_1 = 4.19$, $\widetilde{\rho u} = 0.43$
(a) $\beta = 10°$ (b) $\beta = 15°$ (c) $\beta = 20°$
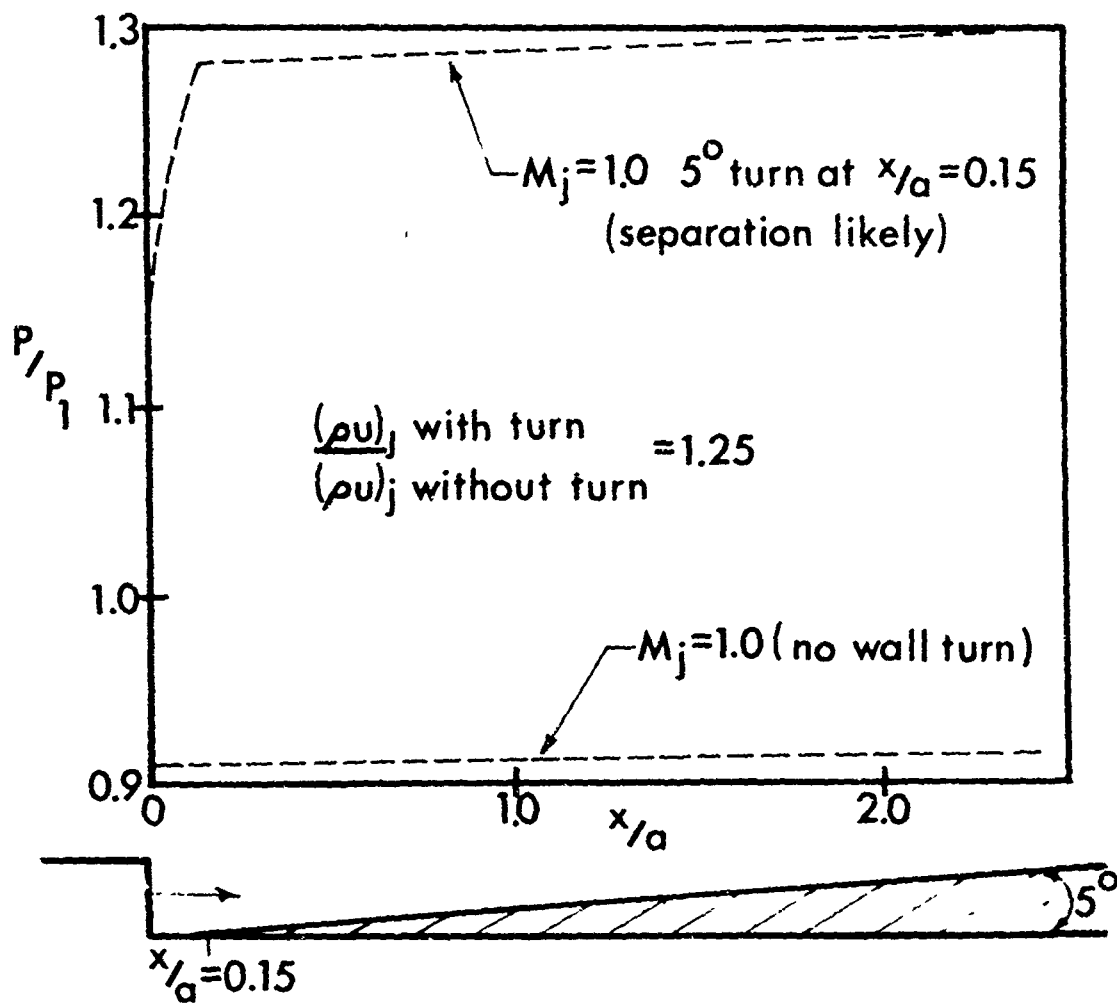
Fig. 43 Effect of Wall-Turn on Streamwise Pressure Distribution: $M_1 = 2.85$, Turbulent Mixing; $M_j = 1.0$, $5°$ Wedge Located 0.15 Slot-Heights Downstream of Injection Station
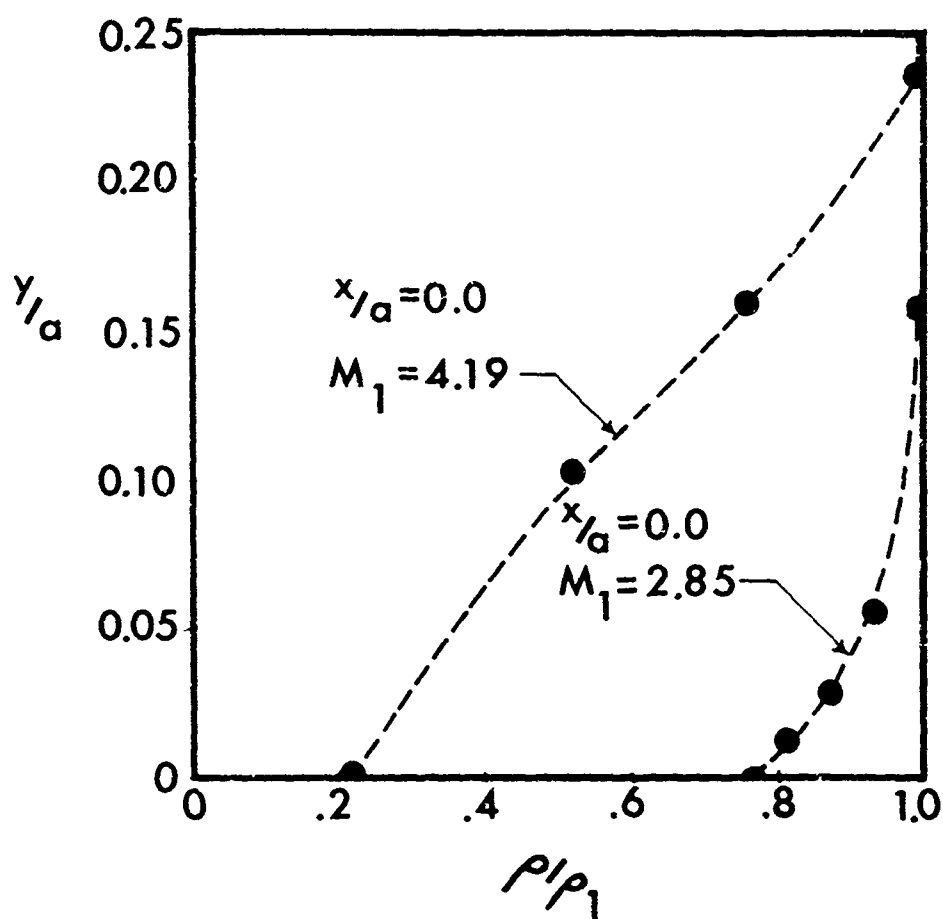
Fig. 44 Initial Splitter Plate Boundary Layer Profiles
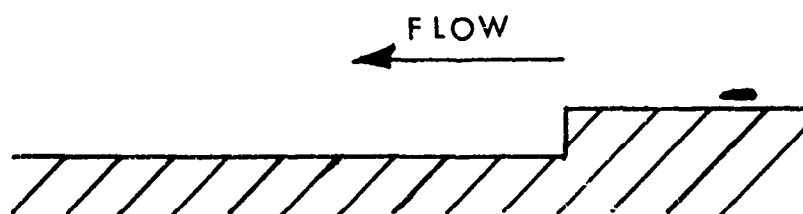
FLOW →

(a)   Schematic of Model Showing Airfoil
       Position.
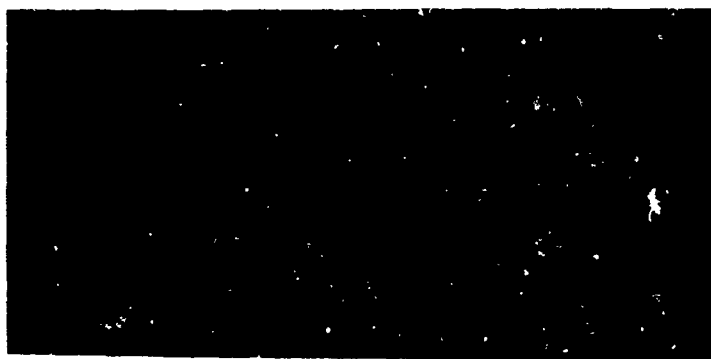
(b)   Spark Schlieren of Flow
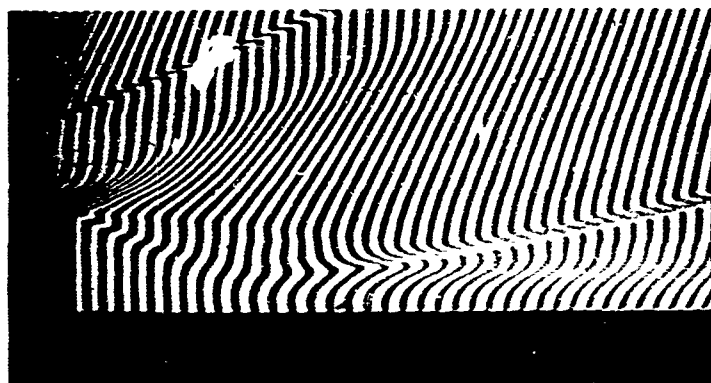
(c)   Interferogram (flow from left to right)

Figure 45   Flow Over Rearfacing Step, Airfoil
             4 Slot Heights Upstream of Step,
             $M_1 = 2.85$

92
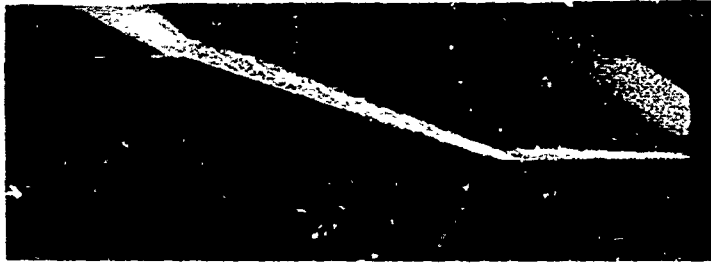
(a)   Wedge 6 Slot Heights Downstream of Airfoil

(b)   Wedge 8 Slot Heights Downstream of Airfoil

Figure 46   Flow Over 20° Wedge, M_1 = 2.85

93
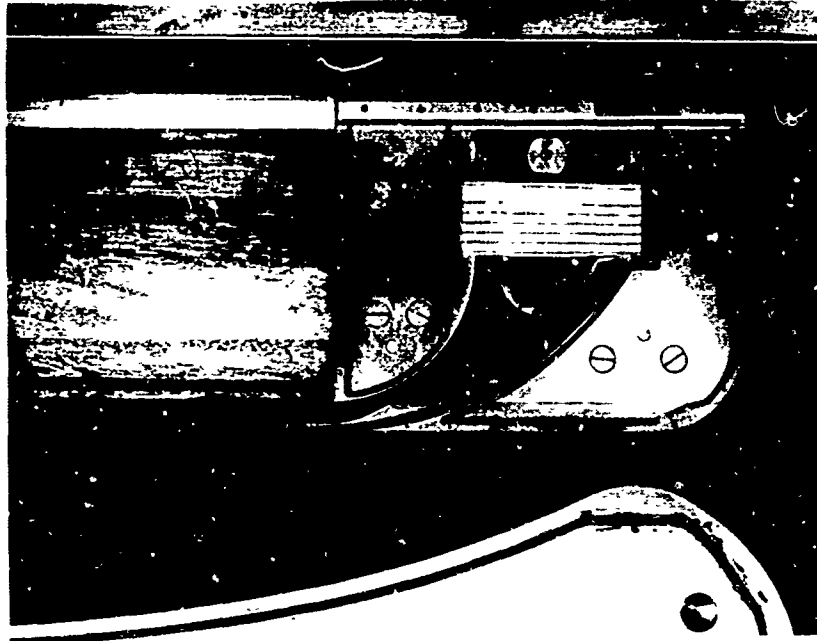
(a) Side View
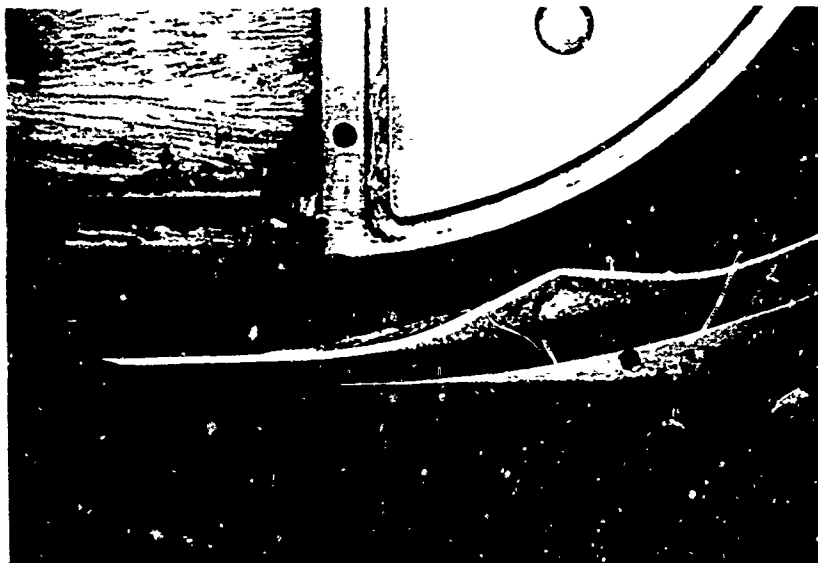
(b) Detail of the Exit Nozzles

Figure 47 DOUBLE PASSAGE INJECTION MODEL
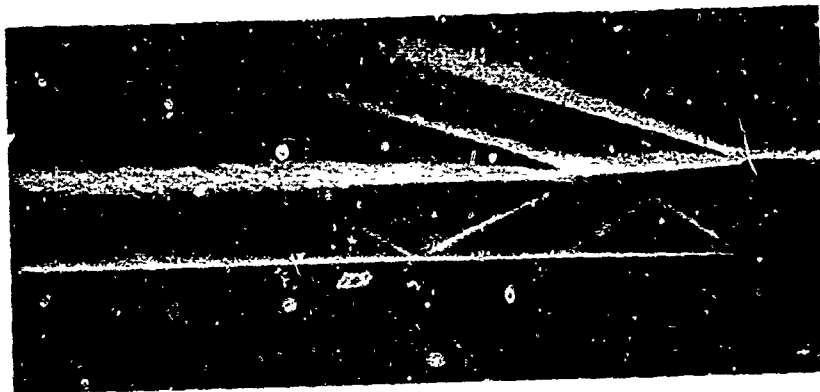
(a) Strong Throttling

(b) Moderate Throttling

Figure 48 SPARK SCHLIEREN WITH DOUBLE FASSAGE
INJECTION SYSTEM

95

REFERENCES

1. T. R. Turner, "Wind-Tunnel Investigation of Boundary- Layer Control
by Blowing on an NACA 65$_5$-424 Airfoil to Effect Drag Reduction",
NASA TN D-2374, July 1964.

2. D I. McRee, J. B. Peterson, A. L. Braslow, "Effect of Air Injection
Through a Porous Surface and Through Slots on Turbulent Skin Fric-
tion at Mach 3", NASA TN D-2427, Aug. 1964.

3. K. R. Czarnecki, "Analytical Investigation of Reduction in Turbulent
Skin Friction on a Flat Plate by Means of Air Injection Through
Discrete Slots", NASA TN D-2102, Nov. 1964.

4. J. B. Peterson, D. I. McRee, J. B. Adcock, A. L. Braslow, "Futher In-
vestigation of Effect of Air Injection Through Slots and Porous
Surfaces on Flot-Plate Turbulent Skin Friction at Mach 3", NASA
TN D-3311, Mar. 1966.

5. P. Bradshaw and M. T. Gee, "Turbulent Wall Jets With and Without an
External Stream", ARC Reports and Memoranda No. 3252, June 1960.

6. R. A. Seban, "Heat Transfer and Effectiveness for a Turbulent Boundary
Layer with Tangential Fluid Injection", Journal of Heat Transfer,
Nov. 1960, pp. 303-312.

7. J. P. Hartnett, R. C. Birkebak, E. R. G. Eckert, "Velocity Distributions,
Temperature Distributions, Effectiveness and Heat Transfer for Air
Injected Through a Tangential Slot into a Turbulent Boundary Layer",
Journal of Heat Transfer, Aug. 1961, pp. 293-306.

8. A. E. Samuel, P. N. Joubert, "Film Cooling of an Adiabatic Flat Plate
in Zero Pressure Gradient in the Presence of a Hot Mainstream and
Cold Tangential Secondary Injection", ASME Paper No. 64-WA/HT-48
Winter Annual Meeting, New York, N. Y., Nov. 1964.

9. R. J. Goldstein, E. R. G. Eckert, R. K. Tsou, A. Haji-Sheikh, "Film
Cooling with Air and Helium Injection Through a Rearward-Facing Slot
into a Supersonic Air Flow", AIAA Journal, vol. 4, no. 6, June 1966,
pp. 981-985.

10. M. Visich, Jr., and P. A. Libby, "Experimental Investigation of Mixing
of Mach Number 3.95 Stream in Presence of Wall, NASA TN D-247, Fe
1960.

11. J. J. Ginoux, "Effect of Gas Injection in Separated Supersonic ·lows",
TCEA Tech. Note. 7, Feb. 1962.

12. H. E. Gilreath, J. A. Schetz, "A Study of Tangential Slot Injection in
Supersonic Flow", Aero. Report No. 66-2, Dept. of Aerospace
Enginee.ing, Univ. of Md., Aug. 1966.

13. H. E. Bailey, A. M. Kuethe, "Supersonic Mixing of Jets and Turbulent Boundary Layers", WADC Tech. Report 57-402, June 1957.

14. P. A. Libby, J. A. Schetz, "Approximate Analysis of the Slot Injection of a Gas in Laminar Flow", AIAA Journal, vol. 1, no. 5, pp. 1056-1061.

15. J. A. Schetz, J. Jannone, "Initial Boundary Layer Effects on Laminar Flows with Wall Slot Injection", Journal of Heat Transfer, Trans. ASME, Series C, vol. 87, 1965, pp. 157-160.

16. J. A. Schetz, S. Favin, "The Ignition of Slot-Injected Gaseous Hydrogen in a Supersonic Air Stream, AIAA Paper No. 66-644, AIAA 2nd Propulsion Joint Specialist Conference, Colorado Springs, Colorado, June 1966.

17. D. R. Chapman, "Laminar Mixing of a Compressible Fluid", NACA Report 958, 1950.

18. D. R. Chapman, D. M. Kuehn, H. K. Larson, "Investigation of Separated Flows in Supersonic and Subsonic Streams with Emphasis on the Effect of Transition", NACA Report No. 1356, 1958.

19. R. F. Weiss, S. Weinbaum, "Hypersonic Boundary-Layer Separation and the Base Flow Problem", AIAA Journ., vol. 4, no. 8, Aug. 1966.

20. S. Weinbaum, "Rapid Expansion of a Supersonic Boundary Layer and its Application to the Near Wake", AIAA Journ., vol. 4, no. 2, Feb. 1966.

21. F. R. Hama, "Experimental Studies on the Lip Shock", AIAA Journ. , vol. 6, no. 2, Feb. 1968.

22. W. D. Hayes, R. F. Probstein, Hypersonic Flow Theory, Academic Press, Inc., New York, 1959.

23. L. D. Landau, E. M. Lifshitz, Fluid Mechanics, Pergamom Press, London 1959.

24. M. Lessen, "On Stability of Free Laminar Boundary Layer Between Parallel Streams", NACA Report No. 979, 1950.

25. T. Tatsumi, T. Kakutani, "The Stability of a Two-Dimensional Laminar Jet", J. Fluid Mech., 4, p. 261-275, 1958.

26. C. C. Lin, "On the Stability of the Laminar Mixing Region Between Two Parallel Streams in a Gas", NACA TN 2887, 1953.

27. J. W. Miles, "On the Disturbed Motion of a Plane Vortex Sheet", J. Fluid Mech., 4, p. 538-552, 1958.

28. J. A. Fejer, J. W. Miles, "On Stability of a Plane Vortex Sheet with respect to Three-Dimensional Distrubances", J. Fluid Mech., pp. 335-336, 1962.

29. M. Lessen, J. A. Fox, H. M. Zien, "On the Inviscid Stability of the Laminar Mixing of Two Parallel Streams of a Compressible Fluid", J. Fluid Mech., pp. 355-367, 1965.

30. M. Lessen, J. A. Fox, H. M. Zien, "Stability of the Laminar Mixing of Two Parallel Streams with respect to Supersonic Disturbances", J. Fluid Mech., pp. 737-742, 1966.

31. W. C. Reynolds, M. C. Potter, "Finite-Amplitude Instability of Parallel Shear Flows", J. Fluid Mech., pp. 465-492, 1967.

32. H. W. Liepman, A. Roshko, Elements of Gasdynamics, J. Wiley and Sons, Inc., New York, 1963, p. 349.

33. L. Crocco, L. Lees, "A Mixing Theory for the Interaction Between Dissepative Flows and Nearly Isentropic Streams", J. Aero. Sci., vol. 19, Oct. 1952.

34. L. Lees, B. L. Reeves, "Supersonic Separated and Reattaching Laminar Flows", AIAA Journ., vol. 2, no. 11, Nov. 1964.

35. B. L. Reeves, L. Lees, "Theory of Laminar Near Wake of Blunt Bodies in Hypersonic Flow", AIAA Journ., vol. 3, no. 11, Nov. 1965.

36. S. Weinbaum, R. W. Garvine, "An Exact Treatment of the Boundary Layer Equations Describing the Two-Dimensional Viscous Analog of the One-Dimensional Inviscid Throat", AIAA Paper No. 68-102, Jan. 1968.

37. S. I. Pai, A Critical Survey of Magnetofluid Dynamics, Part III, "Quasi-One Dimensional Analysis of Magnetogas Dynamics", ARL 63-175, Dec. 1965.

38. A. H. Shapiro, The Dynamics and Thermodynamics of Compressible Fluid Flow, Ronald Press, New York, 1953.

39. J. A. Schetz, H. E. Gilreath, "Tangenitial Slot Injection in Supersonic Flow", AIAA Journ., vol. 5, no. 12, Dec. 1967.

40. A. Ferri, P. A. Libby, V. Zakkay, "Theoretical and Experimental Investigation of Supersonic Combustion", 3rd ICAS Conf. Stockholm, 1962.

41. G. N. Abramovich, The Theory of Turbulent Jets, MIP Press, Cambridge, Mass., 1963.

42. C. M. Sabin, "An Analytical and Experimental Study of the Plane Incompressible Free-Shear Layer with Arbitrary Velocity Ratio and Pressure Gradient", ASME, Ser. P J. Basic Eng., 87, p. 421, 1965.

43. J. S. Linnekin, L. J. Belliveau, "FNOL2, A Fortran (IBM 7090) Subroutine for the Solution of Ordinary Differential Equations with Automatic Adjustment of the Interval of Integration", NOLTR, 63-171, July 1963.

98

DOCUMENT CONTROL DATA - R & D

(Security classification of title, body of abstract and indexing annotation must be entered when the overall report is classified)

1. ORIGINATING ACTIVITY (Corporate author)	2a. REPORT SECURITY CLASSIFICATION
University of Maryland Aerospace Engineering Dept. College Park, Md. 20740	Unclassified
	2b. GROUP N/A

3. REPORT TITLE

RESEARCH ON SLOT INJECTION INTO A SUPERSONIC STREAM

4. DESCRIPTIVE NOTES (Type of report and inclusive dates)

Final Report, June 16, 1967 to August 16, 1968

5. AUTHOR(S) (First name, middle initial, last name)

Joseph A. Schetz, Harold E. Gilreath, Paul J. Waltrup and David P. Lewis

6. REPORT DATE	7a. TOTAL NO. OF PAGES	7b. NO. OF REFS
September 1968	98	43

8a. CONTRACT OR GRANT NO	9a. ORIGINATOR'S REPORT NUMBER(S)
F 33615-67-C-1805	Aero Report No. 68-1
b. PROJECT NO 3012	
c. Task 06	9b. OTHER REPORT NO(S) (Any other numbers that may be assigned this report)
	AFAPL-TR-68-97
d.	

10. DISTRIBUTION STATEMENT This report is embargoed under the U.S. Export Control Act of 1949, administered by the Department of Commerce, and may be released by departments or agencies of the U.S. Government to departments or agencies of foreign governments with which the United States has defense treaty commitments.

11. SUPPLEMENTARY NOTES	12. SPONSORING MILITARY ACTIVITY
	AF Aero Propulsion Laboratory Wright-Patterson AFB, Ohio 45433

13. ABSTRACT   The results of an experimental and analytical study of tangential slot injection into a supersonic stream are presented. The experiments were performed in an atmospheric intake wind tunnel with freestream Mach numbers of 2.85 and 4.19. Injection of air, helium and carbon dioxide at various subsonic Mach numbers and one supersonic condition was considered. Experiments for the flow over of wedges with turning angles between 5° and 25° located on the wall downstream of the injection are also reported.

The principal data are in the form of spark schlieren photographs, interferograms and wall static pressure distributions. Density profiles at several axial stations determined from interferograms are also presented. The transition to turbulence in the shear layer and the character of the turbulence were observed from the spark schlieren photographs. The presence of separation zones was detected by small tufts or threads on the surface.

With subsonic injection. it is found that the initial slot exit conditions are not arbitrary for a given injectant mass flow but are determined by the downstream interaction between the two streams. The flow field has many of the features of the now well-known base-flow problem. A relatively simple analysis is developed which predicts the initial jet exit conditions. Very good agreement with the experimental observations is achieved.

14 KEY WORDS	LINK A		LINK B		LINK C	
	ROLE	WT	ROLE	WT	ROLE	W
Injection						
Fuel Injection						
Gaseous Injection						